UNDERSTANDING PATTERNS OF SCLEROBIONT ENCRUSTATION: METHODOLOGICAL REVIEW AND APPLICATION OF SCLEROBIONT FACIES MODEL IN MIDDLE DEVONIAN APPALACHIAN AND MICHIGAN BASIN PALEODEPTH GRADIENTS

By

Trisha A. Smrecak

A DISSERTATION

Submitted to
Michigan State University
in partial fulfillment of the requirements
for the degree of

Geological Sciences – Doctor of Philosophy

2016

ABSTRACT

UNDERSTANDING PATTERNS OF SCLEROBIONT ENCRUSTATION:
METHODOLOGICAL REVIEW AND APPLICATION OF SCLEROBIONT FACIES
MODEL IN MIDDLE DEVONIAN APPALACHIAN AND MICHIGAN BASIN
PALEODEPTH GRADIENTS

By

Trisha A. Smrecak

Sclerobionts have been a commonly employed litmus test to evaluate a number of paleontological and paleoecological hypotheses. As a result, data compiled on the varied group of organisms have been obtained from highly varied methods, and resulting analyses of sclerobionts are contradictory. Sclerobionts will continue to be used in widely differing studies, but when they are being used to provide insight on community paleoecology or paleoenvironments, it is imperative that scientists use a consistent method for collecting sclerobiont data, or at least understand the biases their chosen method is likely to introduce.

The purpose of this research was twofold: 1) to evaluate the validity of a spatial abundance method, visual estimation, that is both highly valuable as a quick census tool and that has been rigorously employed in Late Ordovician and Modern environments (Smrecak and Brett, 2014; Brett et al., 2012), and suggests that sclerobiont suites may be used as predictive sclerobiofacies models, and 2) to apply visual estimations and other encrustation metrics to evaluate the potential effectiveness of sclerobiofacies in two coeval basins in the Middle Devonian.

Rank abundance of a variety of methods used to assess encrustation was compared on the same sampled sclerobiont assemblage; each method reported significantly different rank orders. The most accurate method for recording sclerobiont encrustation, and baseline for comparison among the other methods, used ArcGIS image digitizing and geospatial data

collecting software to precisely quantify the surface area of a host by each sclerobiont taxon. The method that most closely reflected the rank order produced by ArcGIS was visual estimation. Numerical abundance methods produced a rank order that was 20% different from that produced by ArcGIS. Frequency of encrustation rank abundance was nearly 40% different from ArcGIS rank abundance. Grid overlay methods varied widely based on the counting method used and the grid overlay design chosen.

Visual estimation of spatial abundance was the primary method used to evaluate sclerobiont encrustation patterns in the Middle Devonian Appalachian and Michigan Basins. A number of supporting data metrics were also collected, including encrustation frequency, numerical abundance, and per shell richness, to characterize the sclerobiont encrustation patterns in the basins. Sclerobiont suites in both basins behaved in a manner consistent with what would be predicted by a sclerobiofacies model; an overall decline in encrustation was observed with depth. Some sclerobiont taxa are indicative of particular facies.

Rapid influx of sedimentation in the basin also substantially impacted the observed sclerobiont assemblages. Sclerobionts declined predictably with depth in both the Michigan and Appalachian Basins, but in the Michigan Basin sclerobiont spatial coverage declined from 12% (shallow facies), to 5.4% (moderate facies) to 3.6% (deep facies), but in the Appalachian Basin the decline from 4.3% to 2.48% to 1.25% in those environments. Spatial coverage in the Appalachian Basin is substantially dampened by the high levels of sedimentation. Variability observed within samples inferred to have been from high sedimentation environments suggest that there was a threshold effect from the interplay between sedimentation and eutrophication.

ACKNOWLEDGMENTS

For my parents, who made this possible by supporting me every day in every conceivable

way. For my gram, who would have loved bragging about this accomplishment to anyone who

would have listened. For Joshua, who I hope to continue to parallel. And for Jesse, who showed

me there's life after a dissertation.

With thanks to coffee, and everyone involved in filling my cup with it each morning.

With thanks to Mark Erickson, who got me started down this path and never let me falter, and to

Danita Brandt, who paved that path and outlined it in red ink.

And, as ever, with thanks to my liberal arts degree.

Dissertation: The Journey

Follow the money.

Field work, lots of rock, a

Full Lane cabinet.

Computer screen blinds,

Fossils turned to integers.

A sea without fish.

Hunched and toiling

Evolution rewinds – a

Thesis emerges.

iv

TABLE OF CONTENTS

LIST OF TABLES	vii
LIST OF FIGURES	viii
CHAPTER 1: ASSESSMENT OF TECHNIQUES TO DESCRIBE	
SCLEROBIONT ABUNDANCE AND DISTRIBUTION	1
ABSTRACT	
USE OF SCLEROBIONTS IN PALEONTOLOGICAL STUDIES	2 3 5 7 7
Methods Used to Describe Sclerobionts	5
METHODS	7
Choice of Host Substrate	7
Identification of Sclerobiont Taxa	8
Methods Tested	9
Frequency of Encrustation	9
Numerical Abundance	9
Spatial Abundance	10
Comparing Different Methods – Establishing a Baseline	12
RESULTS	13
ArcGIS Method	13
Rank Order Comparisons	13
Grid Overlays for Assessing Sclerobiont Abundance	14
Preferential Encrustation on Host Valves	16
DISCUSSION	18
Estimation vs. Calculation	18
Comparison of Abundance Methods	21
Assessing Grid Overlay Methods – Rank Abundance	22
Assessing Grid Overlay Methods – Spatial Patterns on Hosts	24
CONCLUSIONS	25
APPENDIX	28
REFERENCES	38
CHAPTER 2: SCLEROBIONT ENCRUSTATION PATTERNS IN THE	
MIDDLE DEVONIAN MICHIGAN BASIN: CHARACTERIZATIONS	
WITH DEPTH	43
ABSTRACT	44
INTRODUCTION	44
Geological Setting	47
METHODS	48
RESULTS	53
Changes in Sclerobiont Suites with Depth	53
Sclerobiont Areal Percent Coverage	55

Sclerobiont Relative Abundance	56
Sclerobiont Richness	57
Frequency of Encrustation	58
DISCUSSION	58
Sclerobiont Assemblage I – Shallow Facies	58
Sclerobiont Assemblage II – Moderate Facies	59
Sclerobiont Assemblage III – Deep Facies	60
Sclerobiont Host Preference and Other Host-Sclerobiont Relationships	61
Host Preference	61
CONCLUSIONS	65
APPENDIX	67
REFERENCES	76
CHAPTER 3: CHARACTERIZING SCLEROBIONT ASSEMBLAGES ALONG	
A MIDDLE DEVONIAN (HAMILTON GROUP) DEPTH GRADIENT,	
APPALACHIAN BASIN, NY, USA AND COMPARISON WITH OTHER	
DEVONIAN SCLEROBIONT ASSEMBLAGES	82
ABSTRACT	83
INTRODUCTION	84
Geological Setting	87
METHODS	89
Host Selection	90
Sclerobiont Data Collection	90
RESULTS	91
Multivariate Analyses	92
Sclerobiont Suite Differences with Depth and Sedimentation	92
Areal Percent Coverage	95
Sclerobiont Relative Abundance	96
Sclerobiont Richness	96
Frequency of Encrustation	97
DISCUSSION	98
Sclerobiont Assemblage I – Shallow Facies	99
Sclerobiont Assemblage II – Moderate Facies	99
Sclerobiont Assemblage III – Deep Facies	100
The Impact of High Sedimentation on Sclerobiont Assemblages	101
Comparison with Other Work	105
CONCLUSIONS	112
APPENDIX	115
REFERENCES	128

LIST OF TABLES

TABLE 1 - Commonly applied sclerobiont encrustation methods	33
TABLE 2 - Rank order of sclerobiont taxa	34
TABLE 3 - Rank order of sclerobiont taxa using various grid overlay methods	35
TABLE 4 - Number and direction of significant rank order shifts with each method	36
TABLE 5 - Number of sclerobionts recorded using each method	37
TABLE 6 - Encrustation metric descriptions	74
TABLE 7 - Observed encrustation metrics in the Michigan Basin by sample and with depth	75
TABLE 8 - Characteristics of host brachiopods	122
TABLE 9 - Encrustation metric definitions	123
TABLE 10 - Observed encrustation metrics by sample with depth	124
TABLE 11 - Compilation of relevant sclerobiont assemblage data	125

LIST OF FIGURES

FIGURE 1 - Grid overlay design and counting methods	29
FIGURE 2 - Idealized line diagram	30
FIGURE 3 - Counting methods and grid overlay design comparisons	30
FIGURE 4 - Change in rank order using ArcGIS and visual estimation methods	31
FIGURE 5 - Changes in rank order of each sclerobiont taxon	32
FIGURE 6 - Michigan Basin locality information	68
FIGURE 7 - Averaged encrustation metrics observed in the Michigan Basin	69
FIGURE 8 - Cluster analysis of Michigan Basin samples	70
FIGURE 9 - Detrended correspondence analysis of Michigan Basin samples	71
FIGURE 10 - Principle coordinate analysis of Michigan Basin samples	72
FIGURE 11 - Taxonomic composition of shallow, moderate, and deep facies in the Michigan Basin	73
FIGURE 12 - Appalachian Basin locality information	116
FIGURE 13 - Averaged encrustation metrics observed in the Appalachian Basin	117
FIGURE 14 - Cluster analysis of Appalachian Basin samples	118
FIGURE 15 - Principle coordinates analysis of Appalachian Basin samples	119
FIGURE 16 - Detrended correspondence analysis of Appalachian Basin samples	120
FIGURE 17 - Taxonomic composition of shallow, moderate, and deep facies in the Appalachian Basin	121

CHAPTER 1: ASSESSMENT OF TECHNIQUES TO DESCRIBE SCLEROBIONT ABUNDANCE AND DISTRIBUTION

ABSTRACT

Patterns of sclerobiont encrustation constitute important data in studies of paleosyn - and autecology, yet methods used to collect this information are not standardized. The variation among different methods may be attributed to the need for uniquely designed methods applied to address a specific question. As a result, comparisons between sclerobiont studies are cumbersome, results are sometimes contradictory, and the interpretive value among published results is low. A comparison of techniques commonly used for computing sclerobiont abundance and distribution upon host substrates revealed that the simplest measure of abundance, numerical abundance, under-reported large colonial organisms and over-reported small colonial and solitary organisms when compared to calculated baseline values obtained from digitized photos in ArcGIS. Spatial abundance methods, also examined, show areal percent coverage estimation over-reports total encrustation, but not significantly.

Methods commonly used to determine sclerobiont abundance including spatial, numerical, and frequency of encrustation methods were applied to a sample set of the snowshoe shaped Ordovician brachiopod *Rafinesquina*. Spatial estimation was the only method to preserve rank abundance calculated by ArcGIS. Frequency of encrustation ranked nearly half the sclerobionts differently than the calculated values in terms of abundance. Most spatially-based grid overlay methods produced different abundance rankings; grid overlays with fewer grid sections better reflected baseline values. Different methods employed in reporting sclerobiont encrustation patterns introduce biases unique to each method. Understanding these biases inherent to each method allows more highly resolved interpretations among previous studies, and promotes more consistent approaches to sclerobiont analysis.

USE OF SCLEROBIONTS IN PALEONTOLOGICAL STUDIES

Paleontological research has incorporated data on encrusting and boring organisms on a range of host substrates as important components of paleoecological, paleoautecological, and taxonomic research. The term 'sclerobiont' is relatively new (Taylor and Wilson, 2002); encrusting organisms have been termed epizoans (e.g. Alvarez and Taylor, 1987), epiphytes (e.g., Taylor, 1990) and epibionts (e.g. Mistiaen et al., 2012). The schema proposed by Taylor and Wilson (2002) follows previous attempts to unify nomenclature (see Walker and Miller, 1992). In modern literature on encrusting and boring communities, the different terms have more restricted meanings that imply the identity and living or dead nature of the host, restrictions that are not always readily identified and thus not usually employed by paleontologists. The present study follows Taylor and Wilson (2002) in using 'sclerobiont' as an all-encompassing term for encrusting and boring organisms upon any substrate and is defined as "any organism (animal or plant) fouling any kind of hard substrate (pg. 523)."

Because numerous sclerobionts may inhabit a common host substrate during the time when the host substrate was living or exposed post-mortem, they record a uniquely time-bound pattern of encrustation (Lescinsky et al., 2002). Sclerobionts can be sensitive environmental indicators, so the patterns of their encrustation may be particularly valuable in interpretation of depth environments (Bordeaux and Brett, 1990; Lescinsky et al., 2002; Smrecak and Brett, 2014). Sclerobionts have been used to infer ecological relationships with their hosts (Bose et al., 2010; Pitrat and Rogers, 1978; Schneider, 2003), and other sclerobionts (Lescinsky, 1997; Liddell and Brett, 1982; Rodrigues, 2007), and to infer the life habits of their hosts (Brandt, 1996; Key et al., 2000; Richards, 1972). Sclerobionts have also been incorporated into studies of taphonomic fidelity (Krause et al., 2010; Lescinsky, 1993, 1995; McKinney, 1995) and

comparative taphonomy (Brett et al., 2012; Lescinsky et al., 2002; Nebelsick et al., 1997; Powell et al., 2011). In hardground settings, sclerobionts have been used to study community evolution throughout geologic time (Taylor and Wilson, 2003) and have shown changes in encrustation patterns with bathymetric changes (Brett et al., 2011; Bordeaux and Brett, 1990; Mistiaen et al., 2012; Smrecak and Brett, 2014).

In an attempt to establish 'best practices' for characterizing patterns of sclerobiont abundance and distribution, the authors examined a collection of the sclerobiont – bearing brachiopod *Rafinesquina* from the Cincinnatian (Katian, U. Ordovician, Ohio and Indiana, USA) following methods used in previous studies. The abundance measures compared herein include 1) numerical abundance (per valve and within-grid regions in various grid overlay designs), 2) frequency of encrustation (the frequency with which a given sclerobiont is observed on a host and, more broadly, the frequency with which a host is encrusted upon in a sample), and 3) spatial abundance (defined as the amount of space each sclerobiont inhabits upon a given host).

It is not surprising that a group of organisms with a widely varied nomenclature and application in paleontological research also has been studied with a wide range of method designs. The methods used to describe the abundance and placement of sclerobionts on their hosts vary dramatically based upon the interest of the researcher and the nature of the host substrate. The nature of characterizing colonial and solitary sclerobionts provides an additional level of complexity that must be considered depending on the goals of research. For example, sclerobiont distribution on arthropods may be significantly impacted by arthropod molting and burrowing behaviors which may impact the susceptibility of their cuticle to encrustation (Brandt, 1996). Bivalve burrowing activity and degree of infaunalization may similarly decrease their susceptibility to encrustation, at least in life (Aberhan et al., 2014; McKinney, 2007). Epibenthic

organisms, like brachiopods, may provide the most consistently available host substrate for sclerobiont encrustation, although even these organisms have areas which are cryptic or in constant contact with the substrate and which may be unsuitable for encrustation during life.

Additionally, particular brachiopod sizes and shell morphologies have been shown to be preferable surfaces for sclerobiont encrustation (Bordeaux and Brett, 1990; Rodland et al., 2004, Rodland et al., 2014).

Methods Used to Describe Sclerobionts

Studies of sclerobionts on host brachiopod substrates are commonly dominated by two types of data, usually collected in service of a particular research question: abundance of sclerobiont taxa, and the spatial location of sclerobionts on the host. Abundance can be measured numerically or spatially, and the location of sclerobionts can be recorded with different degrees of accuracy. There are three recurring styles of methods used to measure both sclerobiont abundance and location: 1) frequency of encrustation, the frequency with which sclerobionts are found on hosts; 2) the number of times each sclerobiont is observed upon a host, called numerical abundance; and 3) the space each sclerobiont occupies on a host, spatial abundance. These methods have similarities in their overall research goals, but researchers have designed a diverse suite of methods within each style to address particular research goals. Most commonly, researchers have a) recorded the presence of a sclerobiont on a host shell (e.g. Pitrat and Rogers, 1978; Richards, 1972) or counted the number of times each occurs on an individual host sample (e.g. Bordeaux and Brett, 1990; Thayer, 1974; Mistiaen et al., 2012), b) counted the number of sclerobionts within designated regions on the host (e.g. Kesling et al., 1980; Sparks et al., 1980; Bishop, 1988; Barringer, 2008; Bose et al., 2010; Shroat-Lewis et al., 2011; Furlong and McRoberts, 2014), c) estimated (Brett et al., 2011; Smrecak and Brett, 2014; Richards, 1972) or

calculated the area of the host covered with each sclerobiont (e.g. Bordeaux and Brett, 1990; Alexander and Scharpf, 1990; Nebelsick et al., 1997) (see Table 1).

The various methods have been designed to address issues that arise because sclerobiont taxa encompass a wide range of colonial and solitary organisms ranging from taxa with small, limited growth size to those that may grow to encrust an entire host substrate. Sclerobiont taxa may also preferentially encrust upon certain locations of the host. Grid overlay methods have been used to quantify those preferences and as a quick censusing method of spatial abundance. Grid overlay design varies widely, from as few as six divisions of the host shell to as many as forty regions, and from equal-area grid designs to grids that divide the host into near-commissure and inter-area regions (e.g. Kesling et al., 1980; Alvarez and Taylor, 1987; Zaton and Borszcz, 2012; see Figure 1). Researchers have also counted the occurrence of a particular sclerobiont taxon as one whole occurrence in each region in which it occurs or as a proportion of an occurrence divided by the number of regions in which each sclerobiont occurs (e.g. Bose et al., 2011).

Sclerobiont abundance can be calculated most precisely by measuring the surface area of both the host substrate and the sclerobionts covering the host. Manual or digital calculation provides the most accurate spatial abundance data, which can be modified to produce numerical abundance or frequency of encrustation data. Unfortunately, these methods are also time consuming and do not translate easily into the field. Researchers have manually calculated these values to the nearest cm² using transparency paper over the host shell or a photograph of the host and outlining and infilling the grid with the area of the host and of the sclerobionts. These data can also be computed using digitized photographs of the host shell and image analyzing software

(Nebelsick, 1996; Lescinsky, 1997); recently, the increasingly ubiquitous spatial mapping software ArcGIS has been used to assess encrustation.

Use of digital techniques, e.g. GIS software, provide pixel-level image data. Digital techniques also permit scaling of host shells, allowing direct comparison of the location of sclerobionts and relative spatial coverage of individual hosts. The host must be relatively flat to permit successfully digitized images upon which to calculate surface area, which excludes some taxa from this technique. An idealized 'map' of the shell and the location and identity of the encrusters – as used in estimation methods – must be made before the method can be applied.

Numerical and spatial abundance methods are favored in more recent research on incorporating sclerobiont encrustation patterns into paleoecological reconstructions. However, just as the nomenclature remains varied despite attempts at refinement (Walker and Miller, 1992; Taylor and Wilson, 2002), no one method predominates. In the last five years alone, grid overlay methods (Bose et al., 2010; 2011), frequency of encrustation methods (Mistiaen et al., 2012), and numerical and spatial abundance methods (Brett et al., 2011; Smrecak and Brett, 2014; Rodland et al., 2014) have all been used. It is therefore of great benefit for researchers interested in integrating sclerobiont community patterns into their research and for broad synthesis of encrustation research to understand the biases introduced by particular methods.

METHODS

Choice of Host Substrate

The large, snowshoe-shaped brachiopod *Rafinesquina* was chosen as an exemplar host. *Rafinesquina* hosts morphologically and taxonomically diverse assemblages of sclerobionts including sheet-like, gumdrop, and runner-form bryozoans, solitary cornulitids and inarticulate brachiopods, colonial corals, a variety of borers, algae, sponges, and scars of taxa preserved

through bioimmuration (Brett et al., 2012; Freeman et al., 2012; Richards, 1972; Smrecak and Brett, 2014). The shape of the *Rafinesquina* is broad, smooth, and concavo-convex, which readily lends the shell to photographic imaging, a requisite for GIS method application, and which is helpful in the successful application of grid overlay methods. A total of 24 valve surfaces, mostly from the external surfaces of valves of articulated *Rafinesquina*, were selected from collections of Smrecak and Brett (2014) and are currently reposited in research collections at Grand Valley State University. The valves were chosen to illustrate the range of sclerobiont taxa and encrustation patterns present on *Rafinesquina*, from fully encrusted to nearly bare surfaces. Preference was also given to host valves that displayed high sclerobiont taxonomic richness.

Identification of Sclerobiont Taxa

Host valves were examined under a dissecting microscope at a magnification of 10 - 30x. Each sclerobiont was identified to major taxonomic group (e.g. bryozoan, cornulitid), and to genus if possible. Bryozoans require destructive thin sectioning to identify, and many encrusting bryozoan colonies are juvenile and are thus lacking in identifying characters. Therefore, bryozoan form taxa, or morphotypes, were established based on a combination of observable characters including zooecial shape and size, the presence or absence of monticules, and growth habit (e.g. gumdrop, sheet-like) following Smrecak and Brett (2014). These form taxa are designated with an "M" to denote morphotype with an associated numerical identifier (e.g. M1). In the samples used in this study, sixteen sclerobiont form taxa were defined.

Methods Tested

Frequency of Encrustation

Frequency of encrustation is a simple measure of the proportion of host shells in a sample upon which encrustation occurs. It can also be more precisely applied to the frequency of encrustation of each sclerobiont taxon in a sample; researchers with an interest in a particular sclerobiont taxon have used versions of this method. In this study, frequency of encrustation (FE) was obtained by 1) noting whether each of the sixteen sclerobiont taxa was present on each host valve, and 2) dividing the total number of host valves encrusted by that taxon (H_e) by the total number of host valves (H_t).

FE = He/Ht

Numerical Abundance

Numerical abundance methods reflect data collection typically referred to as 'relative abundance' in studies focusing on solitary organisms. Numerical abundance methods measure the number of individual sclerobionts on a host valve (e.g. three trepostome bryozoans and two cornulitids) and may extrapolate how many sclerobionts of each taxon might be expected to be observed within a sample. This is commonly referred to as "relative abundance" by other authors (e.g. Rodland et al., 2004). Numerical abundance data provide no information about the area each sclerobiont individual occupies on a host. Abundance data, therefore, reflects larval settlement success and gives equal value to occurrences of small solitary and large colonial sclerobionts. Sclerobiont numerical abundance was calculated in this study by counting the number of times each sclerobiont taxon was observed (S₀) on each host and averaging that value across the sample. Thus:

$$Numerical\ Abundance = \left(\sum So\right) \div Ht.$$

Spatial Abundance

Spatial abundance methods can be estimated, calculated to the nearest pixel using software, or assessed using grid overlays designed to count numerical abundance in different grid sections. The most precise methods calculate the surface area covered by sclerobionts to the nearest cm² or mm², either manually or computed with the help of imaging or GIS software. To emulate those methods, the surface area covered by sclerobionts on each valve was calculated by photographing and digitizing the valve surface. On the surface, the sclerobiont taxa were identified and a reference map of their location was sketched on an idealized line diagram. The image was digitized and scaled to the rest of the sample using ArcGIS software, and the location of each sclerobiont on the host valve was outlined as a polygon feature. This method provided pixel-level spatial abundance data, which were converted to area (cm²) and recorded as a proportion of host valve encrusted. As with numerical abundance, area occupied was averaged across the sample for each sclerobiont taxon. There was a tendency in the method to underestimate surface area from photos of highly convex shells. Even in using the relatively flat Rafinesquina host, four host pedicle valves were too convex to successfully capture sclerobionts and available substrate near the commissure. Therefore, these valves were excluded from the ArcGIS analysis.

Estimated spatial abundance methods were studied, as well. The spatial abundance of each sclerobiont taxon was visually estimated to the nearest whole integer on each host valve following methods outlined in Brett et al. (2011) and refined in Smrecak and Brett (2014). Using the idealized line drawing of the brachiopod (Figure 2), the placement and approximate extent of each sclerobiont was sketched and estimated numerically. Those data were validated by

repeating the process with a subset of ten host valves to ensure consistency of the method. Estimated spatial abundance was averaged across the sample to get the average spatial abundance of each sclerobiont taxon, and to estimate the average proportion of host valves encrusted in the sample.

The study also tested the efficacy of a range of grid overlay methods employed in the literature (see Figure 1). Grid overlays with six, nine, thirteen, and thirty-two relatively equally divided regions were compared following methods used in Bose et al. (2010). A grid overlay with six, unequally divided regions was also used to mimic studies that described encrustation near the commissure vs. in the inter-area of the host valve (e.g. Sparks et al., 1980; Barringer, 2008). Sclerobionts may occur in one grid-defined region or may extend into neighboring sections. Sclerobionts that extend into more than one section of the grid have been counted in different ways. In multiple occurrence counting, each section in which the sclerobiont occurs was counted as a separate occurrence (e.g. Bose et al., 2010). In proportional counting, the number of sections in which a sclerobiont occurs is divided by the sclerobiont occurrence. For example, if a sclerobiont extended into three grid sections it was counted as 0.33 occurrence in each section (Figure 1F). Following the methods of Bose et al. (2010, 2011), the area ratio (R) was calculated for each section of grid in each overlay method by:

$$R = \frac{AR}{AT}$$

Where AR is the area of the grid section and AT is the total area of the host valve. Surface area was totaled for all shells using ArcGIS, and the average shell size was used to approximate the size of each grid region, R_i . The expected number of sclerobionts (E) was calculated by:

$$E = N * R_i$$

Where N is the number of observed sclerobionts in the section of interest (i).

Comparing Different Methods – Establishing a Baseline

The different methods for assessing numerical and spatial abundance produced substantially different numerical outputs, ranging from 0.05 occurrences to 60% of an encrusted surface. Therefore, the rank order abundance of each sclerobiont taxon was recorded for each method. Rank orders and changes in rank order were compared across the methods (see Table 3). Any significant changes in rank resulting from the use of a particular method for a given sclerobiont taxon was recorded. A baseline rank order was selected from the methods applied to allow comparison among all methods. A spatial method was preferred over a numerical method because most spatial methods also collect numerical abundance data during data collection, and a spatial method would allow direct comparison to other spatial methods and also to numerical abundance methods. Spatial abundance rank abundance collected by estimation was selected as the baseline (see Discussion).

Spearman's Rank Correlation and Kendall's Tau (Clarke, 1993; using PAST software from Hammer et al., 2001) were computed for numerical abundance, estimated, and calculated spatial abundance methods to determine changes in rank order among the three methods. The estimation and ArcGIS calculations of spatial abundance ranks were compared to evaluate the difference between the time-intensive calculation methods and field-technique-friendly estimation method.

Spatial abundance methods results were compared to each other and to the spatial map of sclerobiont taxa generated by ArcGIS. One σ and two σ deviations from the expected number of sclerobionts and chi-square tests were also performed to evaluate deviations from the expected number of sclerobionts. The first and last ranked sclerobionts could potentially move up to fifteen positions in their respective rank, but the median taxa could only move seven positions in

either direction. Not every sclerobiont showed two σ deviation rank-order. For the purposes of this research, one σ was considered significant for rank order changes, a change of +/- five positions in rank.

RESULTS

The rank order of the sixteen sclerobionts in order from most to least abundant are provided in Tables 2 and 3.

ArcGIS Method

Rank abundance determined by ArcGIS could not be directly compared to the other methods. Four valve surfaces were omitted from ArcGIS analysis because of their curvature, resulting in the loss of two sclerobiont taxa, bryozoans M3 and M7, from the analysis. A direct comparison in sclerobiont rank abundance between ArcGIS and the estimation method was made by removing data collected on the bryozoan taxa M3 and M7 from the estimation method (Table 2). A per valve comparison of data obtained from ArcGIS and the estimation method was also conducted (Figure 3). There is a clear tendency for the estimation method to overestimate the spatial abundance of sclerobiont taxa, and when five or more sclerobionts are present on a host valve, that overestimation can be significant.

Rank Order Comparisons

Table 2 compares changes in rank order of sclerobiont abundance in numerical and encrustation frequency methods to the baseline estimation method.

Numerical abundance rankings result in change of rank for three sclerobiont taxa: the gumdrop bryozoan M1, which rose in rank abundance, and the sheetlike to branching bryozoan M7 and cystoporid M14, which fell in rank. Three other taxa changed in rank order, but none

significantly. Two small taxa, the gumdrop trepostome M4 and tube-dwelling *Cornulites* rose in rank order. In contrast, the spatially dominant colonial cystoporid bryozoan M6 fell in rank.

The frequency of encrustation method resulted in sclerobiont abundance rankings that deviated nearly forty percent from the baseline. Six sclerobiont taxa showed significant shifts in rank, three positive and three negative. The taxa whose rank changed positively were the small colonial trepostomes M1, M4, and the solitary *Cornulites*. The monticulated trepostome M7, the cystoporid M14, and the inarticulate brachiopods fell in rank. The cystoporid M6 also fell in rank, although not significantly.

Spearman's Rank and Kendall's Tau Correlation were calculated for both the numerical abundance method (rho = -0.09, p = 0.72 and tau = -0.03, p = 0.85) and the encrustation frequency method (rho = -0.4, p = 0.11, tau = -0.28, p = 0.13) as they compared to the baseline. All calculations yielded non-correlation between the different rank order abundances quantified by each method, but none had significant p-values. This is possibly due to the low number of sclerobiont taxa observed on the brachiopods chosen for the study.

Grid Overlays for Assessing Sclerobiont Abundance

The rank abundance of sclerobiont taxa determined by grid overlay methods with six, nine, thirteen, and thirty-two grid regions, and using both previously defined multiple-count and proportional-count methods, are presented in Table 3 and Figure 4. Nine sclerobiont taxa changed rank significantly from the baseline using one or more of the grid overlays. Of these, four taxa were small colonial or solitary sclerobionts (M1, M4, M8, *Cornulites*), three are runner or large colonial sclerobionts (M6, M7, paleotubuliporids, M14), and one displayed a variable morphology (M5). All proportion-count grid overlay methods shifted the small trepostome bryozoan taxon M1 positively, and three of the four shifted the large sheeting trepostome M7,

identified as *Homotrypa*, negatively. Five of the ten grid overlay methods shifted both M1 and M7 significantly in rank order. The sheetlike trepostome M7 only shifted negatively, while the small colonial trepostome M1 primarily shifted positively, in four methods it shifted in rank positively, and only in one shifted negatively.

Of the nine taxa that demonstrated significant rank order shifts using grid overlay methods, six showed significant rank order shifts using the numerical abundance method, as well. Unidentified paleotubuliporid bryozoans, as well as trepostomes M9 and M13 showed results that were consistent in both spatial and numerical abundance methods.

Table 4 shows the number of sclerobiont taxa that changed rank significantly with each grid overlay and counting method. When the multiple count method was applied, all versions of the six-grid overlays, both equally divided and divided into commissure and interarea space, showed similar rank order abundance to the baseline, with only one or two taxa shifting significantly. This result was consistent when the proportion count method was applied to six-grid overlays, as well. When the multiple count method was applied to nine-grid, thirteen-grid, and thirty-two-grid overlays, only slightly more variation in rank order abundance was observed. The proportion-count method resulted in changes in rank order of four or more sclerobionts using grid overlays with more than six sections.

The number of observed sclerobionts in the sample as summed across the grid sections changed from ninety-two to nearly two hundred sclerobionts (Table 5). Numerical abundance recorded one hundred two sclerobionts in the sample. The multiple count method significantly over-reported the number of sclerobionts observed in nine-grid, thirteen-grid, and thirty-two-grid overlays. This is a predictable byproduct of the design of the multiple count method. Regardless

of grid design, proportion-count methods closely matched data obtained with the numerical abundance method.

Preferential Encrustation on Host Valves

The ten combinations of grid overlay design and counting methods were also examined for evidence of more or less encrustation than expected on sections of the host substrate (Figure 5). Sections of the host preferentially encrusted or exhibiting less encrustation than expected were evaluated with two σ deviation from expected levels of encrustation and using chi-squared analysis. Chi-squared analysis and two σ deviation from expected levels reported nearly identical results. However, in two of the ten grid overlay designs, two σ deviation showed significantly more encrustation in a section than expected. This pattern which was not detected with chi-squared analysis. When two significance indicators were not in agreement, the section of the grid being examined was treated as if encrustation were within expected values.

Changes in the design of the grid overlay resulted in changes in reported instances of preferential encrustation of each section (Table 6, Figure 5). Analysis using the evenly divided six-grid overlay with the multiple-count method (Figure 5A) revealed that the central commissure (section 2) was preferentially encrusted and the right commissure (section 3) showed significantly less encrustation than expected. However, a differently designed six-section grid showed different encrustation preferences (Figure 5B). Different counting methods on the same grid overlay designs also significantly altered the reported encrustation in each section (e.g. Figure 5C – 4E).

ArcGIS spatial coverage of sclerobionts on host shells is shown in Figure 5F. The central area of each valve, slightly toward the commissure, was most commonly encrusted. The lateral commissure area was rarely encrusted. The pedicle area was very rarely encrusted. Figure 5F can

be readily compared to the preferentially encrusted or avoided sections reported by each grid overlay method. That the central commissure area exhibits preferred encrustation is in general agreement with the reports of grid overlay and counting methods used to examine the same host valves. Very low encrustation along the lateral commissure surfaces is not well reported by the grid overlay methods. Results from both multiple- and proportional-counting methods, and from evenly and unevenly divided grid overlays with six- and nine- sections reflect the observed lower encrustation in lateral commissure areas.

Using the proportional count method with the thirteen section grid design resulted in greater than expected encrustation in sections 1, 3, and 12, and less encrustation than expected in sections 8 and 10. These results do not agree with other overlays or counting methods. The multiple-count method with the same thirteen-section grid design only showed one instance of more encrustation than expected, in section 13. Neither method yielded encrustation patterns that correlated with those recorded by ArcGIS.

Similarly, the thirty-two section grid design did not reveal encrustation patterns consistent with those recorded with ArcGIS. Although the thirty-two section grid with multiple-count method did support more than expected encrustation along the central commissure sections, but the results suggested that other areas, specifically sections 15 and 21, exhibited less encrustation than expected. Encrustation recorded with ArcGIS showed sclerobiont patterns with encrustation qualitatively at or above what would be expected in those sections. The proportional count method of the thirty-two grid design compounds the differences between ArcGIS and the multiple-count method. Using the method would allow workers to infer that most of the central inter-area exhibit low encrustation, when higher than expected encrustation was recorded by the ArcGIS method.

DISCUSSION

Estimation vs. Calculation

When comparing only the sclerobionts observed with both ArcGIS and estimation, a change in the method produced only one significant change in rank order, a small colonial trepostome M1 (Table 2). M1 ranked seventh with estimation, and when sclerobionts not observed in ArcGIS were omitted from estimation rank order, it ranked fifth. ArcGIS ranked M1 first. Small trepostome M1 was common in the study sample, each individual ranged in size from 2 to 6mm in diameter. M1 generally appeared as the sole, or primary encruster on a host, clustered with other individuals. Estimation requires rounding the percent covered to the nearest integer, resulting in the overestimation of very small M1 colonies. Larger colonies of M1 – though still only around 6mm in diameter – were more likely to be underestimated relative to the size of the host shell. The presence of many, larger M1 colonies in the study sample accounted for the observed underestimation, and subsequent decrease in rank of M1 reported in Table 2. In contrast, the colonial trepostome M8 was generally overestimated but not substantially so, possibly because it was frequently observed with other sclerobiont taxa, which allowed the researcher to easily make proportional size comparisons on the host valve.

Trepostome bryozoans M3 and M7 were not recorded with ArcGIS. These sclerobionts were spatially dominant on the four host brachiopods that were omitted from the ArcGIS study because of the shell convexity, and were not present on other shells used in this study. M3 and M7 ranked fourth and sixth most abundant with estimation, respectively, because they were spatially very dominant on host valves when present, sometimes covering the entirety of the host. Sclerobiont encrustation patterns are dominated by the most abundant sclerobionts, and it is particularly important to consider how using different abundance methods affect the taxa that are

considered most abundant in a sample. Estimation and ArcGIS methods rank the same sclerobiont taxa as the top five most abundant. ArcGIS ranked the five most abundant sclerobionts in the sample as sheetlike cystoporid M6, gumdrop trepostome M2, gumdrop trepostome M1, inarticulate brachiopods, and sheetlike trepostome M5. When the taxa that were not present on hosts examined with ArcGIS (M3 and M7) were omitted, estimation ranked the five most abundant taxa as M6, M2, inarticulate brachiopods, M5, and M1 (Table 2). M5 and M1 changed their relative positions, but the five most abundant sclerobionts taxa remained the same when ranked with either method.

Other research showed that, in the most heavily encrusted samples in the Late Ordovician (Smrecak and Brett, 2014) and Middle Devonian (Smrecak and Brandt, in prep), host valves displayed an average of 2.8 or fewer individual sclerobionts. The estimation method generally overestimated the surface area covered by each sclerobiont, but that this artifact appeared to be significant only when a host was encrusted by more than five sclerobiont individuals (Figure 3). Since encrustation by more than five sclerobionts is not common in Paleozoic sclerobiont assemblages, the relatively quick method of estimating surface area yields results that are statistically consistent with the more precise, time intensive photographic digitization methods like ArcGIS when assessing sclerobiont encrustation spatially.

Collectively, the treatment of sclerobionts by repeatable estimation serves as a reasonable analog for the time-intensive ArcGIS sclerobiont analysis for assessing patterns of individual sclerobiont taxa and for assessing patterns in sclerobiont assemblages as a whole. This is particularly important as there are notable burdens to collecting sclerobiont encrustation data using ArcGIS or other digital photographic methods. First, rarely can a researcher limit host brachiopods to those which exhibit relatively planar, concavo-convex shell shape. Second,

uniserial sclerobionts, including paleotubuliporid bryozoans, hederellids, and auloporid corals, were not easily outlined as polygons in ArcGIS, a prerequisite for this analysis. Taxa that exhibit runner-like patterns branch like tree roots and, sometimes, merge into the path of other runner sclerobionts or back into themselves. Linear patterns like these are most closely replicated in ArcGIS by defining them as line features. In ArcGIS, these features are without spatial dimensions, and therefore cannot be used to calculate surface area. Polygon features in ArcGIS record spatial dimensions needed for surface area calculations but requires the vector points creating the polygon to not cross over themselves. Successfully fitting a polygon to these features required creating numerous smaller polygons, usually fifteen or more for each paleotubuliporid bryozoan. This process was very time-intensive and the results matched observed patterns far less well than other sclerobiont shapes.

Alternatively, researchers using ArcGIS or other digitizing software could choose to outline the widest extent of each uniserial bryozoan or other runner taxon. Arguably, the space between running tendrils of a paleotubuliporid bryozoan is not fully 'available' for encrustation, especially for those taxa which, if successful, would expand over all available surface extending radially from the place where they settled. Outlining the widest extent of uniserial organisms may be a better choice for sclerobiont researchers wishing to use ArcGIS or another similar method, but it inserts the assumption that the entirety of the space in which a runner is found is encrusted. It can also artificially create the impression that spatial competition or overgrowth between multiple organisms is occurring. Solitary sclerobionts were commonly found between branches of uniserial taxa. This occurrence would look like an instance of overgrowth if the widest extent of uniserial taxa was recorded. These interactions could represent sclerobiont-sclerobiont interactions in some way, and the presence of a uniserial taxon in a region of the host

may deter larval settlement in that area, but outlining the widest extent of a uniserial taxon may artificially inflate the appearance of sclerobiont-sclerobiont interactions.

Comparison of Abundance Methods

Numerical abundance methods usually ranked small colonial (e.g. gumdrop morphotype) bryozoans and other solitary taxa highly in terms of rank abundance. Conversely, spatial abundance methods ranked larger colonial, or sheeting, sclerobiont taxa highly, even if only a relative few individuals encrust a large portion of available space. The frequency of encrustation method resulted in changing the rank order of nearly forty percent of sclerobionts from their baseline ranks.

The numerical abundance method resulted in shifts in the rank abundance of three sclerobiont taxa significantly. The cystoporid M14 was rare numerically and spatially. It is unclear if its shift from eleventh to sixteenth, though statistically significant, would affect paleontological interpretations. Sclerobiont taxa that rank low in abundance have shown some interpretive value when they are prevalent in or only found in one particular facies or environment (Brett et al., 2012; Smrecak and Brett, 2014).

The sheetlike trepostome M7, *Homotrypa*, was present only on four valves (see estimation vs. ArcGIS, above), yet it ranked as the sixth most abundant sclerobiont in this sample using spatial abundance. The numerical abundance method ranked M7 as twelfth, a negative shift of six rank positions. Smrecak and Brett (2014) used the abundant M7 as an indicator of shallow water. Had the numerical abundance method been used by Smrecak and Brett (2014), *Homotrypa* would have been interpreted as a rare taxon in all environments. Instead, this sheeting, spatially-dominant taxon was an important indicator of shallow water encrustation patterns and useful in discerning them from moderate environments with significance. Similarly,

numerical abundance ranked M1, a gumdrop trepostome, as the second most abundant taxon in the sample studied herein. This taxon was ubiquitous in Smrecak and Brett (2014), and provided no paleoecological interpretive value.

The frequency of estimation method produced rankings that markedly differed from the baseline. Six of the sixteen taxa changed rank significantly. Inarticulate brachiopods were the only taxon to fall significantly in rank position using the method. They fell from a baseline position in the top five most abundant sclerobionts. The other five sclerobiont taxa increased their rank positions significantly when the frequency of encrustation method was applied. All of these sclerobionts were small colonial or solitary organisms. M1 increased from a rank position of seventh in the baseline to become the most abundant taxon when the frequency of encrustation method was applied. Therefore, frequency of encrustation methods yield sclerobiont rank abundances similar to numerical abundance, usually by significantly inflating the rank of small sclerobiont taxa. Solitary inarticulate brachiopods are the sole exception, being somewhat larger solitary organisms that decrease in rank significantly as evaluated using the frequency of encrustation method (Table 2).

Assessing Grid Overlay Methods – Rank Abundance

Rank abundance of eleven taxa (65% of all sclerobiont taxa) was significantly impacted by at least one of the grid overlay methods. The rank order abundance of the common trepostome bryozoan M1 and the sheeting trepostome M7 changed significantly in every grid overlay and with every counting method. The only other taxon impacted by more than one grid overlay method was M13, a sheet-like to runner trepostome bryozoan. The rank of M13 also shifted negatively in both multiple and proportional count methods. Of the remaining eight taxa, four, all of which were small colonial or gumdrop bryozoans, moved up in rank significantly in

at least one grid overlay. The remaining four taxa, including both large and small bryozoan, fell in rank. The only small taxon to shift negatively in a grid overlay was the cystoporid M8. M8's rank also shifted downward in the ArcGIS calculation, but did not change significantly between spatial and numerical abundance methods.

Most of the significant shifts in rank order were produced by the application of proportion-count methods with more finely divided grid overlay designs. With the multiple-count method, the equally divided six-, thirteen-, and thirty-two-section grid overlay designs each only resulted in one significantly shifted sclerobiont in terms of rank order (Tables 4 and 6). The rank of M1 was significantly shifted in both the six- and nine- section grids; the rank of M8 was significantly shifted only in the thirty-two section grid.

Overall, grid overlays used in concert with the multiple-count method produced eight significant rank shifts, whereas the same grid overlays counted with the proportion-count method produced fourteen significant rank shifts (Table 6). When both multiple- and proportion-counting methods were combined, the six section grid overlay methods, equally and unequally divided sections combined, produced only four significant rank order changes, suggesting that fewer grid sections provide the most accurate results. All more finely divided grid overlays produced at least five significant rank order changes, although using the multiple-count method generally better reflected baseline patterns. In all cases, the six-grid section overlays significantly shifted from the baseline only when another method also showed a significant shift of the same taxon. Six-section grid overlay methods generally better mimicked rank order abundance values reported by the baseline, and multiple-count methods (that is, counting a sclerobiont more than once for every grid section in which it occurs) produced fewer significant deviations from the baseline.

Assessing Grid Overlay Methods – Spatial Patterns on Hosts

Fewer grid sections counted with the multiple-count method yielded results more compatible with the established baseline for rank abundance. However, observed encrustation patterns shown by different grid overlay designs and with different counting methods (Figure 1) were not always in agreement with each other or with encrustation patterns recorded using ArcGIS.

Seven of the ten combined methods showed that the central commissure area was preferentially encrusted, in agreement with observed encrustation patterns in the ArcGIS method. Six of the methods were additionally in agreement, showing that parts of the lateral commissure were avoided. However, four of the six methods suggested that only the right side of the host exhibited less encrustation than expected, which was not well supported by the patterns of encrustation produced by ArcGIS. Almost no encrustation was observed on the left lateral commissure, and no grid overlay method reported the lack of observed encrustation. In fact, the thirteen section grid overlay counted with the proportional counting method suggested that area is preferentially encrusted.

Despite the additional effort required to count sclerobiont encrustation in thirty-two grid overlay methods, the patterns of significantly more- or less- encrusted than expected did not provide the accurate, detailed picture of encrustation that the method was designed to show. Indeed, analyses of preferred encrustation are not better reflections of host/sclerobiont encrustation patterns with thirty-two grid sections than they are with six. Analysis of grid overlay methods for this purpose qualitatively supported the use of unequally divided six section grid overlays to assess preferential encrustation or avoidance of particular regions on the host, but additional refinement of grid design did not correspond to a more accurate, detailed picture of

encrustation patterns on a host. Proportional counting was originally designed to reduce overrepresentation of sclerobionts occurring in more than one section while retaining the ability to
note preferred or avoided areas of the host. The counting method generally increased the
statistical power of the results, providing more preferred or avoided sections than multiple-count
counterparts, but results were usually in direct contrast to those observed with ArcGIS and
multiple-count methods.

Finally, these grid overlays were superimposed on relatively flat host brachiopods, which provided best case scenarios. More globate, biconvex host brachiopods present methodological problems similar to those described for ArcGIS methods, and would further reduce the accuracy of results produced by grid overlays with a higher number of grid sections.

CONCLUSIONS

Sclerobiont abundance can be determined by a count of each sclerobiont taxon or by an assessment of the amount of surface area each sclerobiont taxon occupies on a host. These two methods of assessing sclerobiont encrustation yielded similar rank. Ranking of two of the top three ranked taxa differed between the methods. Frequency of encrustation yielded results in which up to forty percent of taxa rank differently in abundance when compared to numerical and spatial abundance methods. Both numerical abundance and frequency of encrustation shifted taxa predictably, rank order of common small colonial gumdrop bryozoans and solitary organisms increased, while the rank order of spatially dominant bryozoans decreased.

Grid overlay methods for assessing relative abundance differ in the coarseness of the sampled grid size. Fewer partitioned sections in grid overlays generally better reflected sclerobiont abundance as assessed by numerical abundance using the multiple-count method.

Analyses using grid overlays with fewer sections and the proportion-count method predictably

better reflected relative abundance values, as the more grid sections in the overlay design, the more likely a sclerobiont will occur in more than one section. Grid overlay designs, regardless of counting method, generally produced rank orders similar to those seen with numerical abundance or frequency of encrustation, but not to areal abundance methods.

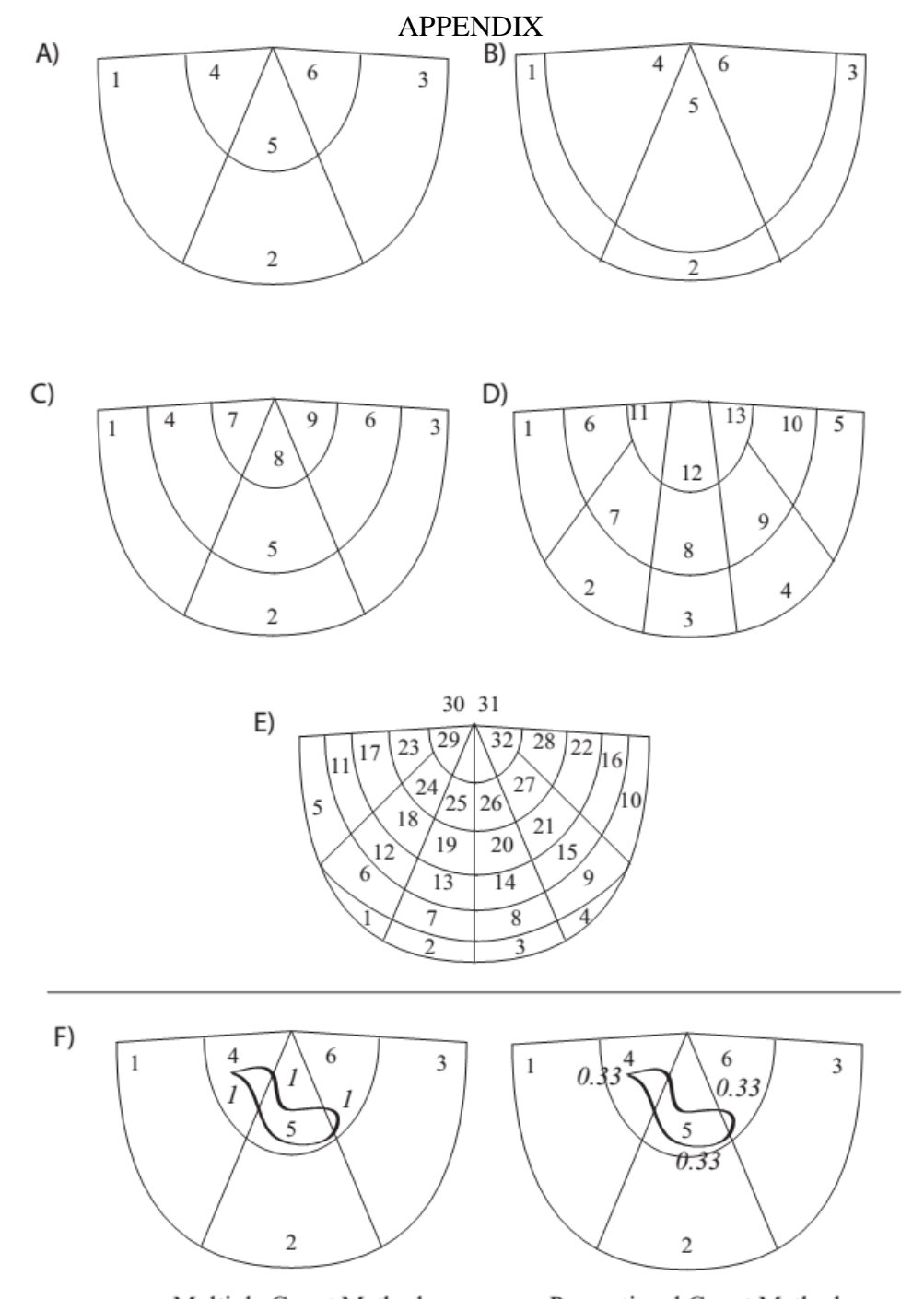
Spatial patterns of sclerobiont distribution were more precisely recorded using outlines of sclerobionts photographed and digitized using ArcGIS software. ArcGIS also accurately reflected areal percent coverage, or spatial abundance. However, an experienced researcher can estimate spatial abundance with similar accuracy for easy field censusing and the ability to conduct meaningful spatial assessments on host shells with varied surface relief. Spatial patterns determined by different grid overlay methods differed from each other and with the results obtained through ArcGIS analysis.

Despite the intuitive conclusion that more finely partitioned grids would result in more precise spatial encrustation pattern data, the most finely divided grid overlays produced results inconsistent with those observed by other methods. Abundance and location data gathered on 6-section grids compared well with baseline patterns observed. Generally, use of grids with fewer sections, together with the multiple-counting method, best approximated the baseline patterns in both sclerobiont assemblage and location data.

More finely divided grid partitions produced more sections which were statistically significantly preferred or avoided. Thirteen-section grid overlays showed fewer preferred or avoided sections than thirty-two-sectioned grids. Use of grids with fewer sections in a grid overlay, combined with the multiple-count method, best approximated the baseline spatial encrustation patterns defined using ArcGIS, even though fewer grid sections examined reduces the number of sections statistically preferred or avoided.

Estimating sclerobiont spatial coverage and counting the number of each sclerobiont taxon present on a host can be used in concert to address abundance in terms of biomass or community importance (spatial) and larval settlement (numerical). When the identities of the sclerobiont taxa are known, attempts to interpret across the methods may be permitted. A law of diminishing returns applies to using grid overlays, as more finely divided grids do not guarantee more precision in characterizing sclerobiont coverage. Spatial sclerobiont patterns are most precisely obtained using ArcGIS software or another image analyzing software, but this method is best applied to host shells with low relief. Grid overlay designs with minimal partitioning provide the closest approximation of patterns recorded using ArcGIS. Understanding how sclerobiont encrustation patterns are characterized by the methods analyzed herein, and the biases inherent to each, allows more highly resolved interpretations among published sclerobiont studies, and promotes more consistent approaches to sclerobiont analysis. Ultimately, a range of methods may still remain useful to researchers for answering particular paleontological questions, but it is important to ensure the chosen method is accurately reporting the patterns with which it was tasked. Understanding how sclerobiont encrustation patterns are characterized by the methods herein, and the biases inherent to each, allows more highly resolved interpretations among published sclerobiont studies and promotes more consistent approaches to sclerobiont analysis.

APPENDIX



Multiple Count Method Proportional Count Method FIGURE 1 – *Grid overlay designs and counting methods*. A) six section equally divided grid. B) Six section unequally divided grid. C) Nine section grid. D) Thirteen section grid. E) Thirty-two section grid. F) Counting sclerobiont occurrences with the multiple count and proportion count method.



FIGURE 2 – *Idealized line diagram*. Line diagram and image of *Rafinesquina* showing location of sclerobionts present.

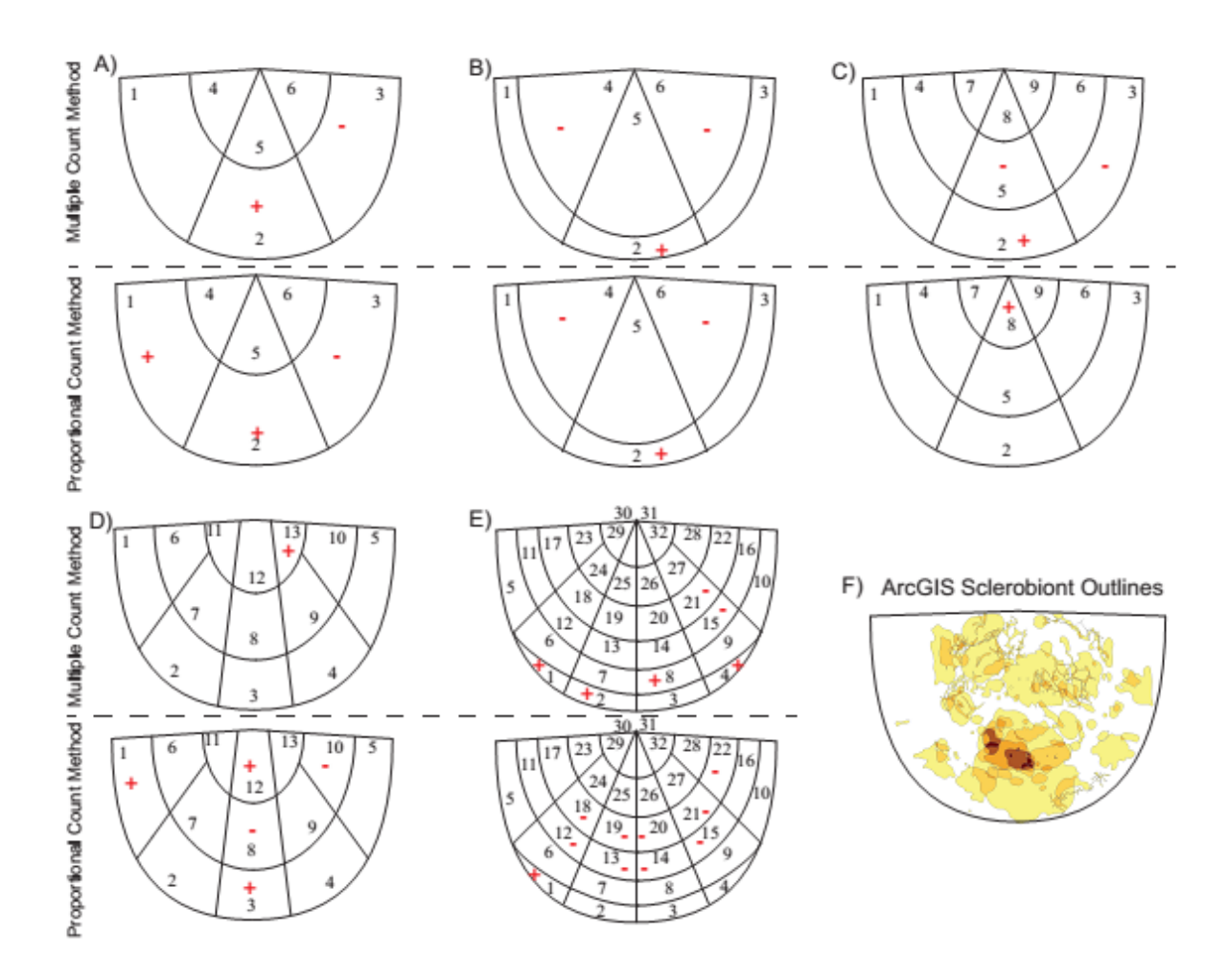


FIGURE 3 – *Counting methods and grid overlay design comparisons*. Comparison of proportion- and multiple- count methods on grid overlay designs. (+) and (-) denote grids that have significantly more or fewer sclerobiont individuals present than expected.

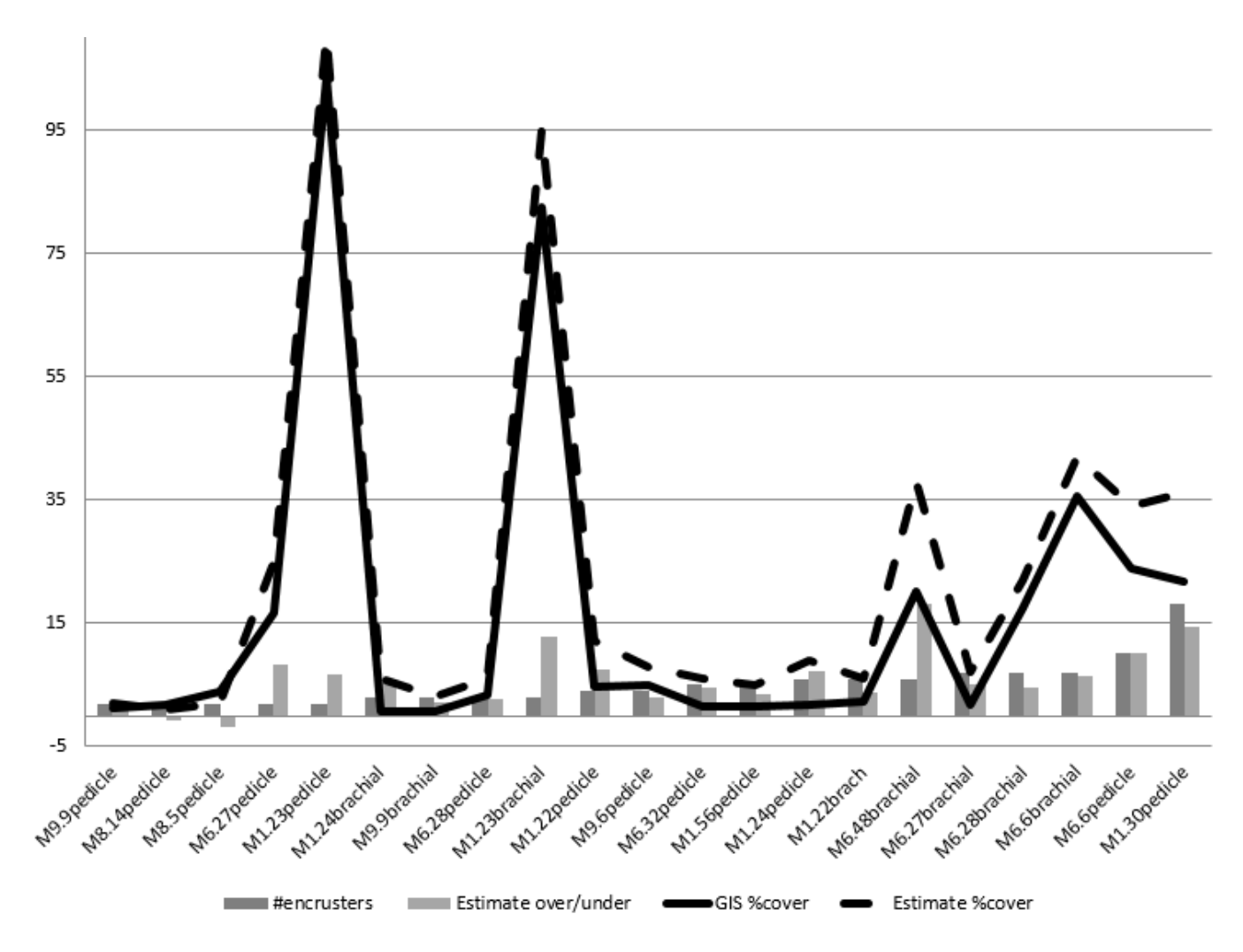


FIGURE 4 – *Change in rank order using ArcGIS and visual estimation methods.* Tracked change in rank of the nine sclerobiont taxa (Y axis) that shifted significantly in rank from baseline when a different method (X axis) was applied.

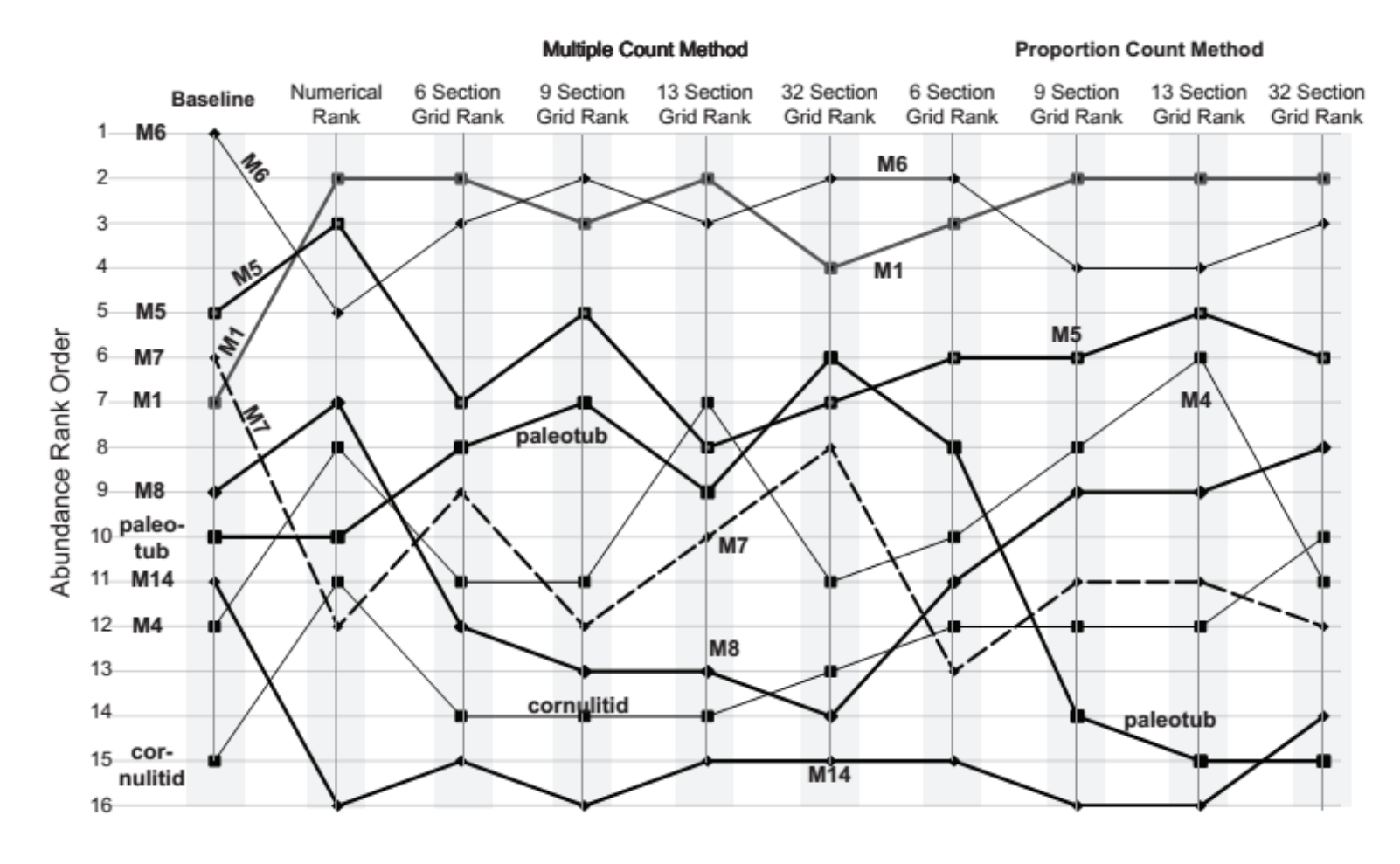


FIGURE 5 – *Changes in rank order of each sclerobiont taxon*. Comparison of data produced with ArcGIS to estimated data for the same 21 brachiopod valves. X axis organized in order of number of sclerobionts present on host from lower to higher. Deviation between estimate and calculated areal coverage changes increases with number of observed sclerobionts, excepting heavily encrusted (<75%) host valves. Average number of sclerobionts per *Rafinesquina* in the region is 2.8 (Smrecak and Brett, 2014).

Sclerobiont Encrustation	
Metric	Metric Description
Areal Percent Coverage	The percentage of host shell surface covered by the sclerobiont(s).
Relative Abundance	The number of individuals or colonies of sclerobionts present.
Sample Richness	The number of encrusting taxa observed in a sample.
Richness Ratio	The number of sclerobiont taxa observed in a sample/total number of sclerobiont taxa observed in basin or study region.
Frequency of Encrustation	The number of host shells encrusted/total number of shells observed.
Maximum Per Host Richness	The highest number of sclerobiont taxa observed on an individual host shell substrate
Average Per Host Richness	The average number of sclerobiont taxa on an individual host shell substrate in a sample

TABLE 1 – *Commonly applied sclerobiont encrustation methods*. Brief description of commonly applied sclerobiont encrustation methods examined in this study.

		Baseline	Numerical Abundance	Frequency of Encrustation
	M6	1	5	5
	M2	2	1	2
	inarticulate brachiopod	3	6	8
аха	M3	4	4	4
Rank Order of Sclerobiont Taxa	M5	5	3	3
ion	M7	6	12	11
rok	M1	7	2	1
cle	Cuffeyella	8	9	9
of S	M8	9	7	6
er	unid. paleotubuliporid	10	10	13
Ord	M14	11	16	16
사 (M4	12	8	7
Rai	unidentified bryozoan	13	14	14
	M13	14	13	12
	Cornulitids	15	11	10
	microconchid	16	15	15

TABLE 2 – *Rank order of sclerobiont taxa*. Rank abundance of sixteen sclerobiont taxa determined by different methods. ** indicates taxon that was not observed with method.

						Grid Overl	d Overlay Designs							
			Multip	ole Count M	ethod		Proportion Count Method							
	녿	6 section	6 section				6 section	6 section						
Baseline Rank Order	Rai	(equal)	(unequal)	9 section	13 section	32 section	(equal)	(unequal)	9 section	13 section	32 section			
M6	1	1	-1	1	1	3	1	1	1	1	1			
M2	2	**5	1	-1	**5	-1	**5	5	**5	**5	**5			
inarticulate brach	3	-2	*-4	*4	-2	1	-2	1	1	1	1			
M3	4	0	0	0	0	3	0	-3	-3	-3	-3			
M5	5	-2	2	-2	3	-2	-2	-2	-2	0	-2			
M7	6	2	1	-1	-3	*4	-1	-1	-1	**6	-1			
M1	7	-2	-1	3	**5	-2	1	1	1	*-4	1			
Cuffeyella	8	2	-2	0	-3	-2	*4	4	*4	0	1			
M8	9	-3	*-4	*4	1	-1	0	0	0	0	*/			
unid paleotubuliporid	10	3	-2	*4	*-4	3	3	3	3	3	**5			
M14	11	1	2	1	2	1	*4	-5	**-5	**-5	1			
M4	12	-3	-3	**-6	2	2	-2	3	3	3	**-6			
UNID BRYO	13	1	**7	*-4	*-4	2	**-7	1	1	-3	*/			
M13 (spider)	14	1	0	1	**-5	**-5	0	3	*-4	0	C			
Cornulites	15	*-4	*4	1	*-4	*-4	*-4	-4	1	*-4	*-4			
microconch	16	0	0	**-5	0	0	0	0	-1	1	**-6			

TABLE 3 – *Rank order of sclerobiont taxa using various grid overlay methods*. Change in rank abundance of sclerobionts with varied grid overlay design and counting methods. Baseline is rank order abundance as determined by estimation. Significant changes in rank (5+ positions) are denoted by **. A change in rank of 4 positions is denoted by *. Positive values indicate an increase in rank as compared to the baseline rank position, negative values indicate a decrease in rank position

				Grid Overlay Methods								Baseline vs. Numerical		Baseline vs. Frequency of Encrustation	
				Multiple	ole Count Pro		Proportional Count #		#Shifts Experienced By All Gri						
Taxa with 1+			spatial	#times shifted	#times shifted	#times shifted	#times shifted	Total	Total	Total # Rank		Significant Shift		Significant Shift	
Significant Rank		Higher Order	morphology:	positively from	negatively from	positively from	negatively from	significant significant Shifts (8			Between Baseline and Shift		Between Baseline and Shift		
Shifts	Taxon Category	Identification	small/large	baseline	baseline	baseline	baseline	positive shifts	negative shift	s possible)		Numerical Method?	Direction?	Frequency Method?	Direction?
M1	gumdrop	trepostome	small	0	1	4	0	4	1	1 5	i	yes	down	yes	up
M4	gumdrop	trepostome	small	0	0	1	0	1	. (0 1	L	yes	down	yes	up
M5	gumdrop	trepostome	small	1	0	0	0	1	. (0 1		no	down	no	up
M6	gumdrop	cystoporid	small	1	0	0	0	1	. (0 1	L	yes	up	no	no change
M7	sheeting	trepostome	large	0	2	0	3	0	!	5 5	i	yes	up	yes	down
MB	gumdrop	cystoporid	small	0	1	0	0	0	1	1		no	up	no	up
M13	sheeting/runner	trepostome	large	0	1	0	2	0		3 3		no	down	no	up
M14	sheeting	cystoporid	large	0	1	0	0	0	1	1 1		yes	up	yes	down
Cornulites	n/a	n/a	small	0	0	1	0	1	. (0 1		yes	down	yes	up
paleotubuliporids	running	paleotubuliporid	large	0	0	0	1	0		1 1		no	no change	no	down

TABLE 4 – *Number and direction of significant rank order shifts with each method.* Description of each sclerobiont taxon shifted significantly by one or more applied method. Number and direction of significant shifts by each method is provided.

		Method Used	Number of Sclerobionts Observed with Method
+		6 section unequal	127
Proportion Count Multiple Coun	Method	6 section equal	128
le C	Me	9 section	142
ltip	1	13 section	146
Mu		32 section	191
unt		6 section unequal	101.99
CC	Method	6 section equal	97.02
tion	Me	9 section	100.94
odo	1	13 section	94.951
Pro		32 section	99.78
		Number of Sclerobionts Observed in Study	102

TABLE 5 – *Number of sclerobionts recorded using each method.* Number of observed sclerobionts in the studied sample when tallied using each sclerobiont encrustation method. Actual number of observed sclerobiont individuals was 102. Significantly different values in bold.

REFERENCES

REFERENCES

- ABERHAN, M., KIESSLING, W., AND FURSICH, F.T., 2014, Testing the role of biological interactions in the evolution of mid-Mesozoic marine benthic ecosystems: Paleobiology, v. 32(2), p. 259-277.
- ALEXANDER, R.R. AND SCHARPF, C.D., 1990, Epizoans on Late Ordovician brachiopods from southeastern Indiana: Historical Biology, v. 4, p. 179-202.
- ALVAREZ, F. AND TAYLOR, P.D., 1987, Epizoan ecology and interactions in the Devonian of Spain: Palaeogeography, Palaeoclimatology, Paaeoecology, v. 61, p. 17-31.
- BARRINGER, J.E., 2008, Analysis of the occurrence of microconchids on Middle Devonian brachiopods from the Michigan Basin: implications for microconchid and brachiopod autecology: unpublished M.S. thesis, Michigan State University, 117 p.
- BISHOP, J.D.D., 1988, Disarticulated bivalve shells as substrates for encrustation by the bryozoan *Cribrilina puncturata* in the Plio-Pleistocene Red Crag of eastern England: Palaeontology, v. 31(2), p. 237-253.
- BORDEAUX, Y.L., and BRETT, C.E., 1990, Medium specific associations of epibionts on Middle Devonian brachiopods: implications for paleoecology: Historical Biology, v. 4, p. 203-220.
- BOSE, R., SCHNEIDER, C., POLLY, P.D., and YACOBUCCI, M.M., 2010, Ecological interactions between *Rhipidomella* (Orthides, Brachiopoda) and its endoskeletobionts and predators from the Middle Devonian Dundee Formation of Ohio, United States: Palaios, v. 25(3), p. 196-208.
- BOSE, R., SCHNEIDER, C.L., LEIGHTON, L.R., AND POLLY, P.D., 2011, Influence of atrypid morphological shape on Devonian episkeletobiont assemblages from the lower Genshaw formation of the Traverse Group of Michigan: A geometric morphometric approach: Palaeogeography, Palaeoclimatology, Palaeoecology, v. 310, p. 427-441.
- BRANDT, D.S., 1996, Epizoans on *Flexicalymene* (Trilobita) and implications for trilobite paleoecology: Journal of Paleontology, v. 70, p. 442-449.
- Brett, C.E., Parsons-Hubbard, K., Walker, S.E., Ferguson, C., Powell, E.N., Staff, G., Ashton-Alcox, K.A., and Raymond, A., 2011, Gradients and patterns of sclerobionts on experimentally deployed bivalve shells: Synopsis of bathymetric and temporal trends on a decadal time scale: Palaeogeography, Palaeoclimatology, Palaeoecology, v. 312, p. 278-304.

- BRETT, C.E., SMRECAK, T., Parsons-Hubbard, K.M., and WALKER, S.E., 2012, Marine sclerobiofacies: Encrusting communities on shells through time and space, *in* Talent, J., ed., Global Biodiversity, Extinction Intervals and Biogeographic Perturbations through Time, UNESCO/International Year of Planet Earth Special Volume, p. 129-155.
- CLARKE, K.R., 1993, Non-parametric multivariate analyses of changes in community structure: Australian Journal of Ecology, v. 18(1), p.117-143.
- FREEMAN, R.L., DATTILO, B.F., MORSE, A., BLAIR, A., FELTON, S., AND POJETA, J.J., 2012, Using taphonomy to reconstruct paleoecological succession and taphonomic feedback in a Cincinnatian (Ordovician, Ohio) storm-disturbed shell bed: Geological Society of America, Abstracts with Programs, v. 44(7), 273 p.
- HAMMER, O., HARPER, D.A.T., and RYAN, P.D., 2001, PAST: Paleontological statistics software package for education and data analysis: Palaeontological Electronica, vol.4 (1): 9 p.
- KESLING, R.V., HOARE, R.D., SPARKS, D.K., 1980, Epizoans of the Middle Devonian brachiopod *Paraspirifer bownockeri*: their relationships to one another and to their host: Journal of Paleontology, v. 54(6), p. 1141-1154.
- KEY, M.M., JEFFRIES, W.B., VORIS, H.K., AND YANG, C.M., 2000, Bryozoan fouling patterns on the horseshoe crab *Tachypleus gigas* (Muller) from Singapore: Proceedings of the 11th International Bryozoology Association Conference, p. 265-271.
- KRAUSE, R.A., Jr., BARBOUR WOOD, S.L., KOWALEWSKI, M., KAUAN, D., ROMANEK, C.S. SIMOES, M.G., and WEHMILLER, J.F., 2010, Quantitative comparisons and models of time averaging in bivalve and brachiopod shell accumulations: Paleobiology, v. 36, p. 304-320.
- LIDDELL, W.D., AND BRETT, C.E., 1982, Skeletal overgrowths among epizoans from the Silurian (Wenlockian) Waldron Shale: Paleobiology, v. 8, p. 67-78.
- LIDGARD, S. AND JACKSON, J.B.C., 1989, Growth in encrusting cheilostone bryozoans: I. Evolutionary trends: Paleobiology, v. 15(3), p. 255-282.
- LESCINSKY, H.L., 1993, Taphonomy and paleoecology of epibionts on the scallops *Chlamys hastate* (Sowerby 1843) and *Chlamys rubida* (Hinds 1845): Palaios, v.8, p. 267-277.
- LESCINSKY, H.L., 1995, The life orientation of concavo-convex brachiopods: overturning the paradigm: Paleobiology, v. 21, p. 520-551.
- LESCINSKY, H.L., 1997, Epibiont communities: recruitment and competition on North American carboniferous brachiopods: Journal of Paleontology, v. 71, p. 34-53.

- LESCINSKY, H.L., EDINGER, E., and RISK, M.J., 2002, Mollusc shell encrustation and bioerosion rates in a modern epeiric sea: taphonomy experiments in the Java Sea, Indonesia: Palaios, v. 17, p. 171-191.
- MCKINNEY, F.K., 1995, Taphonomic effects and preserved overgrowth relationships among encrusting marine organisms: Palaios, v. 10, p. 279-282.
- MCKINNEY, F.K., 2007, The Northern Adriatic Ecosystem: deep time in a shallow sea: Columbia University Press, New York, 227 p.
- MISTIAEN, B., BRICE, D., ZAPALSKI, M.K., and LOONES, C., 2012, Brachiopods and their auloporid epibionts in the Devonian of Boulonnais (France): Comparison with other associations globally, *in* Talent, J., ed., Global Biodiversity, Extinction Intervals and Biogeographic Perturbations through Time, UNESCO/International Year of Planet Earth Special Volume, p. 159-189.
- NEBELSICK, J.H., 1996, Encrustation of small substrates in Tertiary limestones and their importance for carbonate sedimentation, *in* Reitner, J. Neuweiler, and Gunkel, F. (eds.): Global and regional controls on biogenic sedimentation. I. Reef Evolution, Gottinger Arbeiten zur Geologie und Palaontolgie, Geologische Institute, Gottingen, p. 161-167.
- NEBELSICK, J.H., SCHMID, B., and STACHOWITSCH, M., 2007, The encrustation of fossil and recent sea-urchin tests: ecological and taphonomic significance: Lethaia, v. 30, p. 271-284.
- PITRAT, C.W. AND ROGERS, F.S., 1978, *Spinocyrtia* and its epibionts in the Traverse Group (Devonian) of Michigan: Journal of Paleontology, 52(6), p. 1315-1324.
- POWELL, E.N., STAFF, G.M., CALLENDER, W.R., ASHTON-ALCOX, K.A., BRETT, C.E., PARSONS-HUBBARD, K.M., WALKER, S.E., and RAYMOND, A., 2011, The influence of molluscan taxon on taphofacies development over a broad range of environments of preservation, the SSETI experience: Palaeogeography, Palaeoclimatology, Palaeoecology, v. 312, p. 233-264.
- RICHARDS, R.P., 1972, Autecology of Richmondian brachiopods (Late Ordovician of Indiana and Ohio): Journal of Paleontology, v. 46, p. 386-405.
- RODLAND, D.L., KOWALEWSKI, M., CARROLL, M., and SIMOES, M.G., 2004, Colonization of a 'Lost World': Encrustation Patterns in Modern Subtropical Brachiopod Assemblages: Palaios, v. 19, p. 381-395.
- RODLAND, D.L., SIMOES, M.G., KRAUSE, R.A., AND KOWALEWSKI, M., 2014, Stowing away on ships that pass in the night: sclerobiont assemblages on individually dated bivalve and brachiopod shells from a subtropical shelf: Palaios, v. 29, 170-183.

- RODRIGUES, S.C., 2007, Biotic interactions recorded in shells of recent rhynchonelliform brachiopods from San Juan Island, USA: Journal of Shellfish Research, v. 26(1), p. 241-252.
- SCHNEIDER, C.L., 2003, Hitchhiking on Pennsylvanian echinoids: epibionts on Archaeocidaris: Palaios, v. 18, p.435-444.
- SHROAT-LEWIS, R., MCKINNEY, M.L., BRETT, C.E., MEYER, D.L., SUMRALL, C.D., 2011, Paleoecologic assessment of an edrioasteroid (*Echinodermata*) encrusted hardground from the upper Ordovician (Maysvillian) Bellevue Member, Maysville, KY: Palaios, v. 26(8), p. 470-483.
- SMRECAK, T.A., AND BRETT, C.E., 2014, Establishing patterns in sclerobiont distribution in a Late Ordovician (Cincinnatian) depth gradient: toward a sclerobiofacies model Palaios, v. 19, p. 381-395.
- SPARKS, D.K., HOARE, R.D., KESLING, R.V., 1980, Epizoans on the brachiopod *Paraspirifer bownockeri* (Stewart) from the Middle Devonian of Ohio: Museum of Paleontology, The University of Michigan, Ann Arbor, MI, 105 p.
- TAYLOR, P.D., 1990, Preservation of soft-bodied and other organisms by bioimmuration a review: Palaeontology, v. 33, p. 1-17.
- TAYLOR, P.D. and WILSON, M.A., 2002, A new terminology for marine organisms inhabiting hard media: Palaios, v. 17(5), p. 522-525.
- TAYLOR, P.D., AND WILSON, M.A., 2003, Paleoecology and evolution of marine hard substrate communities: Earth-Science Reviews, v. 62, p. 1-103.
- THAYER, C.W., 1974, Substrate specificity of Devonian epizoa: Journal of Paleontology, v. 48(5), p. 881-894.
- WALKER, S.E. AND MILLER III, W., 1992, Organism-substrate relations: toward a logical terminology: Palaios, v. 1, p. 65-74.
- ZATON, M. AND BORSZCZ, T., 2012, Encrustation patterns on post-extinction early Famennian (Late Devonian) brachiopods from Russia: Historical Biology, p. 1-12.

CHAPTER 2: SCLEROBIONT ENCRUSTATION PATTERNS IN THE MIDDLE DEVONIAN MICHIGAN BASIN: CHARACTERIZATIONS WITH DEPTH

ABSTRACT

Sclerobiont encrustation patterns successfully record differences in paleodepth in the Middle Devonian Michigan Basin. Documented using a series of metrics including areal percent cover, relative abundance, richness, encrustation frequency, and taxonomic composition and independently verified with sequence stratigraphy and biofacies analysis, sclerobiont assemblages displayed predictable patterns. Three brachiopod host taxa - *Athyris, Pseudoatrypa*, and *Strophodonta* - exhibited similar encrustation in shallow facies, but sclerobiont encrustation was dampened when *Mucrospirifer* and *Devonochonetes* host valves were used. In deep water facies all brachiopods exhibited similar encrustation. Declines in all measured encrustation metrics, many significant, were observed with depth.

Taxonomically, shallow facies were dominated by encrusting foraminifera, *Ascodictyon*, and *Allonema*. Moderate facies were characterized by trepostome and cystoporate bryozoans.

Trepostome bryozoans dominate in deep environments, accounting for more than double the encrusted area of any other type of sclerobiont in deep water facies. The use of a variety of brachiopod host species is not ideal in assessing encrustation patterns, but sclerobiont assemblages are robust, especially in deeper facies, and can still successfully distinguish changes in relative depth.

INTRODUCTION

Sclerobionts, organisms that encrust both live and dead host shells, are preserved as *in situ*, autochthonous communities (Taylor and Wilson, 2002) and are therefore of great value in paleoecological studies. As such, studies shifted from use primarily in host autecological, host-sclerobiont relationship, and descriptive studies in the 1970s and 1980s (Richards, 1972; Hurst, 1974; Thayer, 1974; Pitrat and Rogers, 1978; Kesling et al., 1980; Spjeldnaes, 1984; references

in Taylor and Wilson, 2002; Wei-Haas et al., 2011) toward paleoenvironmental reconstructions. Sclerobionts are notably impacted by water depth and energy levels, and many researchers posit that sclerobiont assemblages are sensitive to changes in nutrient availability and sedimentation (Lescinsky et al. 2002; Mistiaen et al. 2012; Smrecak and Brett, 2014). Because of their fidelity as preserved communities, sclerobionts have been applied in paleoecological, (Alexander and Sharpf, 1990; Bordeaux and Brett, 1990; Martindale, 1992; Lescinsky, 1997; Bosellini and Papazzoni, 2003; Rodland et al., 2004; Bose et al., 2010; Shroat-Lewis et al., 2010; Brett et al., 2011; Brett et al., 2012; Mistiaen et al., 2012; Richardson-White and Walker, 2012; Zaton and Borszcz, 2012), taphonomic fidelity (Lescinsky, 1993, 1995; McKinney, 1995; Tomasovych et al., 2006; Krause et al., 2010), and comparative taphonomy studies (Brett, 1995; Nebelsick et al., 2007; Lescinsky et al., 2002; Rodrigues, et al., 2008; Brett et al., 2011; Powell et al., 2011).

These studies provided insight into sclerobiont patterns, but results have yielded differing interpretations. In particular, studies differ in the degree to which sclerobionts exhibit host preference according to size or morphologic features, whether hosts might be living or dead during time of encrustation, and to what extent researchers can be confident in sclerobiont and host community fidelity (Tomasovych and Zuschin; 2009; Rodland et al., 2014; Furlong and McRoberts, 2014).

Despite varied accounts of host/sclerobiont relationships and the taphonomic processes working to reduce sclerobiont assemblage fidelity, workers have had success correlating sclerobiont encrustation and paleoenvironmental conditions in Ordovician, Devonian, and modern environments (Alexander and Sharpf, 1990; Bordeaux and Brett, 1990; Lescinsky, et al., 2002; Mistiaen, et al., 2012; Rodland, et al., 2004; Smrecak and Brett, 2014; Walker, et al., 1998; Brett, et al., 2011; Walker, et al., 2011; and see discussion in Brett, et al., 2012). In particular,

Smrecak and Brett (2014) established that suites of sclerobionts could successfully characterize a late Ordovician depth gradient using areal percent coverage. These sclerobiofacies appeared consistent in case studies through to modern examples (Brett et al., 2012). The patterns discerned have been sometimes contradictory, in part due to the noted difficulties above, but also perhaps as a result of methodological differences used to collect sclerobiont encrustation patterns (refer to Chapter 1).

Methods used to analyze sclerobiont encrustation in these and other studies vary widely, inhibiting useful synthesis among temporally constrained studies in different geographic provinces, and in studies across geologic time (Rodland et al., 2014; refer to Chapter 1). Understandably so, as research objectives associated with sclerobionts vary widely, and particular sclerobiont taxa have been called upon to answer questions of taphonomic history and a wide range of whole organisms' autecologies. Analyses have been derived from sclerobiont presence/absence data (e.g. Pitrat and Rogers, 1978), from counts of sclerobiont taxa on each valve or shell (e.g. Bordeaux and Brett, 1990; Thayer, 1974; Mistiaen et al., 2012), and from counting presence of sclerobionts in each of several regions on a host (e.g. Kesling et al., 1980; Sparks et al., 1980; Bishop, 1988; Barringer, 2008; Bose et al., 2010; Shroat-Lewis et al., 2011; Furlong and McRoberts, 2014). Not all studies record the identification of sclerobiont taxa; this further reduces the ability to correlate diversity measures like richness and evenness across studies. Work herein examines sclerobiont assemblages on the eastern margin of the Middle Devonian Michigan Basin along a depth gradient approximated by sequence stratigraphic analysis (Bartholomew et al., 2006) and biofacies analysis (Bartholomew and Brett, 2007; Zambito, 2013), and using a variety of host brachiopods common to the region that are likely to exhibit some degree of sclerobiont encrustation.

Geological Setting

The Michigan Basin began forming as a structural, intracratonic basin in the late Silurian with continued subsidence through the Middle Devonian (Howell and VanderPluijm 1999; Wylie and Huntoon, 2003). Outcrops in the Michigan Basin are uncommon, occurring primarily in quarries, shoreline bluffs, and in drainage exposures along the northeastern and northwestern portions of the northern Lower Peninsula of Michigan. Facies deposited in the Middle Devonian Michigan Basin are also exposed by the Findlay Arch complex on the eastern margin of the basin in Ontario, CA (Bartholomew and Brett, 2007). Most stratigraphic units, although well studied, have been described and characterized by subsurface core analysis (Milstein 1987; Zambito, 2013), and by gamma ray analysis (Wylie and Huntoon, 2003). Lithologies in the Middle Devonian Michigan Basin consist primarily of carbonates and shales that were deposited in shallow water in a subsiding marine carbonate shelf (Kesling et al 1974; Milstein 1987) under semi-arid climatic conditions (Howell and VanderPluijm 1999, Scotese, 2003).

Recent work by Bartholomew et al. (2006) and Bartholomew and Brett (2007) has successfully correlated stratigraphic and biostratigraphic units and in the Michigan Basin with the concurrently deposited units of the Appalachian Basin located across central New York. In particular, Bartholomew and Brett (2007) discerned that member and sub-member scale units reflect third and fourth order, eustatically-driven stratigraphic sequences, and that these that can be traced laterally from the Appalachian Basin. Thus, Michigan Basin deposits are considered extreme distal components of Appalachian Basin sediment packages deposited syonrogenically from Acadian tectonic activity to the modern-day east. The arch complex separating the two basins was not present during the Middle Devonian. Faunal composition supports this argument (Bartholomew et al., 2006). Units in the Michigan Basin are more carbonate-rich and condensed

than their argillaceous corollary facies in the Appalachian Basin (Bartholomew and Brett, 2007). The terriginous source for incoming clastic material in both basins was the second pulse of tectonic activity associated with the Acadian orogenic belt, located along an approximately north-south line at the meridian of present-day Albany, NY (Ettensohn 2008).

Sclerobiont encrustation has been observed in both basins (e.g. Bordeaux and Brett, 1990; Kesling et al., 1980). Higher rates of sedimentation are thought to negatively impact sclerobiont encrustation (Mistiaen et al., 2012) because larval settlement could be deterred by sediment-covered hosts, and because filter feeding organisms are negatively impacted by turbidity. It has also recently been found that sediment composition impacts host presence in the modern (Rodland et al., 2014) and may also impact sclerobiont abundance (Mistiaen et al., 2012), as some sclerobionts are only found when the sediment has a higher concentration of carbonate. Because the Michigan Basin is more carbonate rich and had a generally low sediment input, it is an appropriate basin to test the potential for establishing sclerobiont facies in the Middle Devonian.

METHODS

Sclerobiont specimens were examined in eleven Middle Devonian samples collected from eastern Michigan Basin localities in the northeast Lower Peninsula of Michigan, northern Ohio, and near Thedford, Ontario, CA (Figure 6). Localities in northern Ohio and Ontario form a border between the Michigan and Appalachian bioprovinces, and biofacies analysis reports that these units are compositionally similar to those observed in the Appalachian Basin despite their geographic proximity to the Michigan Basin (Bartholomew and Brett, 2007).

Samples were obtained from museum collections at the University of Michigan Museum of Paleontology (UMMP) in Ann Arbor, MI, and from the Baird and Brett collection at the

Paleontological Research Institution (PRI) in Ithaca, NY. PRI's Baird and Brett Collection is a biostratigraphic representative collection of isolated horizons. This collection was intentionally done to preserve characteristic richness, evenness, and diversity of each sampled horizon. Whole and nearly whole brachiopods were obtained from within these samples, and a limited selection of brachiopod genera were chosen based upon the potential for encrustation and the commonality of the brachiopod within the museum sample. Visual inspection of specimens for sclerobionts was deliberately not done during sample selection to prevent sampling bias. UMMP samples Museum were chosen from taxonomic collections of well-preserved brachiopods with large lot sizes. Each sample had associated high quality locality information. Again, whole and nearly whole brachiopods were selected without regard for presence of encrusters, although effort was made to avoid heavily abraded hosts.

Thirty-to-sixty relatively whole, articulated brachiopods were randomly chosen to mitigate any potential unknown bias from the original collector or from the authors. Efforts were made to ensure the original collection did not 1) focus upon obtaining pristine brachiopod samples, and so included brachiopods exhibiting different degrees of taphonomic degradation, or 2) showcase exemplar encrustation and include only brachiopod hosts with a large portion of the surface encrusted. The author successfully avoided instances of the latter by using bulk lots of the brachiopod host studied. Despite the presence of less well-preserved brachiopods in a lot, it was not always possible to ensure that the original collection did not intentionally omit encrusted brachiopods. However, any collecting bias resulting from the intentional omission of encrusted brachiopods in a museum sample would serve to mute trends observed in this research.

Therefore, museum samples used herein can be considered conservative reflections of the actual sclerobiont patterns at the sampled localities. Relative depths for each sample were estimated

using the stratigraphic information associated with each collection. A relative depth zonation of shallow, moderate, or deep - collectively referred to herein as shallow water samples (SWS), moderate water samples (MWS) and deep water samples (DWS) - was assigned to each sample using a combination of interpreted sequence and biostratigraphic information (Wylie and Huntoon, 2003; Bartholomew et al., 2006; Bartholomew and Brett, 2007).

Brachiopod host genera obtained from this study were primarily *Athyris*, *Atrypa*, *Pseudoatrypa*, and *Strophodonta*, although *Mucrospirifer* and *Devonochonetes* were used or supplemented in samples when not enough host brachiopods of other taxa were found. These lesser-used taxa were included more commonly in samples obtained from PRI. When possible in a sample with a large number of varied brachiopod hosts, separate brachiopod host genera were observed as independent samples to explore the impact of brachiopod host on sclerobiont distribution. Brachiopod host genera were also selected to complement sampling efforts for research in the concurrent Appalachian Basin so that robust comparisons could be made (refer to Chapter 1).

Host preference is always a concern in sclerobiont research. Recent workers have methodically examined potential features of the host bauplans that have been hypothesized to impact sclerobiont settlement. Mistiaen et al. (2012) found that the factors most likely to contribute to encrustation were host size, shell convexity and fold presence, and, to a lesser degree, brachiopod ornamentation and presence of punctae. Host size selection was also observed by Rodland et al. (2004, 2014). Impunctate brachiopods included in this research were the spiriferid *Athyris*, a biconvex brachiopod with smooth shell texture, *Atrypa*, a biconvex to convexi-planar, costate brachiopod, *Pseudoatrypa*, another convexi-planar, costate brachiopod, and the spiriferid *Mucrospirifer*, a biconvex, impunctate brachiopod with prominent costae.

Strophodonta, a concavo-convex, costate strophomenid brachiopod, and *Devonochonetes*, a moderately concavo-convex, costate to finely costellate strophomenid brachiopod with hinge spines, are pseudopunctate. *Devonochonetes* is also the smallest host brachiopod used herein. The orthid brachiopod *Tropidoleptus* is a punctate, concavo-convex brachiopod with broad, rounded costae.

Another contributing factor to sclerobiont encrustation is the potential impact of taphonomic processes like corrosion and abrasion. A debate remains as to the degree of encrustation that occurs pre- and post-mortem, with some sclerobiont researchers generally showing support of encrustation occurring commonly on live hosts (e.g. Alexander and Scharpf, 1990; Bose et al., 2010; Mistiaen et al., 2012), and those interested in sclerobionts for the purposes of taphonomic research suggesting that post-mortem sclerobiont encrustation provides the significant contribution of encrustation to sclerobiont assemblages (e.g. Tomasovych et al., 2006; Tomasovych and Zuschin, 2009).

Host brachiopods were observed using a dissecting microscope at 10-30x maginification. The identity and location of each brachiopod was recorded on an idealized line diagram. The estimated percent of host valve covered by each sclerobiont was also recorded, along with any indication of competition for available space observed between sclerobionts or if the host shell was alive or dead during the encrustation of the sclerobiont. Areal percent coverage estimation methods follow those established in the Shelf and Slope Experimental Taphonomy Initiative (SSETI) and successfully applied in Smrecak and Brett (2014). While the method is inherently subjective, research indicates that it is an effective and relatively rapid way to characterize sclerobiont encrustation (Smrecak and Brett, 2014; Smrecak and Brandt, in prep).

Endoskeletobionts observed were recorded as 'borers' unless they could be readily ascribed to a maker.

Encrustation metrics used in this work are defined in Table 6, and include common methods of assessing sclerobiont suites, such as areal percent coverage, relative abundance, and frequency of encrustation. For the purpose of this study, valves were treated as independent samples. Most brachiopods used in this study were articulated and free of matrix, allowing both exterior valve surfaces to be examined. Pedicle/brachial assignment was recorded during data collection for future work to assess possible valve preference. Sclerobiont taxa were grouped to explore trends related to higher-order taxonomy (e.g. trepostome bryozoans) or morphologic variation (tube-dwelling organisms) with depth.

Multivariate analyses were conducted using both areal percent coverage data and relative abundance data from each sample using PAST software (Hammer et al., 2001). Areal percent coverage was chosen for presentation because it approximates sclerobiont biomass (Jackson, 1977; Rodland et al., 2014) rather than sclerobiont establishment success on the host, recorded with relative abundance. Areal percent coverage has shown in other studies to effectively characterize depth gradients (Smrecak and Brett, 2014; Brett et al., 2012). Two-way cluster analysis was run using PAST software (Jaccard) to examine the relationships among and between sclerobiont samples collected along the depth gradient. Q-mode (areal percent coverage within samples) analysis was not scaled, and R-mode (taxon) analysis was scaled using percent transformation to mitigate the influence of extremely abundant sclerobiont taxa in the dataset. Detrended correspondence analysis and principal coordinate analysis (using Jaccard) were also conducted in PAST to explore sclerobiont encrustation patterns associated with depth. ANOSIM was conducted on the areal percent coverage of each sample to test whether the degree of

difference between samples in each depth zonation was greater than that from among samples within each depth zone.

RESULTS

Encrustation metrics of samples grouped into SWS, MWS, and DWS, are provided in Figure 7 and listed by sample in Table 7. ANOSIM of inter-group variation showed the difference between groups was larger than within-group, but not significantly so (r=0.586. p=0.067). Pairwise ANOSIM showed significant differences between the samples labeled SWS and MWS (r=0.822, p=0.03), but negligible difference between MWS and DWS (r=0.089, p=0.399).

Changes in Sclerobiont Suites with Depth

Two-way cluster analysis (Jaccard; Figure 8), grouped most SWS together, clustered with three MWS and a single DWS (Sample 9). Another cluster grouped two of three DWS together with MWS 10 and 11. SWS 16_Mucro is a subset of SWS 16 showing sclerobiont growth on the brachiopod host *Mucrospirifer*, and it did not cluster with other samples. The *Mucrospirifer* Subsample 16 demonstrated very low encrustation by a less-rich suite of encrusters than observed in other shallow samples, but it was encrusted by mQ and hederellid form B, two sclerobionts that are very common in shallow samples. The DWS 5 and 6 grouped with MWS 10 and outlier MWS 11. MWS 10 had a high concentration of microconchids, unidentified organic remnants, and bryozoans, which were also common in the deep water samples. MWS 11 was obtained from the easternmost locality included in this study, contained a higher than average proportion of the hederellid form A, and the primary host brachiopod in that sample was *Mucrospirifer*. When MWS 11 was removed from cluster analysis, all clusters showed greater

similarity. Three of four SWS grouped very closely (greater than 95% similarity), but the MWS and DWS groupings remained.

R-mode cluster analysis groups most sclerobiont taxa into one of three clusters (Figure 8B). The most closely related cluster groups forms of *Ascodictyon* and *Allonema*, forms mB, mJ, mK, and those that couldn't be assigned to a particular morphotypes together. These forms were most common in SWS (Figure 11). They grouped into a subcluster with taxa that are common in many intervals: hederellid form B, and two broadly categorized unidentified sclerobionts (not more precisely identified because of preservational issues). Ubiquitous sclerobiont taxa, including auloporid corals, *Ascodictyon* form mA, microconchids, and hederellid form A, grouped in another subset of the first cluster. The second cluster included taxa that were most abundant in DWS, comprised of inarticulate brachiopods and trepostome bryozoan forms mD and mG (see Figure 11). The remaining cluster grouped a number of uncommon sclerobionts that occurred primarily in a subset of SWS.

Detrended correspondence analysis showed a depth gradient along axis 1, which explains over 60% of the data. DWS plotted on the left and shallow samples plotting on the right along the axis (Figure 9). SWS 16 was an outlier that grouped well with other SWS in cluster analysis, but fell on the left-hand side of axis 1. Axis 2 was controlled by some factor that does not impact shallow water samples; SWS plotted low on axis two. MWS 10 and 11 and DWS 6, samples that grouped together in cluster analysis, plotted to the left on axis 1 and high on axis 2. MWS 2, 8, and 9 plotted near the center of axis 1 and lower on axis 2. These samples formed a group in cluster analysis. The fistuliporid bryozoan mC (tentatively identified as *Fistulipora*) was only present in Samples 5, 6, and 10, and several sclerobionts in R-mode cluster 2 were not present in Samples 2, 8, and 9.

Principal coordinate analysis provides additional support for those observations (Figure 10). A similar depth gradient is observed on coordinate 1 using PCO, but no SWS appeared as outliers using PCO. All SWS were plotted positively on coordinate 1, and just above and below 0.00 on coordinate 2 axis. The distinctive groupings of the MWS and DWS, however, were even more apparent. MWS 2 and 8 and DWS 9 grouped positively along coordinate 2, while MWS 5, 10, and 11, and DWS 6 occurred in the negative quadrant of the coordinate 2 axis. DWS 11 was the only deep sample to change its grouping using PCO.

Sclerobiont Areal Percent Coverage

Sclerobiont encrustation with respect to areal percent coverage showed a significant decrease from shallow to deep samples, from an average of 12% of valve surface (STDV 6.6) encrusted, to 3.6% (STDV 1.9) in the deep-water samples. A decrease in areal percent coverage between moderate and deep-water samples was also observed but was not statistically significant. Moderate samples0 displayed high variability in terms of areal percent coverage, ranging from just 2.8% of a valve encrusted in Sample 5 to over 9% in Sample 8 (see Table 7).

When sclerobionts were grouped according to similar form taxa (e.g. trepostome bryozoans, tube-dwelling organisms, and *Ascodictyon/Allonema*) a qualitative representation of the composition of sclerobiont suites emerged (Figure 11A). In terms of areal percent coverage, SWS were dominated by foraminifera, coral, and varied form taxa identified as *Ascodictyon* and *Allonema*. MWS were dominated by bryozoans, which made up forty percent of observed sclerobiont coverage. Corals and forms of *Ascodictyon* and *Allonema* were also common, and only slightly less so than observed in shallow samples. Bryozoans expanded as richness declined, and became proportionately more common than sclerobionts such as organic remnants, holdfasts, and foraminifera (Figure 7). DWS were dominated by trepostome bryozoans overwhelmingly

(30% of encrusted valve surfaces). Corals remained nearly as abundant in all depth zones, although the type of coral changed with depth. Encrusting rugose corals were observed mostly in SWS. Forms of *Ascodictyon* and *Allonema* were also similarly abundant in all samples, although some forms were ubiquitous (e.g. form mA), while others were depth restricted. For example, the *Allonema/Ascodictyon* form mR was found only in SWS.

Sclerobiont Relative Abundance

The number of sclerobionts found on brachiopod valves in shallow samples averaged 3.79 (STDV 0.87). In MWS, brachiopods were encrusted upon by 1.3 sclerobionts (STDV 0.34), and by 1.25 sclerobionts (STDV 0.33) in DWS. SWS had a significantly higher number of sclerobiont individuals present on host valves than did hosts from MWS and DWS.

Grouping sclerobiont taxa forms according to higher taxonomic order using relative abundance data allows a picture of how larval settlement patterns change with changing environments (Figure 11B). SWS were dominated by forms of *Allonema* and *Ascodictyon* and foraminifera, and to a lesser extent hederellids and tube-dwelling organisms. MWS showed a similar dominance by *Ascodictyon* and *Allonema*, encompassing 20 percent of observed sclerobionts on host valves. Hederellids and tube-dwelling organisms were also dominant, comprising fifteen percent of observed sclerobionts each. DWS were dominated by tube-dwelling organisms and hederellids, as well. Increasingly higher occurrences of boring organisms and unidentifiable sclerobiont remnants with depth were visible in Figure 11B, they became dominant components of DWS. The observed suites of sclerobionts numerical abundance were more equitable in terms of larval settlement with depth, contradicting the pattern observed from areal percent coverage in this work (Figure 11B).

Sclerobiont Richness

A total of 38 sclerobiont form taxa, including borings (which were not differentiated) and those which were unidentifiable to form level (e.g. unidentified bryozoan, unidentified hederellid) were observed. On average, SWS displayed a richness of 23 distinct sclerobiont forms (STDV 2.05), samples from MWS showed only 15 different sclerobionts, and DWS had a slightly higher richness with an average of 16 form taxa observed (Figure 7). This was a pronounced, significant decline in richness from SWS to those from DWS.

Both average per host richness and maximum per host richness observed showed trends that mimicked sample richness (Figure 7). In SWS, brachiopod hosts showed an average of 3.93 (STDV 1.13) distinct sclerobiont form taxa per shell, including barren shells, whereas MWS were characterized with encrustation of 1.50 distinct sclerobionts (STDV 0.78), and 0.71 sclerobionts encrusted DWS. The difference between SWS and MWS and between SWS and DWS was significant, but the difference between MWS and DWS was not. Maximum per host richness was also highest in the SWS, with an average of 5.5 sclerobionts observed on the most diversely encrusted hosts MWS displayed four different sclerobionts and DWS displayed five sclerobionts on their most diverse brachiopod host valves.

Compositionally, representatives from all thirteen higher order groupings were present in SWS, MWS, and DWS (Figure 11A, B), but hederellid presence was so low (<1%) that they were not visualized on the chart. Richness was more equitable in the shallow and moderately samples. A variety of taxonomic groups were responsible for more than 23% of host valve encrustation. DWS richness was less equitable, and bryozoans dominated the deep samples, accounting for over 40% of host valve encrustation.

Frequency of Encrustation

Seventy-six percent (STDV 0.15) of brachiopod valves from SWS were encrusted by at least one sclerobiont, significantly more frequently encrusted than MWS and DWS. Only forty-one percent (STDV 0.11) of valves in MDS, and 49% (0.10) of valves in DWS were encrusted (Figure 7). Frequency of encrustation followed patterns shown by richness metrics. MDS were slightly less frequently encrusted than those from DWS, but the differences were not significant.

DISCUSSION

Encrustation metrics such as areal percent coverage, numerical abundance, and sclerobiont richness observed on brachiopods throughout the Middle Devonian Michigan Basin decline with depth. Characterization of these metrics reveals a pattern of sclerobiont encrustation that successfully differentiated different depth zones within the basin. A description of the sclerobiont assemblage that characterizes each depth zone follows.

Sclerobiont Assemblage I – Shallow Facies

SWS sclerobiont assemblages are diverse; host brachiopods were encrusted by 27 of 38 sclerobiont taxa (omitting unidentified sclerobiont forms). Individual brachiopods were encrusted by an average of 3.9 sclerobiont individuals, significantly more than observed in any other depth assemblage (Figure 7). The assemblage is dominated by foraminifera (21% of encrusted area), and *Ascodictyon* and *Allonema* (19% of encrusted host area), and corals (14%) (Figure 11A). *Ascodictyon* and *Allonema* were numerically most abundant. Bryozoans, although characteristically spatially dominant organisms on a few shells, were common but not abundant overall. Each bryozoan form took up less than 10% of the total encrusted valve area.

Numerically, bryozoans were a minor component of sclerobiont assemblages in shallow facies. Hederellids covered less than 5% of brachiopod hosts, but were the third most commonly

observed sclerobiont in shallow samples. Seventy-six percent of host valves in shallow water facies exhibited encrustation. Valves were covered on an average of 12% of their surfaces, significantly more than observed in DWS.

SWS 16 was comprised of two different host brachiopod genera; *Mucrospirifer* and *Strophodonta*. These subsamples showed similar encrustation frequency (78% and 88%, respectively), but had substantially different sclerobiont richness. Sclerobiont assemblages encrusting *Mucrospifier* had 11 sclerobiont taxa present, *Strophodonta* sclerobiont assemblages had 27 different taxa present. Two sclerobionts (unidentified hederellids and mH, an encrusting foraminifera) were only found on *Mucrospirifer* hosts. Relative abundance in both samples was consistent with that observed in shallow water facies (3.3 and 5.3, respectively), but areal percent coverage was much higher on *Strophodonta* hosts.

Sclerobiont Assemblage II – Moderate Facies

Sclerobiont assemblages in MWS were significantly less rich than observed in shallow water facies. Fifteen form taxa were present in a sample. Brachiopods observed in those samples were significantly less frequently encrusted; only 40% of host valves in MWS exhibit encrustation. Host valve surfaces in MWS were spatially covered an average of 5.4% by encrusters, which was less than half the encrustation observed in SWS. An average of 1.3 individual sclerobionts were observed on hosts in MWS, which was, again, less than half of what was observed in SWS.

Compositionally, sclerobiont assemblages from MWS were spatially dominated by trepostome and fistuliporid bryozoans. Corals, *Ascodictyon*, and *Allonema* were as spatially abundant in moderate samples as they were in shallow samples (16% vs. 19%), but foraminifera

were a minor component of MWS. Spatially, hederellids still comprised only a fraction of encrusted area in MWS (3% vs. 1%), but were the second most abundant numerically.

Richness metrics and frequency of encrustation in MWS were the lowest of any samples, and were significantly lower than in the SWS. Although they were not significantly lower than DWS, the consistency with which all metrics recorded lower values for MWS than for DWS suggested that another paleoenvironmental factor negatively may impact encrustation in MWS.

Sclerobiont Assemblage III – Deep Facies

Sclerobiont assemblages in DWS were dominated by bryozoans (40% of areal percent encrustation). *Ascodictyon* and *Allonema* and coral were also dominant in DWS. Although not spatially dominant, the tube-dwelling organism *Cornulites* were the most abundant sclerobionts in DWS. On average, 2.6% of host valve surface area was encrusted in DWS by 0.71 individual sclerobionts per valve.

There was no significant difference between MWS and DWS sclerobiont assemblages in terms of relative abundance, areal percent coverage, richness, or frequency of encrustation (Figure 7). The estimated change in depth between moderate and deep facies in the Michigan Basin is minimal, perhaps as little as 10 meters between the shallowest DWS and deepest MWS (estimated from Wylie and Huntoon, 2003), so it is not surprising that the sclerobiont assemblages were statistically similar. There were, however, some notable changes in taxonomic composition. With respect to numerical abundance, DWS showed a 50% decrease in the number of hederellids observed in MWS, and a nearly four-fold decrease in *Ascodictyon* and *Allonema*. Spatially, trepostome bryozoans nearly doubled their coverage from MWS to DWS, crowding out the fistuliporid group for space on host valves. Inarticulate brachiopods were also most

common spatially and numerically in DWF, more than doubling the proportion of encrusted host area. Encrusting foraminifera were nearly absent from DWS (Figure 11A, B).

Sclerobiont Host Preference and Other Host-Sclerobiont Relationships

Sclerobiont assemblages defined by areal percent coverage can clearly differentiate SWS and DWS (Figures 8, 9, 10). DCA and PCO clearly separate these samples, and cluster analysis grouped samples separately. Multivariate analyses do not successfully discern between MWS and DWS. This may be explained by the minimal change in relative depth and, despite substantial proportionate changes therein, the similar taxonomic composition of the samples. The depth gradient in the Michigan Basin is subtle, no truly deep water facies exist. But compositional and other changes in sclerobiont assemblages within the MWS and DWS exist nonetheless. More work on the environmental preferences of particular sclerobiont taxa is needed to understand the factors – aside from depth – that may have contributed to sclerobiont encrustation. Two alternative explanations for the observed similarity between MWS and DWS are discussed below.

Host Preference

Mucrospirifer is a medium-sized, impunctate, rhynchonelliform brachiopod with prominent costae and a fold and sulcus. Devonochonetes is a pseudopunctate host whose small size might potentially deter sclerobiont encrustation. The function of punctae is not fully understood, but some have suggested punctae-bearing brachiopods could secrete sclerobiont-deterring chemicals (Owen and Williams, 1969; Thayer, 1977; Bordeaux and Brett, 1990). Other workers (Bose et al., 2010; Mistiaen et al., 2012) suggested punctae were not significant contributors to the likelihood of encrustation, at least in some environments. Both are considered less desirable host taxa for sclerobiont encrustation. As such, most samples in this work only

included these brachiopod hosts as a minor component of the sample, but in some cases it was necessary to use pseudopunctate brachiopods as a primary or exclusive host for a sample. MWS 8 and 9 were comprised primarily of *Devonochonetes*, and MWS 2 and 11 were comprised primarily of *Mucrospirifer*.

Devonochonetes did not deter sclerobiont encrustation notably. MWS 8 and 9 predominantly consisted of articulated valves of the small brachiopod, but they grouped together with other MWS in all multivariate analyses. They shared similar taxonomic composition and richness (see Figure 8, Table 7) with other MWS. The samples recorded markedly different areal percent coverage (9.3% for MWS 8, 2.6% for MWS 9), but were collected from localities that bracketed the MWS facies, inferred to have been from a particularly shallow horizon of the Ferron Point Fm. (MWS 8), and the shallow portion of the otherwise deep Bell Shale facies (MWS 9).

Mucrospirifer was the primary host in the moderate depth Sample 11 and shallow Sample 2. Shallow Sample 2 grouped with moderate samples in all multivariate analyses. SWS 2 fauna recorded encrustation metric values that were substantially lower than other SWS recorded, particularly in relative abundance and frequency of encrustation metrics (Table 7). Sample 2 was collected from Mucrospirifer hosts in the Silica Shale, a unit that has demonstrated high encrustation on other hosts (Kesling et al., 1980; Sparks et al., 1980; Bose et al., 2010). The lack of encrustation of Mucrospirifer in the otherwise heavily encrusted brachiopods of the Silica Shale suggests that host preference contributed to sclerobiont encrustation patterns observed within the sample. Mucrospirifer was clearly not the preferred substrate for sclerobionts in shallow facies, but the taxonomic assemblage observed in Sample 2 was consistent with other SWS.

MWS 11 data were collected from *Mucrospirifer* hosts and did not group with other samples in cluster analysis. However, in both DCA and PCO (Figures 9 and 10) MWS 11 plotted near other MWS. MWS11 had lower than average richness, areal percent coverage was consistent with other MWS, and relative abundance was nearly double the average of MWS (Table 7). Thus, many sclerobionts attempted to establish themselves on *Mucrospirifer* in the sample, but only a few taxa were successful. This suggests that the brachiopod was not preferentially avoided as a host, and that no characteristic of *Mucrospirifer* was successful in preventing encrustation in MWS, but that the brachiopod may have had some success preventing the establishment of particular sclerobiont taxa.

Because of the evident lack of success of sclerobionts on *Mucrospirifer* in MWS, a subset of *Mucrospirifer* from SWS 16 were also examined to test whether sclerobiont assemblages at that locality were less likely to be encrusted. SWS 16 did not cluster with other shallow samples in cluster analysis, but the sclerobiont areal percent coverage grouped the sample with other SWS in both DCA and PCO. Areal percent coverage and per host richness were substantially lower in *Mucrospirifer* hosts in SWS 16, although other metrics were consistent with SWS.

When SWS *Mucrospirifer* Samples 2 and 16 were included in characterizing shallow sclerobiont assemblages, the sclerobiont assemblages still readily distinguished SWS from MWS and DWS. However, omitting data collected on *Mucrospirifer* hosts significantly changed encrustation metric values in shallow facies. Areal percent coverage and sample richness were most impacted when data from *Mucrospirifer* hosts were included; SWS showed an average areal percent coverage of 15.77% when *Mucrospirifer* samples were omitted. Including them, areal percent coverage in SWS was 10.97%. Richness similarly rose when *Mucrospirifer* samples were omitted; an average of 27 sclerobiont taxa were observed instead of only 21.

However, in environments that show an already reduced sclerobiont encrustation, like deeper water environments, there seemed to be no difference between preferred and avoided hosts. In relative abundance the *Mucrospirifer* – rich Sample 11 showed the highest values compared to other MWS. Many different sclerobiont taxa attempted to settle and establish themselves on *Mucrospirifer*. This sample also recorded areal percent coverage values consistent with other MWS (Table 7), lending support for the idea that sclerobionts were successfully living on *Mucrospirifer*. Yet in SWS, *Mucrospirifer* – rich samples were significantly less encrusted regardless of the metric used. This suggests that evidence of sclerobiont host preference is common in shallow water but absent in deeper water. Average relative abundance of sclerobionts was high on *Mucrospirifer*, suggesting that larval settlement was not deterred by the brachiopod. In moderate depths where a wide range of brachiopod substrates were present, sclerobionts did not appear to have avoided the host valves of *Mucrospirifer*.

Thus, in facies analysis, brachiopods that have previously been reported as deterring sclerobionts can be used as host substrates. In shallow water facies, these brachiopod taxa can be used to gather data about sclerobiont encrustation, but they should not be the sole surface utilized. Researchers using brachiopod taxa that have been inferred to have sclerobiont deterring potential should consider that encrustation observed on the brachiopods may provide a conservative representation of sclerobionts present. In deeper water facies where ideal host brachiopods are not always available, researchers should feel comfortable incorporating brachiopod hosts that have shown prior evidence of being preferentially avoided. In almost all metrics examined herein, valves of avoided brachiopods were encrusted in similar ways as other brachiopod taxa. These results together also provide a basis for re-examination of host preference studies. Those host preference studies that have yielded contradictory interpretations in the

literature may be looking at the same brachiopods but from different paleodepths. Comparing brachiopod host preference should done only on those from similar paleobathymetric regimes, and doing so may enhance the interpretive value of individual studies.

CONCLUSIONS

Sclerobiont assemblages in the Middle Devonian Michigan Basin differ in ways that are discernible taxonomically and through encrustation metrics such as areal percent coverage, relative abundance, richness, and encrustation frequency. Patterns of sclerobiont encrustation change predictably with depth, and can therefore be used to interpret the relative depth of a sample in the region. Areal percent coverage data clearly delineate SWS from DWS using multivariate analyses. MWS and DWS show only a subtle difference between encrustation metric data, likely driven by sclerobiont host avoidance in moderate samples and by the lack of a truly deep, dysphotic water facies in the Michigan Basin during the Middle Devonian. MWS collected from less desirable hosts *Mucrospirifer* and *Devonochonetes* showed depressed values for all encrustation metrics. Yet the taxonomic differences observed between moderate and deep samples can be observed when encrustation patterns of sclerobionts with different life habits are grouped, especially with respect to bryozoans that are more than twice as abundant in deep water facies.

Sclerobiont host preference appears to override depth-related encrustation patterns in shallow facies where a large variety of host surfaces and sclerobiont taxa are common.

Incorporating a large volume of preferentially avoided hosts decreases the observed encrustation patterns using any metric, but especially richness and areal percent coverage. However, in deeper facies, less desirable host brachiopods are commonly encrusted in a manner consistent with other hosts, and need not be omitted from sclerobiont studies. There are thus resulting implications that

to better understand sclerobiont-host relationships requires consideration of the paleoenvironmental conditions under which the encrustation occurs.

APPENDIX

APPENDIX

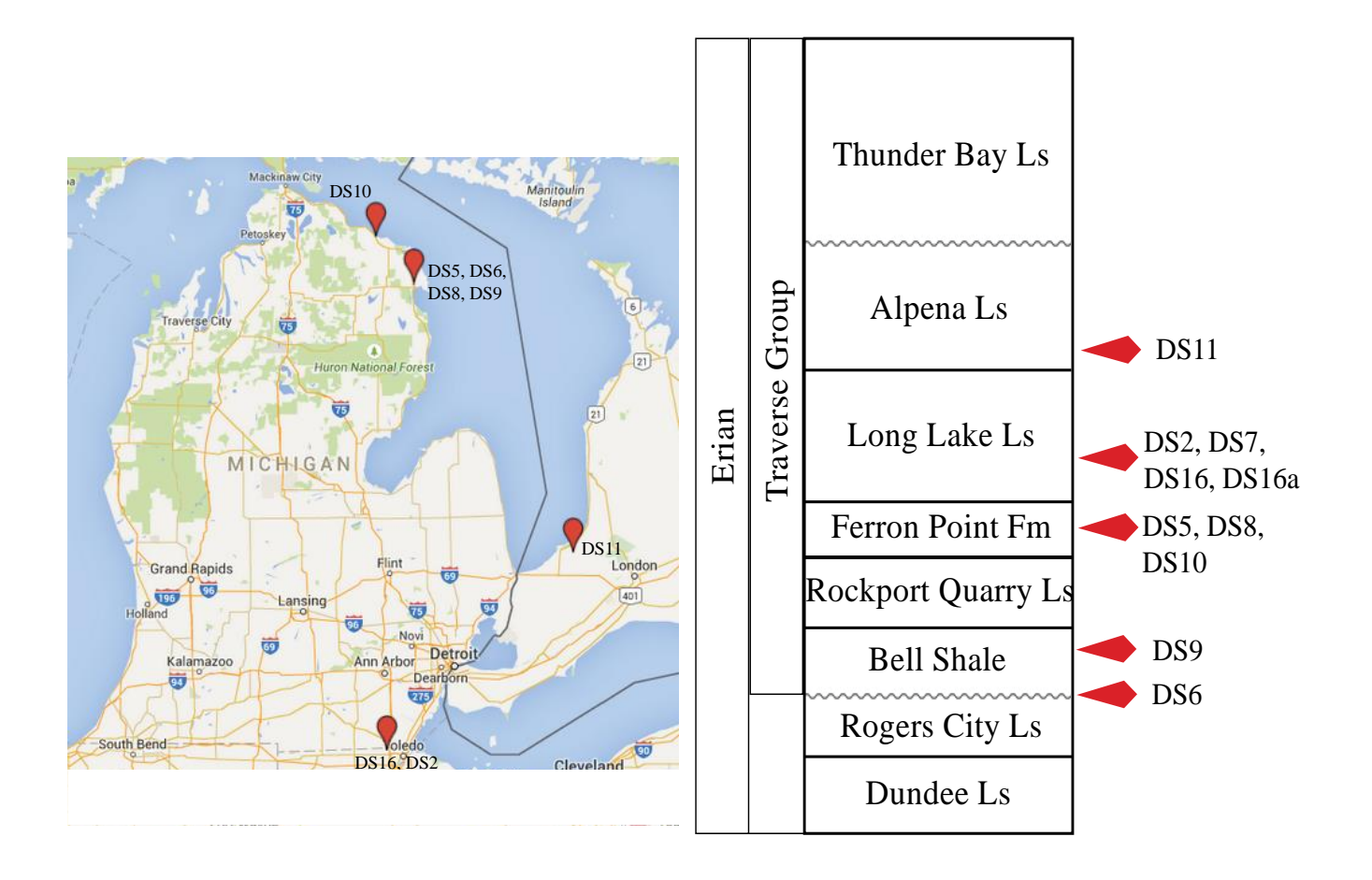


FIGURE 6 – *Michigan Basin locality information*. Locality map and stratigraphic location of samples used in study.

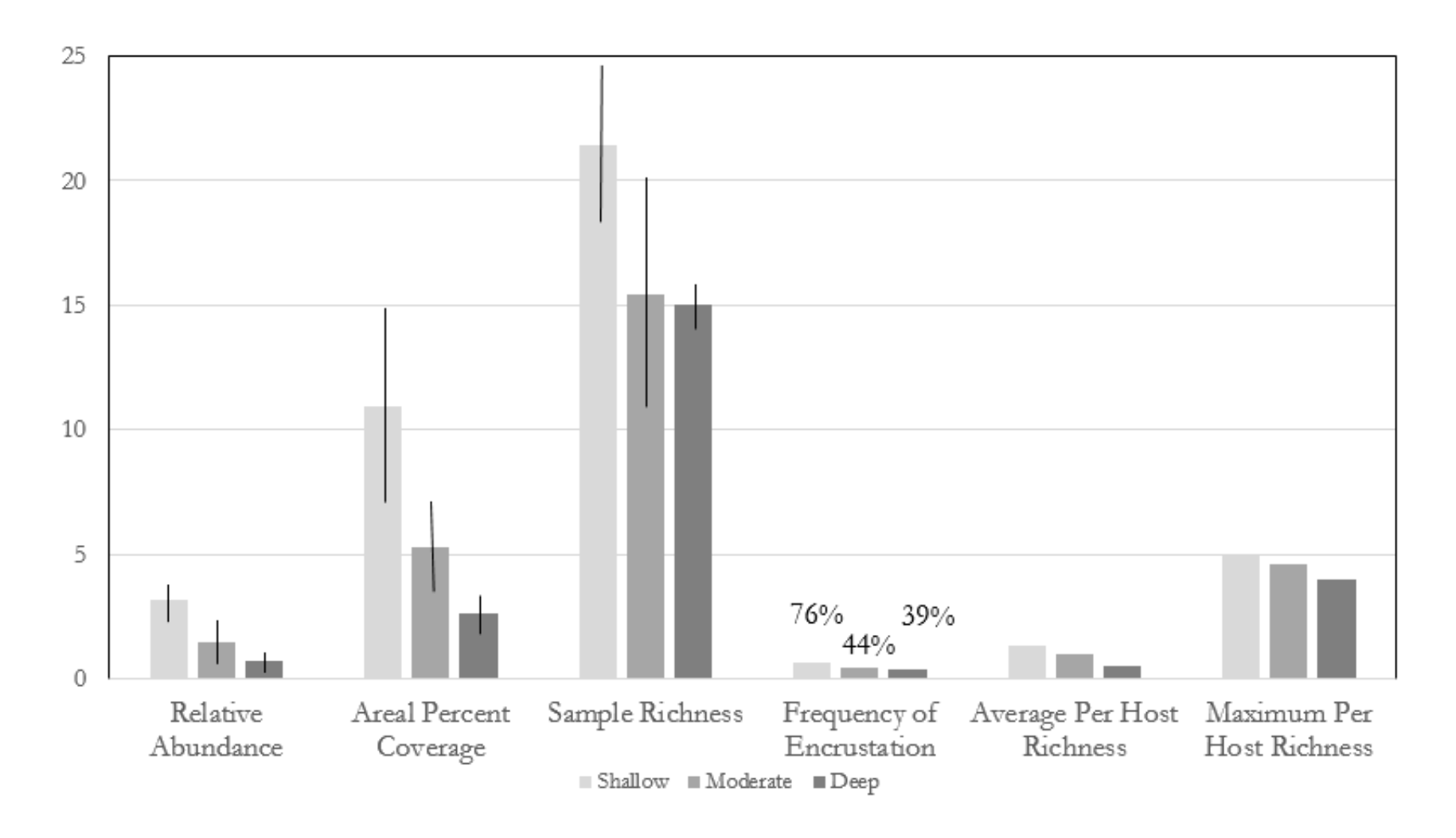


FIGURE 7 – *Averaged encrustation metrics observed in the Michigan Basin*. Encrustation metrics averaged across shallow, moderate, and deep facies samples.

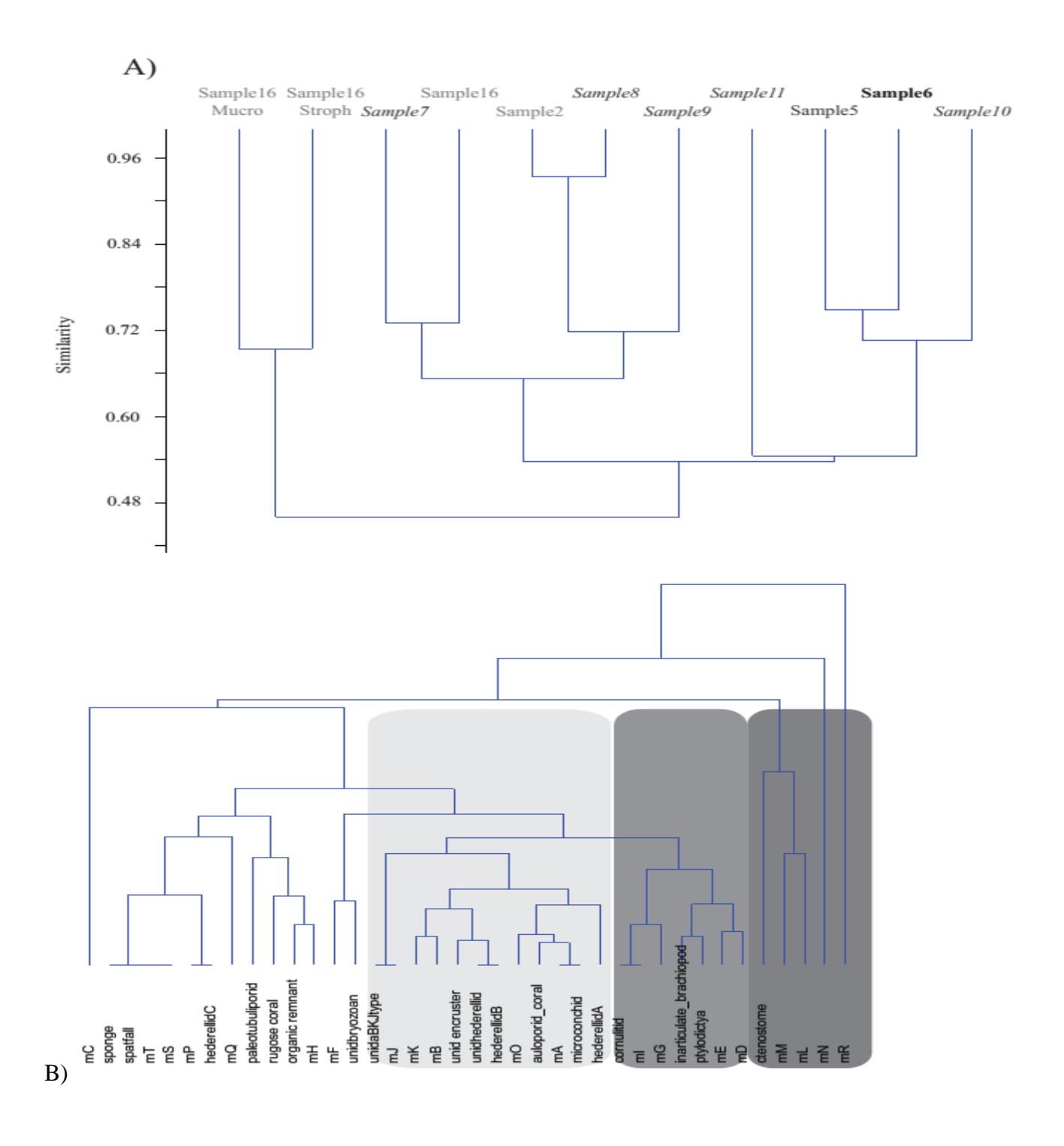


FIGURE 8 – *Cluster analysis of Michigan Basin samples*. A) Q-mode clustering and B) R-mode clustering. Shallow samples in light grey, moderate in dark grey with italics, and deep in black.

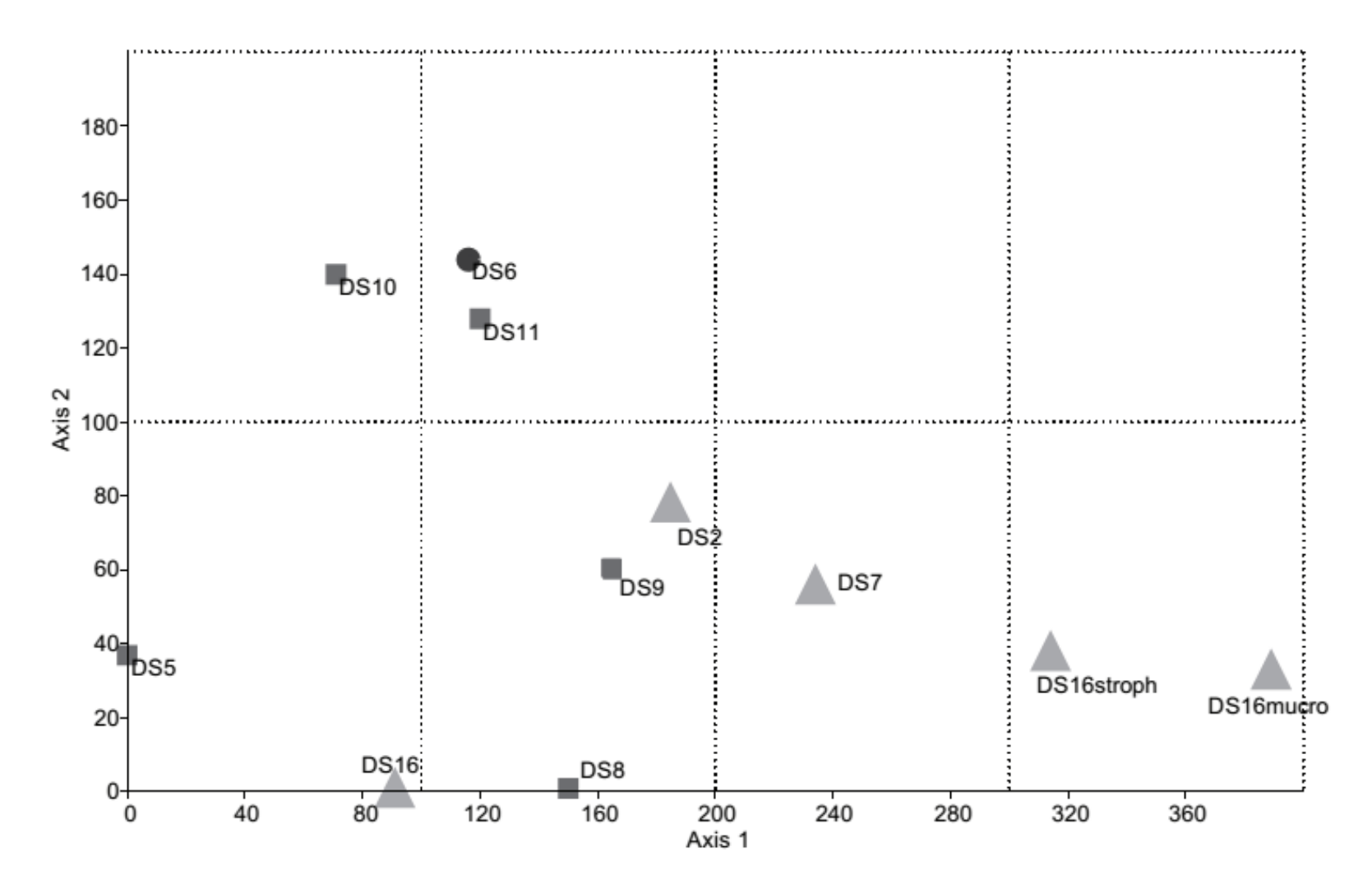


FIGURE 9 – *Detrended correspondence analysis of Michigan Basin samples.* DCA calculated using areal percent coverage data. Shallow samples in light grey triangles, moderate in grey squares, and deep in dark grey circles.

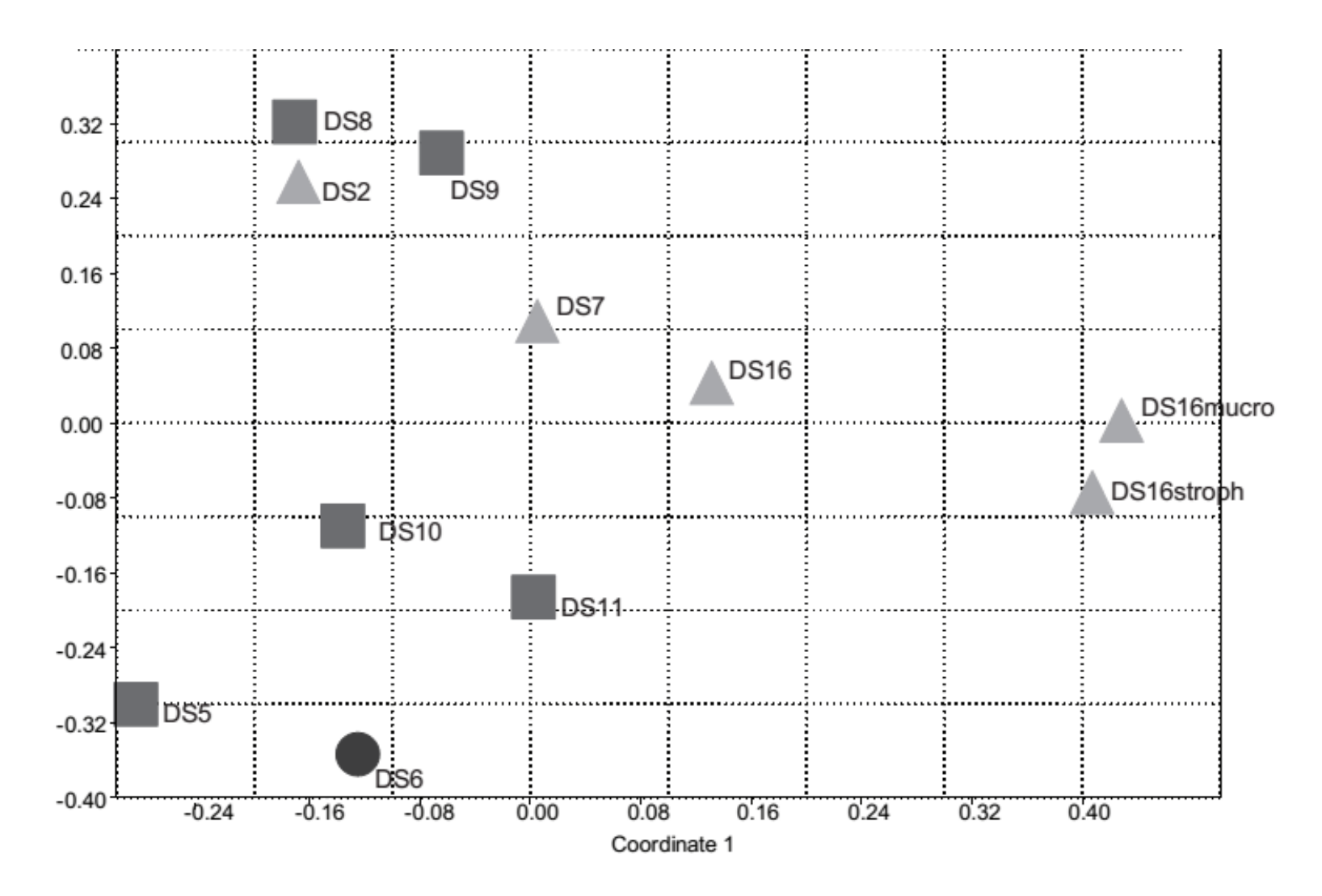


FIGURE 10 – *Principal Coordinate Analysis of Michigan Basin samples*. PCO calculated using areal percent coverage data. Shallow samples in light grey triangles, moderate in grey squares, and deep in dark grey circles.

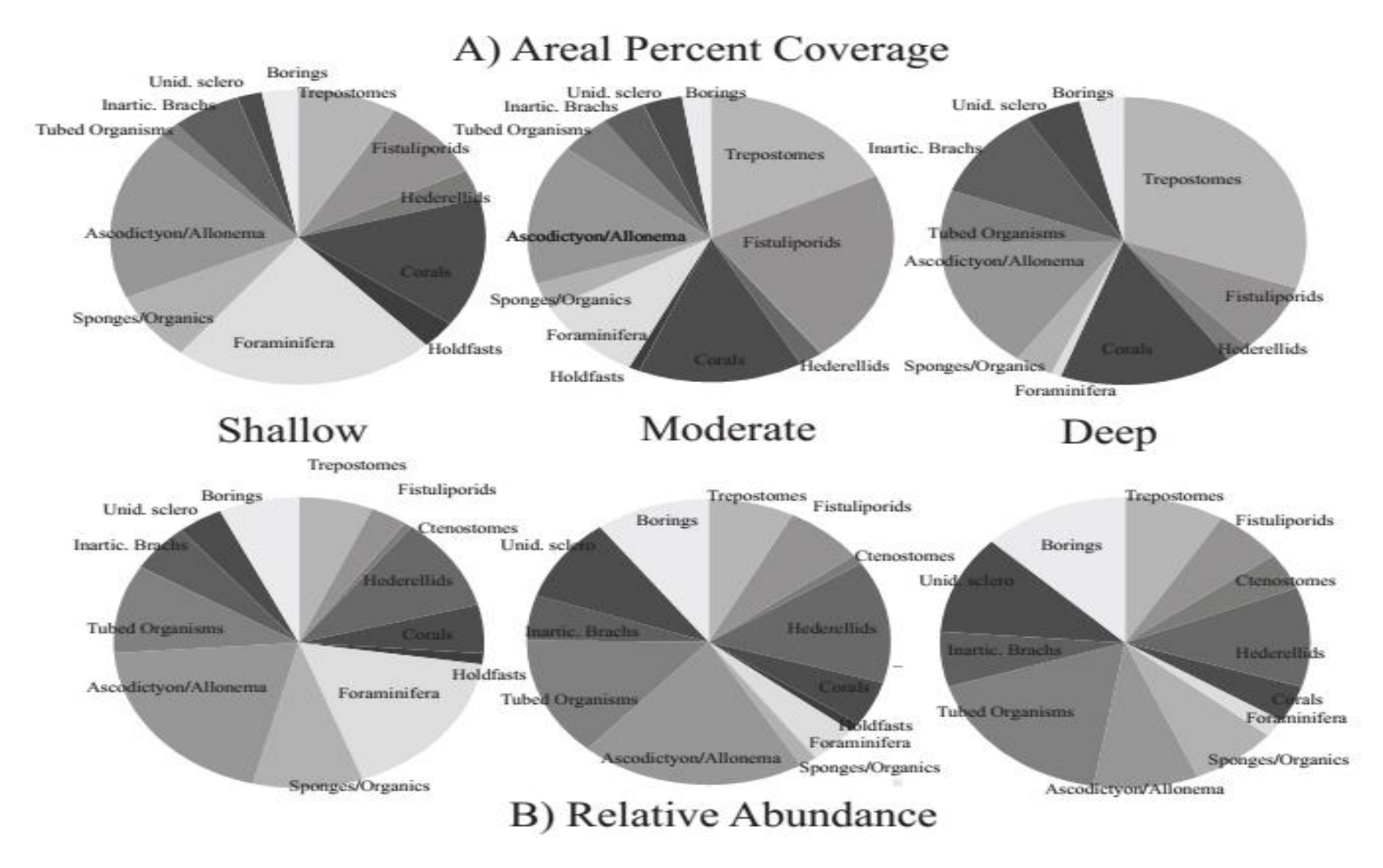


FIGURE 11 – *Taxonomic composition of shallow, moderate, and deep facies in the Michigan Basin.* Relative proportion of different taxonomic groups in shallow, moderate, and deep facies samples, A) according to areal percent coverage, and B) numerical abundance.

Sclerobiont Encrustation	
Metric	Metric Description
Areal Percent Coverage	The percentage of host shell surface covered by the sclerobiont(s).
Relative Abundance	The number of individuals or colonies of sclerobionts present.
Sample Richness	The number of encrusting taxa observed in a sample.
Richness Ratio	The number of sclerobiont taxa observed in a sample/total number of sclerobiont taxa observed in basin or study region.
Frequency of Encrustation	The number of host shells encrusted/total number of shells observed.
Maximum Per Host Richness	The highest number of sclerobiont taxa observed on an individual host shell substrate
Average Per Host Richness	The average number of sclerobiont taxa on an individual host shell substrate in a sample

 $\textbf{TABLE 6} - \textit{Encrustation metric descriptions}. \ Encrustation \ metrics \ used \ in \ this \ study.$

				A ma a l		Eraguanav	A viana ca	Maximum
C 1		A 1	D. Lat	Areal	C 1	Frequency	Average	Maximum
Sample		Assigned	Relative	Percent	Sample	of	Per Host	Per Host
ID	n	Facies	Abundance	Coverage	Richness	Encrustation	Richness	Richness
DS2*	120	shallow	0.78	5.46	16	0.29	0.60	3
DS7	82	shallow	2.50	9.15	24	0.56	1.34	5
DS16	60	shallow	4.02	15.53	29	0.83	1.80	7
DS16_								
Mucro*	60	shallow	3.34	2.05	11	0.78	0.72	3
DS16_								
Stroph	60	shallow	5.28	22.64	27	0.88	2.36	7
Aver	Average Shallow		3.18	10.97	21	0.67	1.37	5
Average (Mucrospirifer								
omitted)			3.93	15.77	27	0.75	1.83	6
DS5	78	moderate	0.63	2.77	12	0.26	0.56	6
DS10	60	moderate	1.02	5.17	21	0.42	0.77	3
DS11*	60	moderate	2.82	4.69	11	0.41	1.05	4
DS6	98	moderate	1.78	4.69	17	0.58	1.46	6
DS8	38	moderate	1.26	9.25	16	0.55	0.98	4
Average Moderate		1.50	5.31	15	0.44	0.96	5	
DS9	95	deep	0.71	2.62	15	0.40	0.51	4
Average Deep		0.71	2.62	15	0.40	0.51	4	

TABLE 7 – *Observed encrustation metrics in the Michigan Basin by sample and with depth.* Encrustation metrics observed in each sample and averaged across shallow, moderate, and deep water facies. * denotes sample with *Mucrospirifer* hosts.

REFERENCES

REFERENCES

- ALEXANDER, R.R. AND SCHARPF, C.D., 1990, Epizoans on Late Ordovician brachiopods from southeastern Indiana: Historical Biology, v. 4, p. 179-202.
- BARTHOLOMEW, A.J., BRETT, C.E., DESANTIS, M, BAIRD, G.C., AND TSUJITA, C., 2006, Sequence stratigraphy of the Middle Devonian at the Border of the Michigan Basin: correlations with New York and implications for sea-level change and paleogeography, Northeastern geology and environmental sciences, v. 28(1), p. 2-33.
- BARTHOLOMEW, A.J., AND BRETT, C.E., 2007, Correlation of Middle Devonian Hamilton Group-equivalent strata in east-central North America: implications for eustacy, tectonics, and faunal proviciality, Geological Society of London Special Publications, v. 278, p. 105-131.
- BARRINGER, J.E., 2008, Analysis of the occurrence of microconchids on Middle Devonian brachiopods from the Michigan Basin: implications for microconchid and brachiopod autecology: unpublished M.S. thesis, Michigan State University, 117 p.
- BISHOP, J.D.D., 1988, Disarticulated bivalve shells as substrates for encrustation by the bryozoan *Cribrilina puncturata* in the Plio-Pleistocene Red Crag of eastern England: Palaeontology, v. 31(2), p. 237-253.
- BORDEAUX, Y.L., and BRETT, C.E., 1990, Medium specific associations of epibionts on Middle Devonian brachiopods: implications for paleoecology: Historical Biology, v. 4, p. 203-220.
- BOSE, R., SCHNEIDER, C., POLLY, P.D., and YACOBUCCI, M.M., 2010, Ecological interactions between *Rhipidomella* (Orthides, Brachiopoda) and its endoskeletobionts and predators from the Middle Devonian Dundee Formation of Ohio, United States: Palaios, v. 25(3), p. 196-208.
- Bose, R., 2013, Quantitative analysis strengthens qualitative assessment; a case study of Devonian brachiopod species, Palaeontologische Zeitschrift, v.87(2), 169-178.
- Brett, C.E., Parsons-Hubbard, K., Walker, S.E., Ferguson, C., Powell, E.N., Staff, G., Ashton-Alcox, K.A., and Raymond, A., 2011, Gradients and patterns of sclerobionts on experimentally deployed bivalve shells: Synopsis of bathymetric and temporal trends on a decadal time scale: Palaeogeography, Palaeoclimatology, Palaeoecology, v. 312, p. 278-304.
- BOSELLINI, F.R. AND PAPAZZONI, C.A., 2003, Palaeoecological significance of coral-encrusting foraminiferan associations: a case-study from the Upper Eocene of northern Italy, Acta Paleontologica Polonica, v. 48(2), p. 279-292.

- BRETT, C.E, 1995, Sequence stratigraphy, biostratigraphy, and taphonomy in shallow marine environments: Palaios, v. 10, p. 497-516.
- BRETT, C.E., SMRECAK, T., Parsons-Hubbard, K.M., and WALKER, S.E., 2012, Marine sclerobiofacies: Encrusting communities on shells through time and space, *in* Talent, J., ed., Global Biodiversity, Extinction Intervals and Biogeographic Perturbations through Time, UNESCO/International Year of Planet Earth Special Volume, p. 129-155.
- ETTENSOHN, F.R., 2008, Chapter 4: The Appalachian Foreland Basin in Eastern United States, *in* Miall, A.D., ed., Sedimentary Basins of the World, Vol. 5, The Sedimentary Basins of the United States and Canada, p. 105-179.
- FURLONG, C. AND MCROBERTS, C.A., 2014, Commensal borings from the Middle Devonian of central New York: ecologic and taxonomic review of *Clionoides, Clinolithes*, and *Canaliparva* n. ichnogen., Journal of Paleontology, v. 88, p. 131-145.
- HAMMER, O., HARPER, D.A.T., and RYAN, P.D., 2001, PAST: Paleontological statistics software package for education and data analysis: Palaeontological Electronica, vol.4 (1): 9 p.
- HOWELL, P.D., AND VAN DER PLUIJM, B.A., 1999, Structural sequences and styles of subsidence in the Michigan Basin, GSA Bulletin, v. 111(7), 974-991.
- HURST, J.M., 1974, Selective epizoan encrustation of some Silurian brachiopods from Gotland, Palaeontology, 17, p. 423-429.
- JACKSON, J.B.C., 1977, Competition on marine hard substrata: the adaptive significance of solitary and colonial strategies, The American Naturalist, v. 111(980), p. 743-767.
- KESLING, R.V., HOARE, R.D., SPARKS, D.K., 1980, Epizoans of the Middle Devonian brachiopod *Paraspirifer bownockeri*: their relationships to one another and to their host: Journal of Paleontology, v. 54(6), p. 1141-1154.
- KRAUSE, R.A., Jr., BARBOUR WOOD, S.L., KOWALEWSKI, M., KAUAN, D., ROMANEK, C.S. SIMOES, M.G., and WEHMILLER, J.F., 2010, Quantitative comparisons and models of time averaging in bivalve and brachiopod shell accumulations: Paleobiology, v. 36, p. 304-320.
- LESCINSKY, H.L., 1993, Taphonomy and paleoecology of epibionts on the scallops *Chlamys hastate* (Sowerby 1843) and *Chlamys rubida* (Hinds 1845): Palaios, v.8, p. 267-277.
- LESCINSKY, H.L., 1995, The life orientation of concavo-convex brachiopods: overturning the paradigm: Paleobiology, v. 21, p. 520-551.
- LESCINSKY, H.L., 1997, Epibiont communities: recruitment and competition on North American carboniferous brachiopods: Journal of Paleontology, v. 71, p. 34-53.

- LESCINSKY, H.L., EDINGER, E., and RISK, M.J., 2002, Mollusc shell encrustation and bioerosion rates in a modern epeiric sea: taphonomy experiments in the Java Sea, Indonesia: Palaios, v. 17, p. 171-191.
- MCKINNEY, F.K., 1995, Taphonomic effects and preserved overgrowth relationships among encrusting marine organisms: Palaios, v. 10, p. 279-282.
- OWEN, G. AND WILLIAMS, A., 1969, The caecum of articulate brachiopods, Proceedings of the Royal Society B., 172, p. 197-202.
- MARTINDALE, W., 1992, Calcified epibionts as palaeoecological tools: examples from the Recent and Pleistoncene reefs of Barbados: Coral Reefs, v. 11, 167-177.
- MILSTEIN, R.L., 1987, Middle Devonian Traverse Group in Charlevoix and Emmet counties, Michigan, Geological Society of America Centennial Field Guide North-Central Section, 4p.
- MISTIAEN, B., BRICE, D., ZAPALSKI, M.K., and LOONES, C., 2012, Brachiopods and their auloporid epibionts in the Devonian of Boulonnais (France): Comparison with other associations globally, *in* Talent, J., ed., Global Biodiversity, Extinction Intervals and Biogeographic Perturbations through Time, UNESCO/International Year of Planet Earth Special Volume, p. 159-189.
- NEBELSICK, J.H., SCHMID, B., and STACHOWITSCH, M., 2007, The encrustation of fossil and recent sea-urchin tests: ecological and taphonomic significance: Lethaia, v. 30, p. 271-284.
- PITRAT, C.W. AND ROGERS, F.S., 1978, *Spinocyrtia* and its epibionts in the Traverse Group (Devonian) of Michigan: Journal of Paleontology, 52(6), p. 1315-1324.
- POWELL, E.N., STAFF, G.M., CALLENDER, W.R., ASHTON-ALCOX, K.A., BRETT, C.E., PARSONS-HUBBARD, K.M., WALKER, S.E., and RAYMOND, A., 2011, The influence of molluscan taxon on taphofacies development over a broad range of environments of preservation, the SSETI experience: Palaeogeography, Palaeoclimatology, Palaeoecology, v. 312, p. 233-264.
- RICHARDS, R.P., 1972, Autecology of Richmondian brachiopods (Late Ordovician of Indiana and Ohio): Journal of Paleontology, v. 46, p. 386-405.
- RICHARDSON-WHITE, S., and WALKER, S.E., 2011, Diversity, taphonomy and behavior of encrusting foraminifera on experimental shells deployed along a shelf-to-slope bathymetric gradient, Lee Stocking Island, Bahamas: Palaeogeography, Palaeoclimatology, Palaeoecology, v. 312, p. 305-324.

- RICKARD, L.V., 1984, Correlation of the subsurface Lower and Middle Devonian of the Lake Erie region, Geological Society of America Bulletin, v. 13, p.149-186.
- RODLAND, D.L., KOWALEWSKI, M., CARROLL, M., and SIMOES, M.G., 2004, Colonization of a 'Lost World': Encrustation Patterns in Modern Subtropical Brachiopod Assemblages: Palaios, v. 19, p. 381-395.
- RODLAND, D.L., SIMOES, M.G., KRAUSE, R.A., AND KOWALEWSKI, M, 2014, Stowing away on ships that pass in the night: sclerobiont assemblages on individually dated bivalve and brachiopod shells from a subtropical shelf, Palaios, v. 29(4), p.170-183.
- RODRIGUES, S.C., SIMOES, M.G., KOWALEWSKI, M., PETTI, M.A.V., NONATO, E.F., 2008, Biotic interaction between spionid polychaetes and boucardiid brachiopods: paleoecological, taphonomic, and evolutionary implications, Acta Palaeontologica Polonica, v. 53(4), p. 657-668.
- SCOTESE, C., 2003, PALEOMAP Project, www.scotese.com. Last accessed 7/17/2015.
- SHROAT-LEWIS, R., MCKINNEY, M.L., BRETT, C.E., MEYER, D.L., SUMRALL, C.D., 2011, Paleoecologic assessment of an edrioasteroid (*Echinodermata*) encrusted hardground from the upper Ordovician (Maysvillian) Bellevue Member, Maysville, KY: Palaios, v. 26(8), p. 470-483.
- SMRECAK, T.A., AND BRETT, C.E., 2014, Establishing patterns in sclerobiont distribution in a Late Ordovician (Cincinnatian) depth gradient: toward a sclerobiofacies model Palaios, v. 19, p. 381-395.
- SMRECAK, T.A, AND BRANDT, D., *in prep*, Assessment of techniques used to describe sclerobiont abundance and distribution.
- SPARKS, D.K., HOARE, R.D., KESLING, R.V., 1980, Epizoans on the brachiopod *Paraspirifer* bownockeri (Stewart) from the Middle Devonian of Ohio: Museum of Paleontology, The University of Michigan, Ann Arbor, MI, 105 p.
- SPJELDNAES, N., 1984, Epifauna as a tool in autecological analysis of Silurian brachiopods, Palaeontology Special Papers, v. 32, p. 225-235.
- TAYLOR, P.D. and WILSON, M.A., 2002, A new terminology for marine organisms inhabiting hard media: Palaios, v. 17(5), p. 522-525.
- THAYER, C.W., 1974, Substrate specificity of Devonian epizoa: Journal of Paleontology, v. 48(5), p. 881-894.
- THAYER, C.W., 1986, Respiration and the function of brachiopod punctae, Lethaia, 19, p. 23-31.

- TOMASOVYCH, A., FURSICH, F.T., OLSZEWSKI, T.D., 2006, Modeling shelliness and alteration in shell beds: variation in hardpart input and burial rates leads to opposing predictions: Paleobiology, v. 32(2), p. 278-298.
- TOMASOVYCH, A., and ZUSCHIN, M., 2009, Variation in brachiopod preservation along a carbonate shelf-basin transect (Red Sea and Gulf of Aden): environmental sensitivity of taphofacies: Palaios, v. 24, p. 697-716.
- WALKER, S.E., PARSONS-HUBBARD, K., POWELL, E.N., and BRETT, C.E., 1998, Bioerosion or bioaccumulation? Shelf-slope trends for epi- and endobionts on experimentally deployed gastropod shells: Historical Biology, v. 13, p. 61-72.
- WALKER, S.E., PARSONS-HUBBARD, K., RICHARDSON-WHITE, S., BRETT, C.E., and POWELL, E.N., 2011, Alpha and beta diversity of encrusting foraminifera that recruit to long-term experiments along a carbonate platform-to-slope gradient: paleoecological and paleoenvironmental implications: Palaeogeography, Palaeoclimatology, Palaeoecology, v. 312, p. 325-349.
- WEI-HAAS, M.L., GLUMAC, B., and CURRAN, H.A., 2011, *Sphenothallus*-like fossils from the Martinsburg Formation (Upper Ordovician), Tennessee, USA: Journal of Paleontology, v. 85(2), p. 353-360.
- WRIGHT, J.D. AND WRIGHT, E.P., 1961, A study of the Middle Devonian Widder Formation of Southwestern Ontario, Contributions to the Museum of Paleontology, University of Michigan, v. 16(5), p. 287-300.
- WYLIE, A.S., JR., AND HUNTOON, J.E., 2003, Log-curve amplitude slicing: visualization of log data and depositional trends in the Middle Devonian Traverse Group, Michigan Basin, United States, AAPG Bulletin, v. 87(4), p. 581-608.
- ZAMBITO, JAMES, 2013, A revised stratigraphic framework for the Middle and Upper Devonian of the Northern Michigan Basin, AAPG Annual Convention and Exhibition, Pittsburgh, Pennsylvania, May 19-22, 2013.
- ZATON, M., and BORSZCZ, T., 2012, Encrustation patterns on post-extinction early Famennian (Late Devonian) brachiopods from Russia: Historical Biology, p.1-12.

CHAPTER 3: CHARACTERIZING SCLEROBIONT ASSEMBLAGES ALONG A MIDDLE DEVONIAN (HAMILTON GROUP) DEPTH GRADIENT, APPALACHIAN BASIN, NY, USA AND COMPARISON WITH OTHER DEVONIAN SCLEROBIONT ASSEMBLAGES

ABSTRACT

The well-studied Middle Devonian Hamilton Group strata of the Appalachian Basin, Eastern USA, contain units that are well-constrained in terms of paleoenvironmental conditions and the basin is thus an excellent location to study changes in sclerobiont assemblages with depth. Sclerobiont assemblages in the Hamilton Group reflect paleobathymetric zonations recorded independently by light-sensitive microendolith suites and supported by sequence stratigraphic interpretations. Areal percent coverage, frequency of encrustation, and relative abundance of sclerobiont assemblages declined with increasing depth, patterns which are consistent with others in the Middle Devonian, as well as those observed in the Late Ordovician and Carboniferous. Shallow environments were dominated by colonial hederellids (incertae cedis). Deep environments hosted a less diverse sclerobiont fauna, characterized by ctenostome and fistuliporid bryozoans, and to a lesser extent, cornulitids. Cornulitids were more abundant in environments with higher sedimentation/turbidity. Despite predictable patterns of decline in encrustation metrics, brachiopods from the Middle Devonian Appalachian Basin are much less encrusted in shallow and moderately deep environments than they are in the coeval Michigan Basin, the Late Ordovician fauna of the Cincinnati Arch region, and qualitatively less encrusted than other locations and times spanning the Paleozoic. The combination of a predictable decline in encrustation metrics consistent with other studies along with markedly low values of encrustation supports the interpretation that sclerobiont assemblages are very sensitive to paleobathymetry, and that other paleoenvironmental factors, in this case sedimentation, can be readily identified in sclerobiont assemblages. This research adds to the growing body of work supporting the use of sclerobiont suites as effective paleobathymetric indicators, and contributes to the potential viability of a sclerobiofacies model applicable throughout geologic time.

INTRODUCTION

Sclerobionts are organisms that live encrusted upon live or dead host substrates (Taylor and Wilson, 2002). These animals have been widely used in host autecological research and in studies of interactions between the whole organism host taxon and an individual sclerobiont taxon or suite of taxa (e.g. Richards, 1972; Vinn and Wilson, 2012). Sclerobionts are part of an emerging body of literature applying suites of organisms as paleoenvironmental indicators and proxies for physical and taphonomic perturbations (Lebold, 2000; Brett et al., 2012; Tomasovych et al., 2006; Rodrigues, 2008; Krause et al., 2010; Brett et al., 2011; Powell et al., 2011; Barclay et al., 2013). Sclerobionts are thought to be sensitive to a combination of water depth and energy, light penetration, nutrient availability, and sedimentation (Brett et al. 2012; Lescinsky 2002; Mistiaen et al. 2012; Smrecak and Brett, 2014), although the influences of these abiotic factors on sclerobiont assemblages are difficult to differentiate from one another.

In some cases, sclerobionts are more sensitive to paleoenvironmental changes than their host taxa (Lescinsky et al., 2002; Smrecak and Brett, 2014), and their study may eventually permit differentiation of the often-conflated paleoenvironmental conditions to which they are sensitive. As a result, increasingly more research has been devoted to sclerobiont assemblage structure, which has also prompted work on the relationship between sclerobionts and their hosts. Sclerobiont suites have been shown to have been impacted not only by paleoenvironmental changes, but also by the choice of host, whether the host is living or dead at the time of encrustation, and by the host morphology.

If ontogeny causes changes in the shape, size, or life habit of the host taxon (e.g. a transition from an epibenthic to a semi-infaunal life habit), the potential area upon which sclerobionts may settle and grow can change, as well. If living hosts had the ability to deter

sclerobionts, potential observed biases in sclerobiont assemblages could be attributed to their relationship with the host and not to changing paleoenvironmental conditions (e.g. Brandt, 1996; Key, et al., 1999, 2000). If encrustation is occurring primarily post-mortem, the above conditions are less likely to influence sclerobiont assemblages, but a new suite of taphonomic considerations must be considered.

High frequencies of sclerobionts on host shells have been interpreted as a taphonomic byproduct of repeated exhumation and reburial (Parsons-Hubbard et al. 1999; Lescinsky et al. 2002; Tomasovych et al. 2006; Tomasovych and Zuschin 2009). Taphonomic processes can also degrade sclerobiont preservation on hosts (Davies et al. 1989; Tomasovych and Zuschin, 2009). The impact of taphonomic alteration on sclerobiont suites has not yet been fully explored. However, some workers suggested that sclerobiont communities establish themselves primarily during the life of the host (Lebold, 2000; Lescinsky et al. 2002; Bose et al. 2010). Observations of some live-live interactions between host and sclerobiont (e.g. sclerobionts growing in line with inhalant currents, host shell mottling around a sclerobiont) support those findings. Experiments on deployed host shells in Lee Stocking Island, Bahamas, showed that both sclerobiont diversity and areal percent coverage peak early after deployment and decline thereafter, suggesting that sclerobiont assemblages on a given host are not continually increasing until final burial of the host (Brett et al., 2011). Both peri- and postmortem impacts to sclerobiont assemblages must be considered when studying encrustation patterns on any host taxa, and any methods used to collect data on sclerobiont patterns should provide means to account for these potential biases.

Methods used to analyze sclerobiont encrustation vary widely, which has prevented useful synthesis among temporally constrained studies in different geographic provinces, and

between studies through geologic time. Analyses have been derived from sclerobiont presence/absence data (e.g. Pitrat and Rogers, 1978), from counts of sclerobiont taxa on each valve or shell (e.g. Thayer, 1974; Bordeaux and Brett, 1990; Mistiaen et al., 2012), and from counting presence/absence of sclerobionts in each of several squares in a grid overlay of the host shell (e.g. Kesling et al., 1980; Bose et al., 2010; Furlong and McRoberts, 2014). Further, some studies have focused on recording indications of live-live relationships between the host and sclerobionts (e.g. Rodland et al., 2014), while others have focused on taphonomic impacts (e.g. Tomasovych and Zuschin, 2009). Not all studies have recorded the identification of sclerobiont taxa, further reducing the ability to correlate diversity measures like richness and evenness among studies. The disparity of methods used in assessing sclerobionts likely contribute much to the varied, sometimes conflicting, results observed in similar studies (Smrecak and Brandt, *Chapter 2*).

Here we document suites of sclerobionts across a well-studied Middle Devonian

Appalachian Basin depth gradient using a variety of host brachiopod taxa. In addition we explore sclerobiont encrustation patterns from areas interpreted to have both background and episodically higher levels of sedimentation influx. This work builds on previous successful attempts to correlate sclerobiont encrustation with relative depth in Ordovician, Devonian,

Carboniferous, and modern environments (Alexander and Scharpf 1990; Bordeaux and Brett 1990; Lescinsky, 1997; Walker et al 1998, 2011; Brett et al 2011, 2012; Smrecak and Brett 2014), some of whom also showed evidence of a sclerobiont response to sedimentation/turbidity, and uses well-constrained sequence-stratigraphy to place sampled units in a known depositional context.

Geological Setting

The Middle Devonian Appalachian Basin is a foreland basin formed as a result of the Acadian Orogeny and filled by the erosion of the orogen (Ettensohn, 2008). The resulting package of sediments form a clastic wedge that thins westward from 900 meters to less than 90 meters (Rickard, 1984) (Figure 12). Third- and fourth- order depositional sequences have been identified in this package of rocks, termed the Hamilton Group. Each formation represents a third- order sequence (e.g. Skaneateles Fm.). The high-stand systems tracts in each sequence shows evidence of fourth-order depositional sequences and thin carbonate layers that can be traced laterally across the basin (Brett and Baird, 1996; Bartholomew and Brett, 2007). During the Middle Devonian, the Appalachian Basin was located in the subtropical, semi-arid climatic belt (Howell and VanderPluijm, 1999; Scotese, 2003).

The Hamilton Group outcrop belt is located near the I-90 corridor in New York State, which has allowed workers easy examination of these facies as they change laterally. It is also one of the most complete and fossiliferous Paleozoic stratigraphic sections globally, has been extensively studied in terms of stratigraphic and biostratigraphic correlation, and has been the framework for a number of paleoenvironmental studies (Brett and Baird, 1986 and papers therein; Bordeaux and Brett, 1990; Bartholomew and Brett, 2007; VerStraeten, 2007; Zambito, 2013).

Another proxy for relative depth in the Middle Devonian Appalachian Basin is the use of microendolith suites. Microendolithic borings (primarily algal, fungal, and bacterial borings) have been studied along known depth gradients in modern environments (Glaub and Bundschuh, 1997; Glaub et al., 2007). Fossil microendoliths assemblages provide a light sensitivity proxy that can allow samples to be placed in shallow euphotic, deep euphotic, and dysphotic settings.

This provides a proxy for both turbidity and relative depth along the gradient, and can be used independently of sequence stratigraphy to position samples along a depth gradient (Glaub et al., 2007, Vogel and Brett, 2009). Patterns of microendolith distribution have been used to establish ichnocoeneses along ancient paleodepth gradients (Vogel et al., 1987; Glaub et al., 2007). Vogel et al. (1987) studied microendolithic boring communities in the Middle Devonian Hamilton Group of New York State. In combination, microendolith suites, sequence stratigraphy, and biofacies analysis provide a substantive framework upon which to analyze patterns of sclerobionts and permits the assignment of sampled units to relative depth and euphotic zonations. Smrecak and Brett (2014) established sclerobiont patterns in the Ordovician-aged Cincinnatian Arch region that independently reflect the relative euphotic zonations established by microendoliths, affirming the ability to use sclerobionts to discern gradients independent of other biological and physical parameters.

Sequence stratigraphy and biofacies analysis also function as effective proxies for sedimentation rate. Hardgrounds and maximum flooding surfaces record times of very low sedimentation, while the middle highstand systems tract is characterized by a rapid influx of sediment into the corresponding basin, sometimes accompanied by dysoxic or anoxic conditions (Brett, 1995). For this reason, units deposited during highstand systems tracts have been known to yield lagerstätten-style preservation. A multi-proxy approach to interpreting paleoenvironmental conditions has shown success across the Middle Devonian Appalachian Basin (e.g. Brett and Baird, 1996; Bartholemew, et al. 2006) and methods used in the Appalachian Basin have provided a baseline for interpretation of less commonly studied intervals (e.g. Bartholemew and Brett, 2007; VerStraeten et al., 2011). Biofacies analysis in the Middle Devonian Appalachian basin has been used to discern depth as well as low- and high-

sedimentation samples (Brett, 1990; Brett et al., 2007). Therefore, samples collected in the Middle Devonian Appalachian Basin could be assigned a background sedimentation or high sedimentation sample (HSS) designation herein.

METHODS

Appalachian Basin sclerobionts were examined from 18 sampled units collected from south of the I-90 corridor in central New York (Figure 12). Eleven sampled units were collected by the authors in the field, and seven came from collections held at the Paleontological Research Institution (PRI). Field samples were obtained from approximately thirty centimeter-thick horizons from known stratigraphic locations (Figure 12). The majority of field and museum samples were obtained from horizons that were previously studied for microendoliths by Vogel et al (1987) and reflect depositional changes in strata laterally across the basin. Museum samples were obtained from representative stratigraphic samples collected from known stratigraphic horizons as a part of the Baird and Brett stratigraphic collection held at PRI. Only whole or nearly whole brachiopods found in those samples were included in analysis. Thirty-to-sixty brachiopods were collected from each museum sample or field locality. Museum specimens are reposited at PRI, field samples are currently located in the collections of the Department of Geological Sciences at Michigan State University.

Microendolith suites of Vogel et al. (1987) provided an independent proxy for relative depth/turbidity in the Middle Devonian Appalachian Basin. Samples in this study were grouped into shallow-, moderate-, and deep-zonations, and were coded as background- or high-sedimentation environments.

Host Selection

Host variability was minimized by selecting the brachiopod taxa that were present in most of the samples. The brachiopods *Athyris*, *Tropidoleptus*, *Strophodonta*, and *Mucrospirifer* fulfilled this criteria. Generally one brachiopod genus was analyzed per sampled unit. If at least 20 specimens of multiple genera were present within a sampled unit, two or three brachiopod genera were used to test for inter-host variability patterns in sclerobiont encrustation and to assess if hosts were preferentially avoided by sclerobionts. Size, relief of costae, and presence of punctae on host brachiopods have been suggested to contribute to observed encrustation patterns (e.g. Alexander and Scharpf, 1990; Rodland et al., 2004). Table 8 summarizes the morphological features of select host taxa.

Sclerobiont Data Collection

Brachiopod shells were examined with a dissecting microscope using a magnification of 10 - 30x. Following Smrecak and Brett (2014), the identity and location of each sclerobiont morphotype was recorded on an idealized line drawing of the host. The following data were collected: 1) identity of sclerobiont, 2) estimated areal percent of host valve covered by each sclerobiont, 3) number of each sclerobiont taxon present, 4) location of each sclerobiont on the valve, 5) sclerobiont position relative to other sclerobiont taxa, 6) color of host valve, 7) abrasion of host valve, and 8) fragmentation of host valve. Collection of areal percent coverage followed methods established in the Shelf and Slope Experimental Taphonomy Initiative (SSETI) and applied by Smrecak and Brett (2014). Endoskeletobionts observed were recorded as 'borers' unless they could be readily ascribed to a specific maker (e.g. ctenostome bryozoans).

Encrustation metrics are listed in Table 9. Pedicle and brachial valves of each host were treated independently, therefore the data compiled are and not differentiated by valve type. As

such, any sclerobiont taxon preference for a cryptic or exposed valve surface was not considered herein. Frequency of encrustation reflects the frequency with which a valve, interior or exterior surface, articulated or not, is encrusted upon. Ninety percent of the brachiopods used in this study were articulated and free of matrix, allowing both exterior valve surfaces to be examined.

Sclerobiont taxa were grouped by life habit and growth morphology, and taxonomically when possible, to characterize sclerobiont assemblage compositional trends. Sclerobionts were identified to genus when possible, or given a distinct morphotypic assignment. Morphotypes were commonly assigned to bryzoans (e.g. trepostome mA) based on characteristics like zooecial shape and size and colony morphology.

Multivariate analyses were conducted using areal percent coverage data from each sample with PAST software (Hammer et al., 2001). Cluster analysis was run on data compiled from all samples using PAST software (Jaccard) to characterize the relationships among and between sclerobiont samples collected along the depth gradient. Detrended correspondence analysis and principal coordinate analysis (Jaccard) were conducted in PAST to characterize sclerobiont encrustation patterns associated with depth and sedimentation. ANOSIM was used with areal percent coverage data to test if inter-sample variation was greater than intra-samples for each depth zone.

RESULTS

Encrustation metrics are defined in Table 9 and characterized by depth and by sample in Figure 13 and Table 10. Metrics were also averaged at each depth both by including and omitting samples characterized as high sedimentation localities (HSS).

Multivariate Analyses

When HSS were omitted, ANOSIM showed statistically significant dissimilarity between groupings (r=0.637, p=0.0443). Pairwise ANOSIM (Clarke, 1993) shows differences, though not statistically significant, between shallow water samples (SWS) and deep water samples (DWS) (r=0.846, p=0.216). When HSS were integrated into depth zone sample groups, the statistical distinction between the groups was no longer evident (r=0.3498; p=0.0173). However, using pairwise ANOSIM, SWS and moderate water samples (MWS) showed some difference (r=0.5021; p=0.007) and MWS and DWS were also dissimilar (r=0.601; p=0.025). HSS samples displayed wide variation with respect to encrustation metrics such as relative abundance, areal percent coverage, and frequency of encrustation (see Table 10) regardless of depth designation. Four sclerobiont taxa (two bryozoan morphotypes, paleotubuliporids, and sponge remnants) were only present in samples designated HSS. In addition, HSS commonly included sclerobiont taxa that were particularly dominant in a given depth zone, suggesting they may be hardy taxa. For example, the cystoporate bryozoan mM (tentatively identified as holdfasts of Sulcoretepora) and encrusting foraminifera mT occur only in SWS and HSS, whereas the ptylodictinine bryozoan form mX occurs exclusively in deep and high sedimentation samples. Because sclerobiont taxa that were otherwise depth-restricted also occurred in HSS, the statistical power of ANOSIMsupported groupings was weakened when high sedimentation samples are included.

Sclerobiont Suite Differences with Depth and Sedimentation

Q-mode cluster analysis (Figure 14) grouped most DWS (Jaccard), separating them from a cluster of SWS and MWS. An additional cluster of two SWS (Samples 20 and 22) and a MWS (Sample 29) was also observed. MWS 18, *Tropidoleptus* Subsample of MWS 18, and MWS 28 clustered together at greater than sixty percent, and were grouped with a SWS cluster consisting

of SWS 26 and *Atrypa* Subsample of SWS 26. The observed grouping between MWS and SWS was also recorded in PCO (see Figure 15).

DWS 12 and 13 grouped together in both cluster analysis and PCO (Figures 14, 15), and along with DWS 14 were collected in the far western portion of the Appalachian Basin in the Ludlowville (Figure 12). Sample 14 is a DWS with relatively high areal percent coverage, richness, and frequency of encrustation for deep water facies (Table 10), driven partly by high auloporid coral encrustation. Sample 12 was unique in that it had the highest observed richness in this study. The higher encrustation metrics observed at DWS 12 and 14 and their proximity to each other in the distal portion of the basin may explain why some similarity measures group DWS 14 with other DWS, and why DWS 12, 13, and 14 cluster separately from other deep samples in other multivariate analyses.

Principal Coordinates Analysis (PCO) was used to test whether spatial abundance of sclerobiont taxa (the areal percent coverage encrustation metric) was able to discern relative depth zonations. PCO axis 1 (Figure 15) accounted for sixty-six percent of the variance and arranged samples generally from shallow to deep, SWS falling on the left side of axis one, MWS in the center, and DWS on the right side. The spread along axis two may be the result of a combination of faunal composition and overall sample richness. Samples with unusually high richness (e.g. greater than 15 sclerobiont forms) plotted higher on axis two, and those with markedly lower richness (e.g. less than five sclerobiont forms) plotted low on axis two.

Some samples did not fall predictably in PCO. MWS 29 grouped with SWS in cluster analysis and plotted with them in PCO. The MWS *Mucrospirifer* Subsample 28 plotted near DWS on axis 1. Sample 21 and Sample 27 (DWS) were collected from localities in the central portion of the basin near the collecting localities of most MWS. These two samples grouped high

on axis 2 and closer to MWS. *Strophodonta* subsample 28 (MWS) and the Sample 4 (DWS) nearly overlap in PCO. Both samples showed very low richness – three and two sclerobionts, respectively – and had low areal percent coverage.

Samples from HSS did not plot together, nor did they consistently plot with other samples from the same depth designation. Usually they plotted toward the shallow side of axis one. The HSS DWS and subsamples of Sample 19 grouped with SWS. DWS 19 and its subsamples showed very high richness, higher than all but one SWS (Table 10). The HSS from SWS and MWS that showed very low encrustation (Samples 15 and 17, respectively) plotted near DWS. HSS SWS 23, however, plotted near other SWS. Sample 23 did not have high areal percent coverage or relative abundance, but richness and taxonomic composition in Sample 23 closely reflected values observed in other shallow samples.

Detrended correspondence analysis (DCA) grouped samples according to their respective depths. A depth gradient is visible on axis one (56% explained; Figure 16). Samples from DWS plotted to the left and samples from SWS plotted to the right. Significant overlap between MWS and DWS was evident in the center of the graph. Sample 19 (HSS, DWS) plotted with SWS in PCO, but in DCA, both the *Mucrospirifer* and *Athyris* subsampled hosts found in Sample 19 grouped with other DWS. HSS SWS were treated similarly by both PCO and DCA. An outlier unique to DCA was a *Mucrospirifer* subsample of Sample 26 (SWS); it plotted unusually high on axis two and aligned with DWS on axis one. PCO and cluster analysis both placed *Mucrospifer* Subsample 26 with other SWS. Taxonomically, this sample resembled other SWS, but encrustation metric values were generally depressed (Table 10).

Areal Percent Coverage

Host brachiopod areal percent coverage in shallow-, moderate-, and deep- samples are provided in Table 10. There was a decline in areal percent coverage with depth, although the differences between shallow- to moderate- and from moderate- to deep- were not significant. When an outlier with uniquely high encrustation was removed (DWS 12), the difference between SWS and DWS encrustation was statistically significant. Sample 12 had much higher sample richness and areal percent coverage than other deep samples, and had higher richness than any other sample in this study.

Values of areal percent coverage were generally low in all depths, declining from 4.31% in SWS to 2.48% in MWS and 1.25% in DWS. HSS had slightly higher areal percent coverage values, and when these samples were removed, these values were further depressed (Figure 13, Table 10).

Nearly half of the encrusted area on host brachiopods in SWS was covered by hederellids (Figure 17). In DWS, hederellids only covered five percent of the encrusted area. Forms of *Ascodictyon* and *Allonema* encrusted increasingly more area on host shells with depth. This is true whether HSS were included or not, suggesting that depth was the primary control on spatial coverage by these taxa. Bryozoans encrustation increased with depth. In SWS, bryozoans covered very little area on host valves (around 3-5%), even though they were colonial organisms with potentially large spatial footprints. Trepostomes encrusted an average of 1-3% in samples from all depth zones, though they were more common in deeper water. Fistuliporids were uncommon in SWS and nearly absent in MWS, but covered twelve percent of encrusted host brachiopods in DWS. Holdfasts and unidentifiable encrusters covered a consistent, if low, percentage of valves despite changing depth.

Sclerobiont Relative Abundance

Brachiopod host valves in SWS were encrusted by an average of 1.57 sclerobionts (STDV 0.25), those in MWS by 0.72 sclerobionts (STDV 0.23), and those in DWS were encrusted by 0.60 sclerobionts (STDV 0.24). SWS relative abundance was statistically significantly different from both moderate and deep samples, but MWS and DWS were not significantly different. The difference between SWS and DWS increased when the outlier Sample 12 (see Areal Percent Coverage, above) was removed from the deep group, but was not significant.

Sclerobiont relative abundance data were also be grouped according to generalized forms to compare settlement success in different depth zones (Figure 17). This grouping permitted direct comparison between the spatial composition (areal coverage, Figure 17A) and numerical composition (relative abundance) of sclerobiont taxa in each environment. In SWS, sponge and other organic remnants were the most commonly observed sclerobionts, followed by forms of *Ascodictyon* and *Allonema*. MWS and DWS were dominated by borings, endobionts that comprised over 50% of the observed bionts in those samples. Tube-dwelling organisms, which include a broad taxonomic group of solitary microconchids, cornulitids, and vine-like tubuliporate bryozoans, were the next most commonly observed sclerobionts in moderate and deep samples.

Sclerobiont Richness

Forty-four sclerobiont forms occurred in the 18 samples observed. Sample richness varied widely: some samples had as few as two or three sclerobiont forms present; others have up to 18 or 20 different sclerobiont forms present (Table 10). Sclerobiont richness was highest in MWS; an average of 13.25 sclerobiont forms were present on average in a sample (STDV 3.71),

but MWS also displayed high variability. MWS were slightly less rich, with an average of 13 sclerobiont form taxa present in each sample (STDV 3.94). Deep samples had an average of only 8 (STDV 1.98). Sclerobiont richness in SWS and MWS differed significantly from those in DWS.

Average per-host richness ranged between 0.80 and 1.10 in samples from all environments. The differences between samples from all depths were not significant, despite very high maximum per-host richness values on shells in some samples – 6 or 7 different sclerobiont forms on one host. Both SWS and MWS were more likely to record avariety of sclerobiont forms on a single host than hosts collected from DWS.

DWS 12, a sample from the distal portion of the Appalachian Basin, had the highest richness observed in the study. Sample 12 hosted 20 sclerobiont taxa and incorporated 44% of the observed sclerobiont taxa in the study. The next highest sample richness was found in Sample 18 (MWS), with 19 sclerobiont taxa, then from Sample 19 (DWS, HSS) with 18 sclerobionts present. A subset of *Strophomena* hosts in Sample 18 (MWS) had only 3 sclerobionts present. Samples from MWS displayed variable richness. In contrast, SWS consistently showed 30% of the observed sclerobionts (see Table 10).

Frequency of Encrustation

As with areal percent coverage and relative abundance, frequency of encrustation decreased with depth (Figure 13). The decline from SWS, which were encrusted 62% of the time, (STDV 0.07) to MWS, of which 54% were encrusted (STDV 0.10), was not significant. Only 41% of DWS brachiopods were encrusted (STDV 0.19); significantly less than the frequency of encrustation observed in brachiopod samples from SWS.

DISCUSSION

A recent review of sclerobiont encrustation patterns across depth gradients in different regions and during different geologic time periods documents predictable declines in with depth (Brett et al., 2012). Not all encrustation metrics were assessed in every study, and taxonomic composition of sclerobiont assemblages inherently changes through time, but it is apparent that sclerobiont assemblages are sensitive sclerobiofacies proxies capable of discerning relative depth zonations. Sclerobionts may also secondarily record turbidity levels (Mistiaen et al., 2012; Smrecak and Brett, 2014).

Research on sclerobiont assemblages has generally been limited to those regions where encrustation is fairly ubiquitous across formations, hosts, and inferred environments (e.g. Cincinnatian of Ohio, Kentucky, and Indiana) or on units expressing unusually high encrustation (e.g. the Silica Shale). Particular units within the Middle Devonian Appalachian Basin appear to have these epibole-quality sclerobiont facies (e.g. the Kashong Shale, Bordeaux and Brett, 1990), but as evidenced herein, when examined across the Appalachian Basin, heavy encrustation was not ubiquitously observed. Sclerobiont assemblages can be used to discern both depth and sedimentation/turbidity in the Appalachian Basin. Moreover, the Middle Devonian Appalachian Basin records less encrustation than other regions (see discussion below, Table 11), yet the paleoenvironmental signals provided by sclerobionts are discernible.

The reason for lower encrustation in the Appalachian Basin may lie in its proximal position to the Acadian Mountains. The impact of sedimentation is difficult to decouple from other paleoenvironmental factors, like nutrient availability, because sediment and nutrient load are both incorporated into marine environments by runoff. Both the sequence stratigraphic (Brett, 1995; VerStraeten, 2007) and microendolith suites (Vogel et al., 1987) provide independent

evidence of turbidity that may or may not correspond to increased nutrient load. However, the tectonic pulses may have provided sediment influx from erosion of the highlands that swamped impacts of eutrophication on sclerobionts within the basin (Ettensohn, 2004, 2008).

Three distinct sclerobiont assemblages can be described from the Middle Devonian Appalachian Basin. Commonalities exist between them and their HSS counterparts, but the impact of sedimentation on sclerobiont assemblages is observable, and has also been characterized below.

Sclerobiont Assemblage I – Shallow Facies

SWS were characterized by 1.56 scleorbiont individuals covering 4.3% of host brachiopod valve surfaces. Over 60% of valves were encrusted by one or more sclerobionts by an average of 13 different sclerobiont taxa. Taxonomically, shallow water sclerobiont assemblages were heavily dominated by hederellids, in particular hederellid A, which accounted for 40% of the encrusted area on host valves. Forms of *Ascodictyon* and *Allonema* (especially mB and mK forms), and organic remnants that resemble algal crusts were also most common in SWS (Figure 17). The cryptostome (?) bryozoan mE (tentatively identified as *Paleschara*), the trepostome mM, and a foraminifera mT occurred only in shallow facies not influenced by influxes of high sedimentation rates and turbid waters. Borings were a trivial component of both relative abundance and areal percent coverage of shallow sclerobiont assemblages.

Sclerobiont Assemblage II – Moderate Facies

Sclerobiont assemblage II is characterized by an average of 0.80 individual sclerobionts encrusting 2.5 percent of host brachiopod valves. Over 50% of valves examined are encrusted. These values are consistently lower than those observed in Sclerobiont Assemblage I. Per-host and average richness in Sclerobiont Assemblage II is nearly as high as Sclerobiont Assemblage I,

but is markedly more variable (Figure 13). Most other studied sclerobiont depth gradients (see discussion in Brett, et al, 2012) showed decreasing richness with depth in sclerobiont encrustation independent of geography or age.

Dominant taxonomic groups in Sclerobiont Assemblage II are similar to observed in shallow facies, but differ proportionately – hederellids (18%), organic remnants (21%), and tube-dwelling organisms (21%) – are equally common in Sclerobiont Assemblage II. In the Shallow Assemblage I, hederellids encrusted nearly 40% of hosts, while the other sclerobiont taxa encrusted only 14% of host surfaces combined. Although not abundant, the trepostome bryozoan mV, the cystoporate bryozoan mL, and crinoid holdfasts occurred only in Sclerobiont Assemblage II. In contrast with Sclerobiont Assemblage I, borings, including the common taxon *Vermiformichnus*, comprised over fifty percent of observed encrusters in Sclerobiont Assemblage II (Figure 15). Borings were more commonly observed in Sclerobiont Assemblage II than in any other sampled environment. Areal percent coverage in Sclerobiont Assemblage II is far lower than observed in the samples from a particular MWS unit of Bordeaux and Brett, (1990), and from equivalent facies using a different methodology (unpublished data; Brett et al, 2012), but their measured richness and taxonomic composition was consistent with data herein (Table 10).

Sclerobiont Assemblage III – Deep Facies

Samples from the deepest water environments were consistently grouped together regardless of similarity metric used, supporting the conclusion that sclerobiont assemblages from the Appalachian Basin track water depth. Sclerobiont Assemblage III is characterized by less than 2% of valve surfaces encrusted by an average of 0.62 individual sclerobionts. This was significantly less than observed in Sclerobiont Assemblage I, and was consistent with trends

observed by Bordeaux and Brett (unpublished data) (Table 11; see discussion below). Sample richness in Sclerobiont Assemblage III was significantly lower than the other facies. Fewer than nine sclerobiont taxa were present in any given sample. Less than half of the surfaces examined in this zone were encrusted. Hosts that were encrusted had an average richness 20% lower than Sclerobiont Assemblages I and II, and maximum richness was significantly lower (Figure 13). In addition to significantly lower values in almost all encrustation metrics, Sclerobiont Assemblage III harbored an entirely different suite of sclerobionts. *Ascodictyon* and *Allonema* forms were the dominant surface area encrusters, followed by fistuliporid and ctenostome bryozoans (Figure 17). In Sclerobiont Assemblages I and II these taxa were very minor areal components of sclerobiont assemblages. Sclerobiont Assemblage III encrustation patterns were consistent with those of Bordeaux and Brett (1990) and trends observed in deep facies as generalized by Brett et al (2012).

The Impact of High Sedimentation on Sclerobiont Assemblages

Sclerobiont encrustation metrics described herein allow meaningful and predictable encrustation patterns to emerge along an idealized Middle Devonian depth gradient in the Appalachian Basin. Secondary patterns likely related to sedimentation and sequence stratigraphic depositional conditions have emerged, as well.

Sclerobiont assemblages from shallow and deep water HSS facies share some affinity with their respective Sclerobiont Assemblages I and III. In PCO, HSS plotted generally on the shallow side of axis one. Both SWS 23 and DWS 19 and subsamples showed higher than average richness that was consistent with other shallow-water samples (Figure 15, Table 10). DCA, however, plotted HSS more variably (Figure 16). Samples 19 and 23 still plotted with other SWS, but Sample 19 subsamples *Athyris* and *Mucrospirifer* plotted with other DWS. DCA

appears to have been more sensitive to differences in sclerobiont assemblages driven by brachiopod hosts than to impacts of sedimentation.

HSS SWS shared more taxonomic affinities with Sclerobiont Assemblage II.; both were dominated by hederellids, organic remnants, *Ascodictyon* and *Allonema* forms, and tubedwelling organisms. HSS DWS, however, showed some taxonomic differences to that seen in Sclerobiont Assemblage III. HSS DWS was similar to Sclerobiont Assemblage III in that 35-40% of covered host surfaces were dominated by forms of *Ascodictyon* and *Allonema*, but lacked most other characteristic taxa. Fistuliporid and ctenostome bryozoans, very common in Sclerobiont Assemblage III (Figure 17A), were nearly absent in HSS DWS. Other sclerobiont taxa, were only present in the HSS DWS environments. For example, tubuliporid bryozoans and the monticulated trepostome mS occurred only in DWS with high sedimentation.

HSS DWS had substantially higher relative abundance than their counterparts from lower sedimentation environments; the difference between them was statistically significant (Figure 13). This trend is consistent with other observed encrustation patterns in the Middle Devonian Appalachian Basin (Bordeaux and Brett, 1990), and with patterns observed comparing sclerobiont assemblages on hardground fauna to those on soft-bottom fauna (Smrecak, 2013). Despite this, areal percent coverage in HSS DWS was the lowest observed (Table 10).

With respect to areal percent coverage, high sedimentation depressed encrustation in deep environments and enhanced it in shallow environments. Sclerobiont encrustation should be depressed when sedimentation is increased, as the presence of sediment on a host can prevent larval settlement, and the filter-feeding sclerobionts already established may be negatively impacted by increased sediment. Thus, HSS DWS predictably displayed the lowest encrustation observed (Table 10). Yet HSS SWS samples showed the highest areal percent coverage values in

this study, 6.66%, which was significantly higher than that seen in Sclerobiont Assemblage I (Table 10). The higher areal percent coverage in HSS SWS could reflect the impact of sedimentation abrading some sclerobionts and providing room on the host for additional encrustation, or reflect an increase in nutrient availability that accompanies increased turbidity. High areal coverage in HSS samples was primarily driven by one of the two sampled units collected from the Kashong Shale, but has been observed in other research (Bordeaux and Brett, 1990), and suggests that conditions in the Kashong Shale were uniquely suited to sclerobiont encrustation. More work is needed to understand the discrepancies observed in encrustation among the Kashong Shale and other units.

Sample richness was positively impacted by increased sedimentation. HSS SWS recorded higher sample richness than Sclerobiont Assemblage I, III and HSS DWS. Only MWS recorded higher sample richness. HSS DWS had higher sample richness than deep samples, as well. Thus, it appears additional sedimentation cultivated the potential for a wider variety of sclerobionts to establish themselves on a host, despite their later success or failure. It may also be that most larvae were not preferentially seeking particular depth regimes, but were only looking for a preferred microhabitat (e.g. cryptic or within current) (Taylor and Wilson, 2003). The incumbent larvae's later success by any measure (i.e. areal coverage, relative abundance) would be the result of a combination of environmental factors, not effective larval settlement. This argument is also supported by the observation that maximum per host richness was higher when sedimentation increased, regardless of the inferred depth from which samples were taken (Table 10). Additionally, holdfasts increased in areal percent coverage in the HSS DWS, showing nearly twice the covered surface areas as they did in any other observed facies. This indicates success by those forms able to rise above the sediment-water interface.

The variation in other encrustation metrics lends credence to the use of areal percent coverage as a primary tool for assessing sclerobiont encrustation patterns, with support from other metrics like relative abundance and richness. Both relative abundance and richness were markedly impacted by fluctuating environmental conditions, but areal percent coverage appeared to consistently reflect long term environmental conditions, e.g. relative depth. Variations introduced by high sedimentation merely drove high areal percent encrustation values higher and low values lower (Table 10). Frequency of encrustation was depressed slightly in both HSS SWS and DWS when compared with samples from Sclerobiont Assemblages I and III (Table 10), and was most sensitive to changing depth regimes.

Richness may also have responded to the sample's position stratigraphically. The observed spread in PCO on axis 2 (Figure 15) was likely driven by sclerobiont richness. The underlying cause for the difference in richness may have been the overall increase in sediment or turbidity during the times those samples were being deposited. Almost all sampled horizons that fall at -0.80 or below on axis 2 in PCO were deposited in the middle to upper portion of the highstand sequence tract (Brett and Baird, 1996; Brett et al., 2011b). In the siliciclastic-dominated environments of the Appalachian Basin, sclerobiont encrustation might be predicted to be lower during the highstand systems tract because of the release of sediment that was previously trapped landward by rising sea level (Brett, 1998). Thus, during the highstand, environmental conditions were more turbid across the basin, and increased sediment funneled into the basin may have covered host shells or precluded more sensitive sclerobionts from encrusting before a diversity of encrusting fauna could develop.

Areal percent coverage for those samples that plotted low in PCO showed reduced encrustation when compared to the average for SWS and MWS. Average areal percent

encrustation for SWS 20 and 22 was 2%; Sclerobiont Assemblage I documented areal percent coverage at 2.4%. *Rhipidomella* SWS 26 was not included because it was interpreted to have been deposited during a transgressive sequence tract. Other samples from the same horizon plotted in the upper portion of Figure 15. The average areal percent coverage value for the four moderate samples that plot below -0.08 of Figure 15 was around 1.4%, lower than the average observed 2.43% when all moderate samples were considered together. It appears that sclerobiont richness and areal percent coverage responded to basinwide increases in sedimentation.

Comparison with Other Work

This work documents the ability of sclerobiont assemblages to discern depth and sedimentation in the Appalachian Basin, and permits comparison between other Middle Devonian sclerobiont assemblages geographically, and other sclerobiont assemblages temporally.

Sample collection localities were originally selected to represent varied depths and sedimentation rates based upon sequence stratigraphy and biofacies (Bartholomew et al., 2006; VerStraeten, 2007), and suites of light-sensitive microendoliths (Vogel et al., 1987). These groupings were evidenced in cluster analysis. PCO and DCA support and refine these groupings, even when HSS SWS and DWS were incorporated into the analysis. These relative depth groupings, based on sclerobiont areal percent coverage data, emerged regardless of the type of host brachiopod used as substrate in the sample, and despite a lateral facies change from a siltier facies to a more condensed, argillaceous facies. Only localities with evidence of unusually high sedimentation rates as compared to the other samples in this study show discernable differences in encrustation patterns. Within these samples, the patterns are most significant in DWS.

Sclerobiont Assemblage I was characterized by relatively high values in all encrustation metrics, and this is consistent with other studies. Sclerobiont Assemblage I, however, has significantly lower encrustation than has been recorded in other work (Table 11), and Sclerobiont Assemblages I and II had lower than expected areal percent coverage during times of highstand sequence stratigraphic conditions. The lowered encrustation observed basinwide may be attributed to the higher sedimentation observed within the basin, but increased sedimentation locally appeared to increase encrustation, specifically in the Kashong Shale (Bordeaux and Brett, 1990).

Bordeaux and Brett (1990) conducted sclerobiont research on *Spinacyrtia* samples in the Appalachian Basin collected from the Middle Devonian Kashong Shale. In the same lithologic unit, Bordeaux and Brett (1990) documented much higher areal percent coverage by sclerobionts, 20 to 30 percent areal coverage of hosts compared to 6.66% in this study. However, other encrustation metrics observed by Bordeaux and Brett (1990) were consistent with the present study, showing an average richness of sixteen sclerobiont form taxa, and an average of 1.9 sclerobionts per valve. Taxonomically, sclerobionts observed in Bordeaux and Brett (1990) and this work were also consistent (Brett et al., 2012; Table 11). The method employed to estimate sclerobiont coverage likely overinflated encrustation and significantly contributes to the differences observed (Brett, *pers. comm.*).

The Middle Devonian Michigan Basin – Most notably, areal percent coverage and relative abundance of sclerobiont assemblages are markedly lower in the Appalachian Basin than in the coeval Michigan Basin, especially in shallow facies (SWS; see discussion below). The Appalachian Basin was a deeper, cooler, and more turbid basin than the Michigan Basin, and was also faunally distinct in terms of the macrobenthic assemblages (Bartholomew and Brett,

2007). Michigan Basin sclerobiont assemblages more closely mimic patterns observed with decreasing paleodepth (Smrecak and Brandt, *Chapter 1*) (Table 11) than do Appalachian Basin sclerobiont assemblages. It is therefore apparent that, basinwide, some paleoenvironmental factor apart from depth was mitigating sclerobiont encrustation in the Appalachian Basin.

HSS SWS recorded the highest observed areal percent encrustation, at 6.66%. This value is lower than observed in the shallow facies shown in a number of studies discussed by Brett et al. (2012), and lower than correlative units in the Michigan Basin (Smrecak and Brandt, *Chapter 1*). At 11%, the Kashong Shale Sample 15 has the highest observed areal percent encrustation in this study, and was also nearly twice as high as almost any other studied sample observed in this work. Eleven percent areal coverage was exceptionally high in this work, but still much lower than values reported in other studies, including the coeval Michigan Basin. Eleven percent encrustation was also, qualitatively, lower than has been observed in other regions during the Middle Devonian (Table 11) (Ager, 1961, 1963; Mistiaen et al., 2012; Kesling et al., 1980; Sparks et al., 1980; Brett et al., 2012; Smrecak and Brandt, *Chapter 2*).

Sclerobiont encrustation patterns in the shallow and moderate facies, and to a lesser extent the deep facies, can be directly compared to work conducted in the Middle Devonian Michigan Basin. Intervals in the Michigan Basin were correlated as extreme distal components of Appalachian Basin units and sclerobionts found within those units can thus be directly compared as proximal and distal analogs. Shallow facies in the Michigan Basin contained host brachiopods that exhibited over three times higher areal percent coverage (15%) than the 4.31% observed in SWS of the Appalachian Basin. Michigan Basin hosts also recorded higher relative abundance, with nearly four encrusters per valve as compared to only 1.8 sclerobionts per valve in the Appalachian Basin. Hosts in the Appalachian Basin also recorded fewer encrusters and

less areal coverage than their corollaries in the MWS of the Michigan Basin, although the difference was less apparent (Table 11).

The Appalachian Basin deep facies represents a deep to dysphotic setting as a result of the migrating foredeep associated with Acadian orogenic activity (Ettonsohn, 2006, 2008). These facies also recorded times of dysoxia and may have contributed to regional extinction events (e.g. Baird and Brett, 2008), although no samples were collected from the deepest portion of this facies in this work. However, some deep samples examined herein showed evidence of pyrite replacement, an indication of dysoxic conditions. No samples collected in the Middle Devonian Michigan Basin record those same conditions, as the basin was inferred to have been shallower; only some units in the Bell Shale provide an analog to DWS in the Appalachian Basin.

Therefore, the deepest portion of the Michigan Basin deep facies represent shallower environments than the deepest portion of the Appalachian Basin DWS. The sclerobiofacies model predicts that the Appalachian Basin DWS will show less encrustation than the DWS in the Michigan Basin.

Other Paleozoic Comparisons— While absolute values of other encrustation metrics, like relative abundance and frequency of encrustation values from the Late Ordovician Cincinnati Arch region were consistent with those observed in the Middle Devonian Appalachian Basin (Smrecak and Brett, 2014; see Table 11), areal percent coverage values observed herein were, again, substantially lower. This trend is also true when work herein is compared to other Middle Devonian sclerobiont studies (e.g. Kesling et al., 1980; Mistiaen et al., 2012) and the Carboniferous of North America (e.g. Lescinsky, 1993; Brett et al., 2012; see Table 11). Even sclerobiont assemblages in modern environments (Brett et al., 2011) show encrustation trends consistent with other studies mentioned and contrasting the observed sclerobiont trends

documented herein (Table 11). Possible explanations for the observed trends include choice of host, turbidity, nutrient availability, and the methods used to collect sclerobiont encrustation data.

Brachiopod Host Preference – In this work, multiple brachiopod taxa were used as substrates. Other researchers, including Smrecak and Brett (2014), Kesling et al. (1980), and Lescinsky (1993), limited their research to a single, ubiquitous host substrate. Bordeaux and Brett (1990) also focused on a taxonomic variety of host brachiopod substrates, but limited their stratigraphic range to a two meter interval in the relatively shallow and turbid Kashong Shale. Bordeaux and Brett's (1990) primary goal was to assess evidence of host preference by sclerobionts. Of the brachiopods used in both Bordeaux and Brett (1990) and this work, Athyris, Devonochonetes, and Mucrospirifer exhibited negligible to slightly negative deviations in frequency of encrustation compared to average observed, and Tropidoleptus and Mediospirifer showed negligible positive deviations in frequency of encrustation. Since the brachiopod taxa used herein were preferentially avoided or encrusted – but only slightly – a minor component of the observed differences in areal percent coverage data between the studies could be attributed to host specificity. It cannot account fully for the observed difference.

Sedimentation and Nutrient Availability – The depositional environment associated with the Middle Devonian Kashong Shale studied in the Appalachian Basin may be, in some ways, unique to the basin. The samples in this work and from Bordeaux and Brett (1990) that were collected from the Kashong Shale were more highly encrusted than observed in other samples across the basin. The locality from which Kashong Shale samples were collected was close to terrigenous source material. The samples were inferred to be from a shallow, high sedimentation environment.

The Kashong Shale was interpreted to be deposited in a more turbid environment (Vogel et al., 1987), but its sequence stratigraphic position in the upper transgressive sequence tract suggests that some component of the sediment could have been trapped inland, perhaps permitting temporary pauses in sedimentation. Conversely, increased turbidity could have been coupled with increased eutrophication during the deposition of the Kashong Shale. The pattern of increased turbidity resulting in higher areal percent coverage and increased diversity in the Devonian was also discussed by Brett et al. (2012), who attributed the observed increase to a boost in productivity associated with eutrophic conditions.

Increased nutrients and sedimentation are incorporated into marine environments by runoff, and sclerobionts observed in higher sedimentation environments in shallow water were positively impacted in terms of areal percent coverage. If sclerobionts responded to nutrient load, sclerobiont assemblages in DWS would have been positively impacted by increased nutrient availability during times of higher sedimentation, but this pattern was not observed. Sclerobiont assemblages from high sedimentation deeper water facies showed less areal percent coverage than those samples from background sedimentation deep water facies (Table 10).

Change in Methodology – A potential difference in the methods used to assess areal percent coverage may account for some portion of the observed variation reported among the studies. Organisms that display runner-type growth patterns, like the hederellids, are difficult to quantify in terms of areal percent coverage (Smrecak and Brandt, Chapter 2). Yet they are particularly common in Middle Devonian sclerobiont assemblages, especially those located in shallow facies. The use of different methods on runner-type organisms like hederellids produce widely varied results (Smrecak and Brandt, Chapter 1) could result in a large disparity in encrustation that is wholly an artifact of the data collection method used.

Smrecak and Brandt (*Chapter 1*) estimated the space actively covered by encrusting organisms, and colonial organisms with runner-type growth patterns put out 'shoots' in multiple directions, thereby gaining access to different regions of a host shell surface while maintaining minimal actual surficial coverage of the host valve. A censusing method that estimates the covered host surface by counting the number of gridded regions on a host in which a given sclerobiont occurs can inflate the recorded amount of surface covered, especially as compared to organisms like sheeting bryozoans and large inarticulate brachiopods (Smrecak and Brandt, Chapter 1). The grid region censusing method was used by Bordeaux and Brett (1990), Kesling et al. (1980), and Sparks et al. (1980). Smrecak and Brandt (Chapter 1), however, used the same methodology as this research and the documented trend of low areal percent coverage in the Middle Devonian Appalachian Basin persisted. Thus, the abundance of hederellids in the study region coupled with differing methodologies may account for a portion of the difference between observed areal percent coverage values in the studies. However, even when consistent methods were applied, the difference remained visible. The differences observed in sclerobiont encrustation patterns when other methods are applied also serves to highlight the difficulty associated with successfully crafting generalizations among sclerobiont studies when varied methods are used.

Samples from the western Appalachian Basin contained hosts with higher areal percent coverage than their facies counterparts in the eastern portion of the basin (Figure 12, Table 10). Hosts collected from deep facies in the western Appalachian Basin were encrusted on an average of at least 1.1% of their shells, and up to 7% in the condensed intervals exposed on the coast of Lake Erie. In contrast, the average areal percent coverage of hosts by sclerobionts in the eastern portion of the basin was 0.37%. Hosts from SWS collected in the eastern portion of the basin

have an average areal percent coverage of 1.63%, while hosts from shallow samples in the western portion of the basin were encrusted on 8.15% of valve surfaces. There was no discernable difference in samples from moderate facies. Despite the apparent proximal – distal trend, sclerobiont assemblages changed in predictable ways along paleodepth.

Although encrustation patterns were generally depressed in the Middle Devonian Appalachian Basin, sclerobiont encrustation successfully recorded changes in relative depth, and can be used to establish a sclerobiont facies gradient, or sclerobiofacies. The depressed areal percent coverage observed in this study, and the observed variations in those patterns associated with areas of high sedimentation, support the claim of Mistiaen et al., (2012) and Smrecak and Brett (2014) that sclerobionts are also sensitive to sedimentation regimes, although this relationship is still not fully understood. Comparing values recorded by encrustation metrics between the proximal, sediment-laden Appalachian Basin and the distal Michigan Basin further supports the ability of sclerobiont assemblages to discern both paleodepth and sedimentation changes.

CONCLUSIONS

Establishing predictable trends in sclerobiont encrustation along a Middle Devonian depth-related gradient and adds to the growing understanding of sclerobiont patterns in different environments through time. Despite comparatively low areal coverage of host surfaces compared to other regional Devonian studies and to trends observed in other environments throughout geologic time, a sclerobiont depth gradient is discernable and strengthens the sclerobiofacies model (Brett et al., 2011; Smrecak and Brett, 2014). Frequency of encrustation and relative abundance of sclerobiont taxa, two easily obtained and commonly used measures of sclerobiont encrustation, are not sufficient for sclerobiont assemblage analysis. These and other encrustation

metrics, however, provide effective supporting data when used in concert with sclerobiont areal percent coverage estimates. Combined, measures of sclerobiont encrustation can be used to successfully establish the relative depth of sampled locations. These results are in accordance with independent depth proxies. Sclerobionts are sensitive to sedimentation, an environmental metric difficult to separate entirely from eutrophic conditions (Brett et al., 2011; Mistiaen et al., 2012), but one that impacts both larval settlement and establishment of sclerobionts. Samples in the distal Appalachian Basin were more highly encrusted, regardless of depth assignment, than their correlative samples in the proximal Appalachian Basin.

Comparison with similar horizons in the extremely distal, coeval Michigan Basin suggests that sediment load played a role in both areal percent coverage and relative abundance of sclerobiont assemblages, and dampened encrustation across the Appalachian Basin. In fully inhabited, diverse environments where biofacies indicators are subtle, sclerobiont assemblages may be effective indictors of a variety of paleoenvironmental conditions. Brachiopods collected from horizons within the highstand systems tract displayed substantially less richness and were less encrusted than those collected during other sequence stratigraphic intervals, likely because of increased sediment.

Middle Devonian Appalachian Basin sclerobiofacies, defined by patterns of areal percent coverage of particular suites of sclerobiont taxa, and supported with sample richness, frequency of encrustation, and relative abundance, provide an effective proxy for paleodepth. Areal percent coverage decreased predictably with depth despite the overall lowered values of encrustation across the Appalachian Basin. Consistent, heavy encrustation by hederellids, for example, is characteristic of shallow water deposition, cornulitid encrustation is indicative of both higher rates of sedimentation and deeper water, consistent with patterns observed in Ordovician

encrusting communities (Smrecak and Brett, 2014), and bryozoan dominance indicates deep water deposition in the Middle Devonian Appalachian Basin. Sclerobiofacies defined in the Middle Devonian Appalachian Basin display patterns that are in accordance with established sclerobiofacies for other geologic and depositional settings (Brett et al., 2012; Smrecak and Brett, 2014), and are useful proxy indicators for paleoenvironmental conditions.

APPENDIX

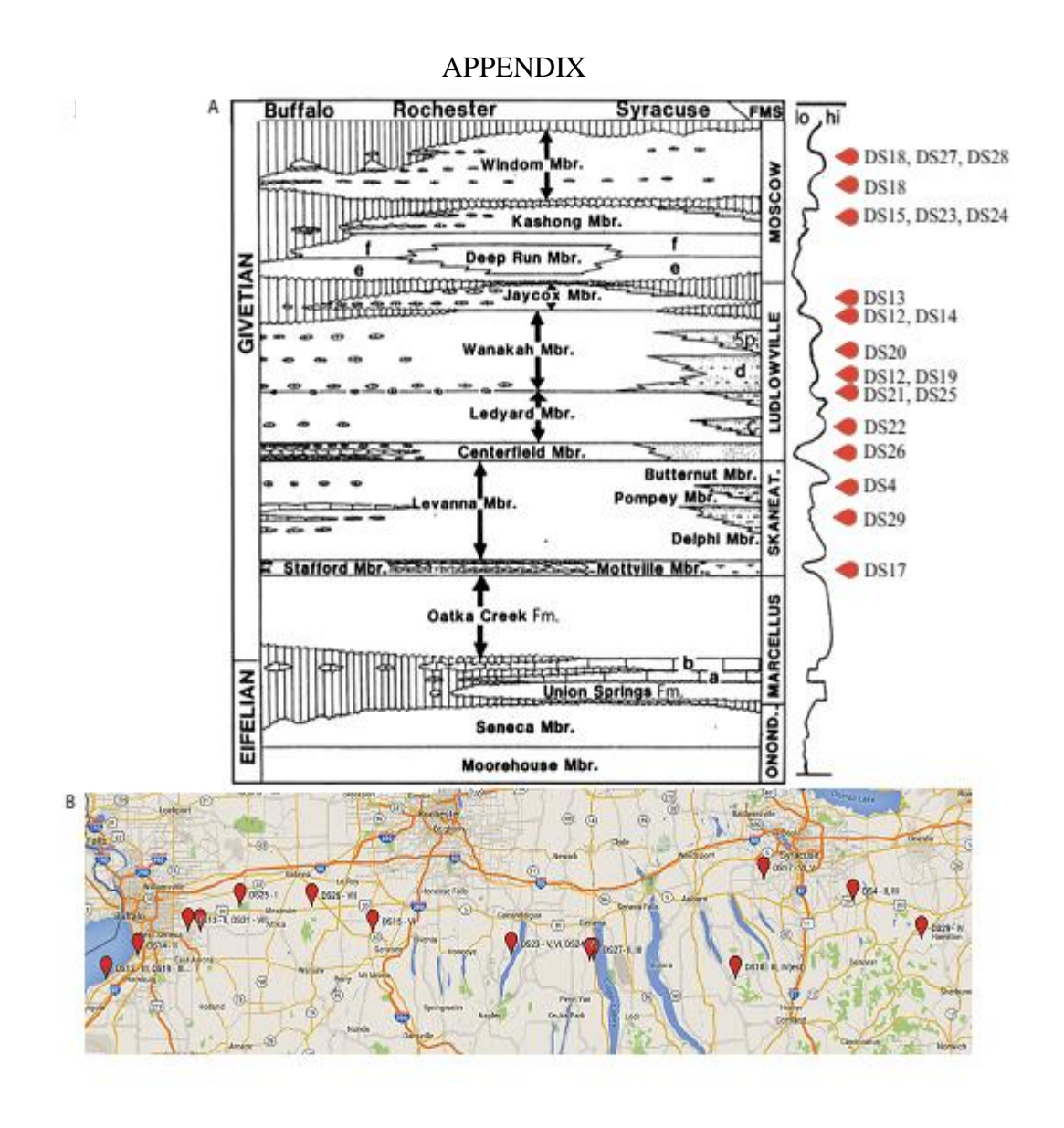


FIGURE 12 – *Appalachian Basin locality information*. Stratigraphic (A) and geographic (B) location of sampled brachiopod hosts (modified from Google Maps). Regional stratigraphy modified from Brett and Baird (1996). Roman numerals indicate depth/turbidity zonation of sampled horizon following Vogel et al. (1987).

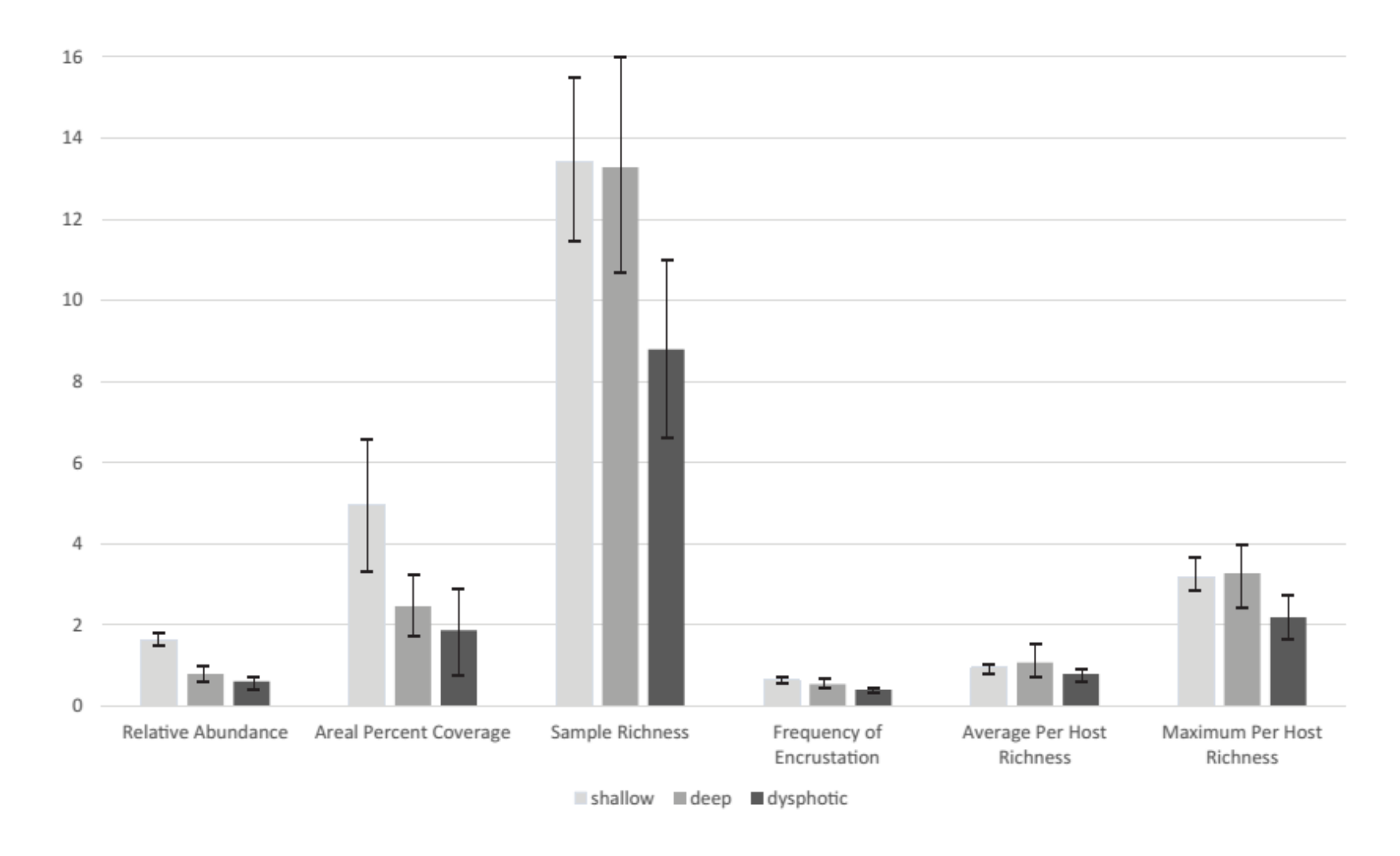


FIGURE 13 – *Averaged encrustation metrics observed in the Appalachian Basin*. Histogram of encrustation metrics averaged from samples within each designated depth zonation. Samples designated to be from high sedimentation environments are included in their respective shallow and moderate facies groupings.

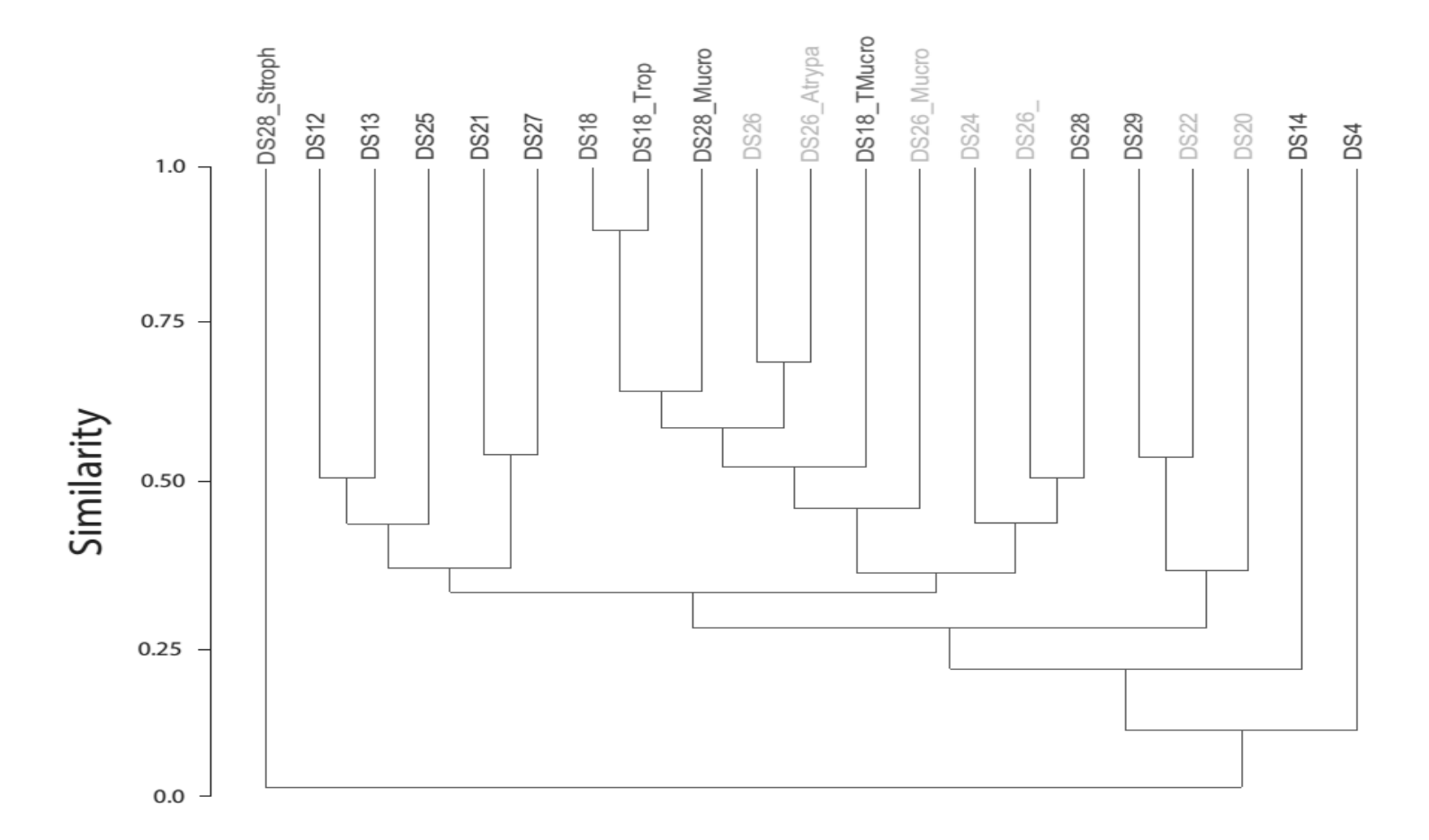


FIGURE 14 – *Cluster analysis of Appalachian Basin samples*. Cluster analysis using areal percent coverage data and Jaccard similarity.

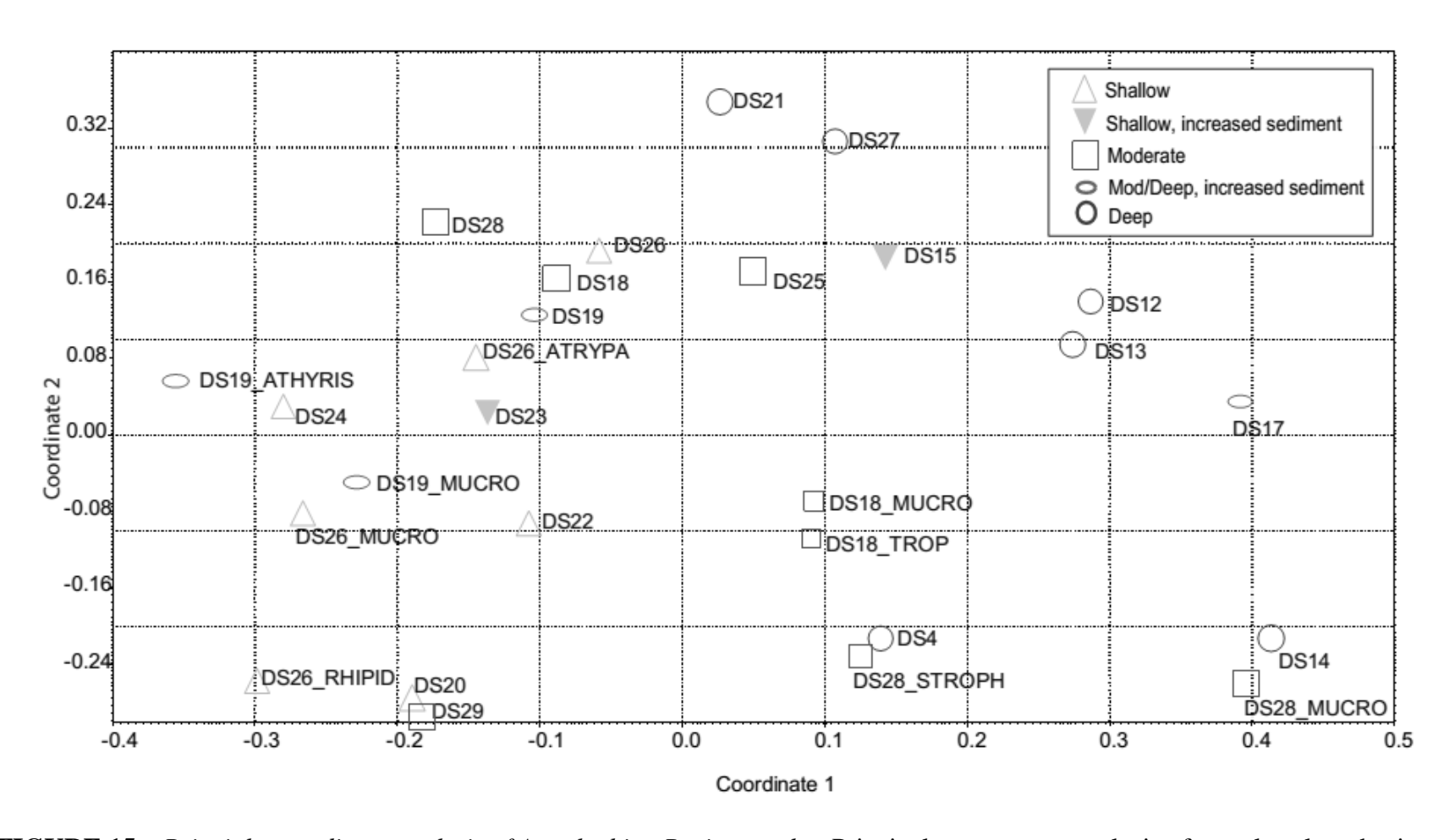


FIGURE 15 – *Principle coordinate analysis of Appalachian Basin samples.* Principal components analysis of samples plotted using areal percent coverage data.

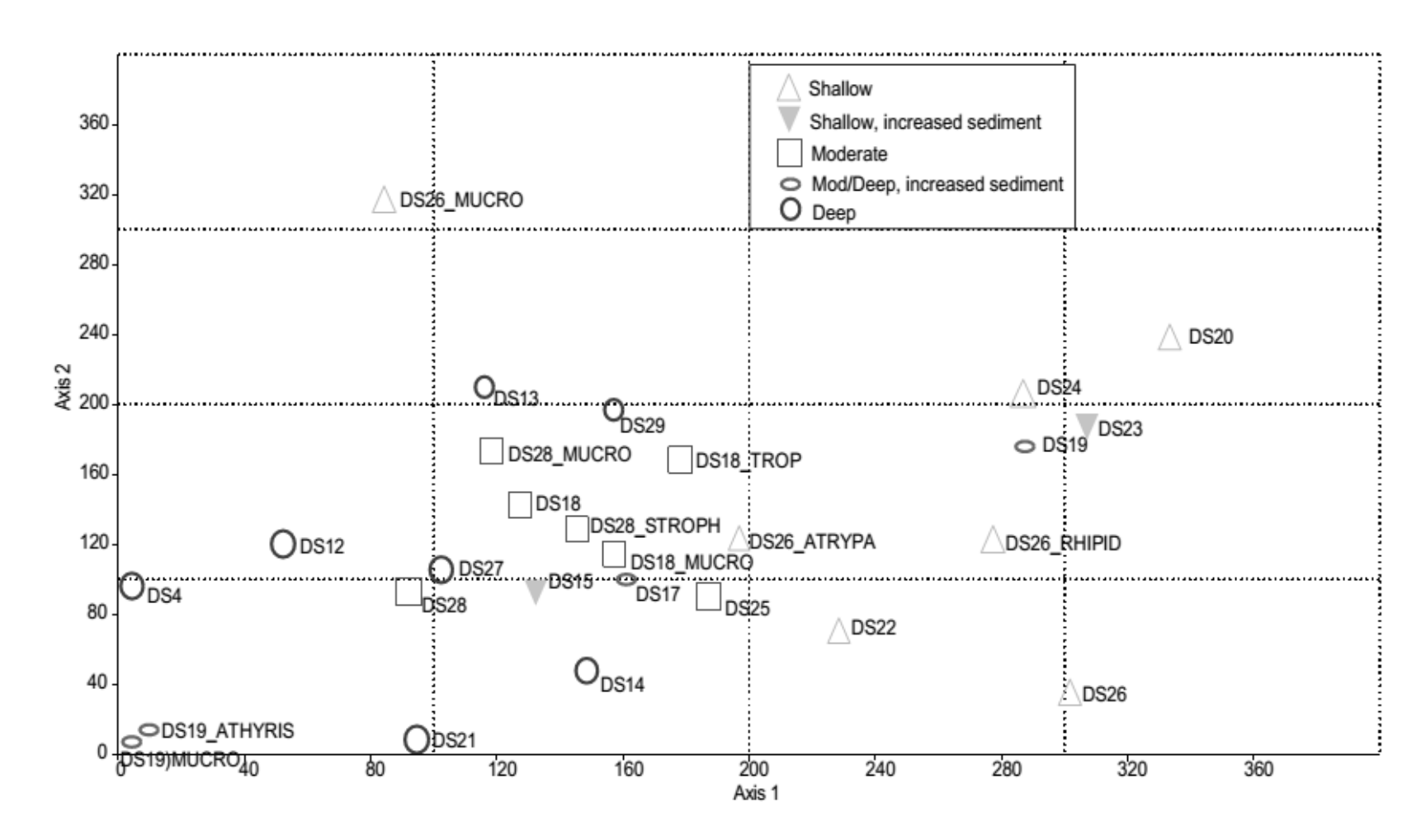


FIGURE 16 – *Detrended correspondence analysis of Appalachian Basin samples.* Detrended correspondence analysis of samples plotted using areal percent coverage data.

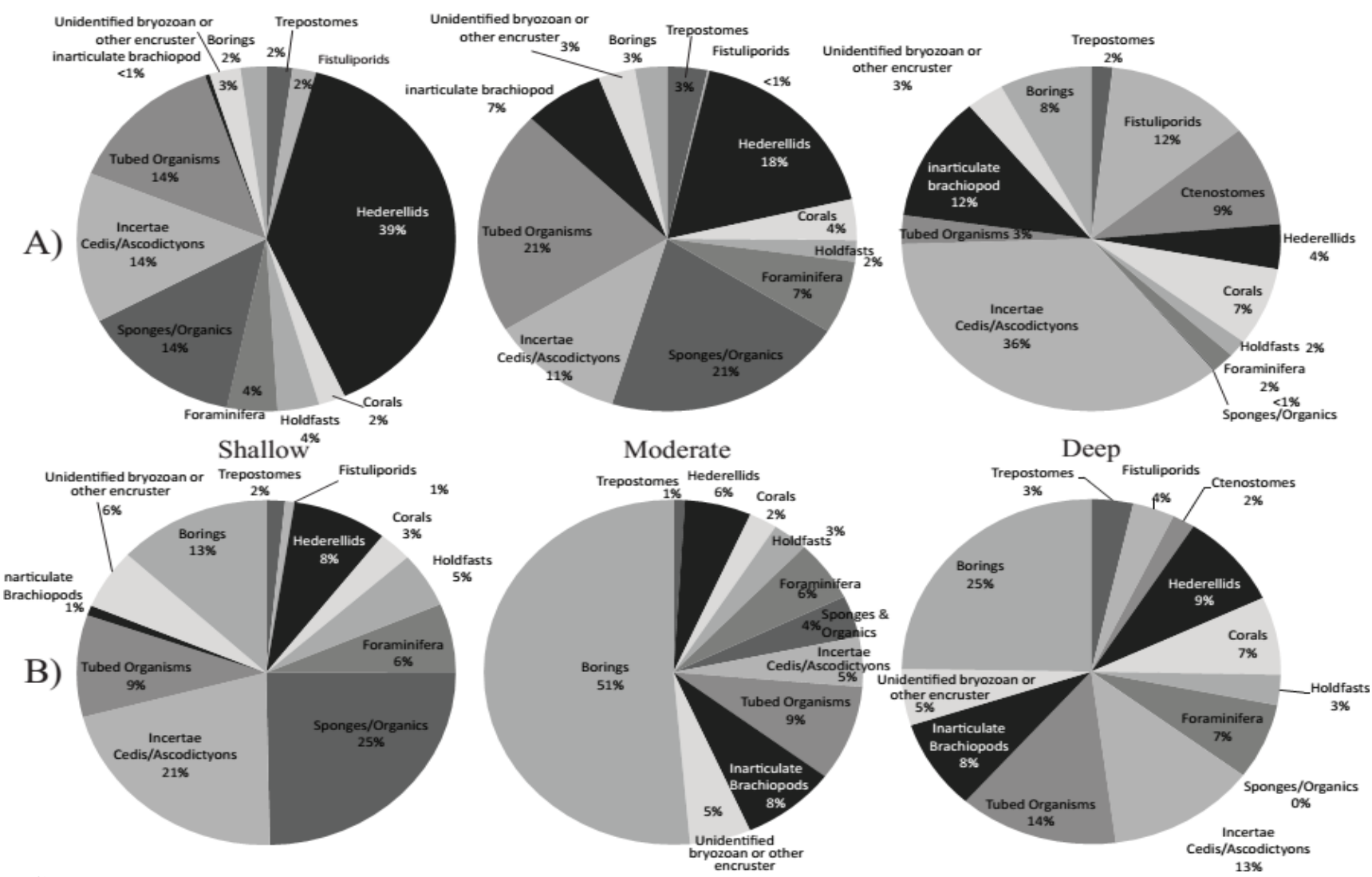


FIGURE 17 – *Taxonomic composition of shallow, moderate, and deep facies in the Appalachian Basin.* Proportion of different sclerobiont forms in different depth zonations based on A) areal percent coverage and B) relative abundance.

	Punctae	Shape	Ornamentation		
Athyris	impunctate	biconvex	smooth		
Tropidoleptus	punctate	concavo-convex	broad costae		
Strophodonta	pseudopunctate	concavo-convex	finely costellate		
			prominent		
Mucrospirifer	impunctate	biconvex	costae		

TABLE 8 – Characteristics of host brachiopods. Data obtained from Kaesler, 1997.

Sclerobiont Encrustation	
Metric	Metric Description
Areal Percent Coverage	The percentage of host shell surface covered by the sclerobiont(s).
Relative Abundance	The number of individuals or colonies of sclerobionts present.
Sample Richness	The number of encrusting taxa observed in a sample.
Richness Ratio	The number of sclerobiont taxa observed in a sample/total number of sclerobiont taxa observed in basin or study region.
Frequency of Encrustation	The number of host shells encrusted/total number of shells observed.
Maximum Per Host Richness	The highest number of sclerobiont taxa observed on an individual host shell substrate
Average Per Host Richness	The average number of sclerobiont taxa on an individual host shell substrate in a sample

 $\textbf{TABLE 9} - Encrustation \ metrics \ definitions.$

			ico	ž	ation thess				
Locality	n	Facies Designation	Sequence Stratigraphic p.	Relative Abundance	Areal Percent Coverges	Sample Richness	Frequency of Encrustation	Average Per Host Richnes	Maximum Per H
DS20	38	shallow		1.75	1.65	20	0.52	1.08	U
DS22	30	shallow		1.10	2.48	15	0.70	0.73	3
DS24	54	shallow		1.49	1.41	10	0.35	0.59	3
DS26	53	shallow		1.29	5.30	16	0.65	0.82	3
DS26_Muc	15	shallow		1.25	2.14	9	0.73	0.50	2
DS26_Rhir	20	shallow		0.85	2.60	8	0.55	1.24	2
DS26_Atry	14	shallow		1.93	9.93	11	0.64	1.98	3
Average S	hallow			1.38	3.64	12.7	0.59	0.99	3.14
DS15	60	high sedir	nentation	3.37	11.01	15	0.73	0.67	5
DS23		high sedir		1.08	2.31	15	0.48	0.73	3
Average H				2.23	6.66	15.0	0.61	0.70	4.00
SHALLOW	3			1.57	4.31	13.2	0.60	0.93	3.33
DS17	57	moderate		0.09	1.16	5	0.07	0.37	4
DS18	112	moderate		0.60	3.73	19	0.64	0.97	4
DS18_Muc	30	moderate		0.43	2.03	12	0.62	0.94	4
DS18_Stro	56	moderate		0.77	5.42	18	0.67	2.32	4
DS28	33	moderate		1.24	1.79	14	0.52	0.68	3
DS28_Muc	10	moderate		0.60	1.20	4	0.40	0.44	1
DS28_Stro	12	moderate		1.33	1.67	9	0.67	1.18	3
DS29	48	moderate		0.66	0.71	8	0.33	0.29	1
Average N	1oderate			0.72	2.43	11.57	0.51	0.99	3.29
DS4	60	deep		0.02	0.03	2	0.02	0.10	1
DS13		deep		0.92	2.03	15	0.47	1.12	3
DS14		deep		0.77	5.62	11	0.88	1.56	4
DS21		deep		0.93	1.11	12	0.57	0.67	2
DS25		deep		0.66	1.43	17	0.28	1.05	4
DS27		deep		0.43	1.78	8	0.39	0.92	2
Average D				0.62	2.00	10.83	0.43	0.90	2.67
DS19	71	high sedir	nentation	0.86	0.88	17	0.44	0.74	4
		high sedir		1.39	2.23	7	0.44	0.74	3
DS19_Ath									4
DS19_Muc		high sedir	nemation	0.75	0.62	14	0.416	1.72	
Average H	เรเเวยฉบย	= h		1.00	1.24	12.67	0.45	1.09	3.67
omitted				0.83	1.34	12.50	0.43	0.98	3.17
DS12	62	moderate		1.02	7.90	20	0.76	1.37	4

TABLE 10 – Observed encrustation metrics by sample with depth. Averaged across shallow, moderate, and deep water facies. Samples presumed to be from high sedimentation environments are included in Figure 13; average encrustation metric values are calculated herein both with and without high sedimentation samples.

					Depositional		Relative	Frequency of	
Citation	Location	Host	Sclerobionts Present	Substrate/Fms.	Environment	% Cover	Abundance	Encrustation	Richness
			trepostomes, hederellids,						
	Western Canada Sed	Desquamatia, Spinatrypina,	cornulitids, microconchids,	Firebag Mbr calcareuous					
Barclay et al., 2013	Basin, NE Alberta	Pseudoatrypa	Ascodictyon	interval in shale package	shallow	N/A	N/A	21%	9
		December 6 de la contraction	trepostomes, hederellids,	Hay River Fm most					
Paralay at al 2012	Northwest Tarritories	Desquamatia, Spinatrypina,	cornulitids, microconchids, Ascodictyon	calcareous zone (firebag is	shallow			50%	
Barclay et al., 2013	Northwest Territories	Pseudoatrypa	· ·	laterally contiguous)	Stidilow			50%	
		Desquamatia, Spinatrypina,	trepostomes, hederellids, cornulitids, microconchids,						
Barclay et al., 2013	Northwest Territories	Pseudoatrypa	Ascodictyon	Upper Twin Falls Fm.	deeper			44.40%	
barciay et al., 2015	Northwest remitancs	1 эсийний ура	corals, inarticulate	opper rwiir raiis riii.	иссреі			77.7070	
		Cyrtospirifer, Schizophoria, Athyris,	brachiopods, spirorbids,						
Brice and Mistiaen,		Atrypa, Douvillina, Nervostrophia,	bryozoans, cornulitids,						
1992	France	Eoschuchertella	hederellids	Beaulieu				28.60%	
		Cyrtospirifer, Schizophoria, Athyris,							
Brice and Mistiaen,		Atrypa, Douvillina, Nervostrophia,							
1992	France	Eoschuchertella		Beaulieu				39.80%	
		Cyrtospirifer, Schizophoria, Athyris,							
Brice and Mistiaen,		Atrypa, Douvillina, Nervostrophia,							
1992	France	Eoschuchertella		Beaulieu				22.70%	
		Cyrtospirifer, Schizophoria, Athyris,							
Brice and Mistiaen,	_	Atrypa, Douvillina, Nervostrophia,		_				45.000	
1992	France	Eoschuchertella		Ferque				16.00%	
Duine and Mintings		Cyrtospirifer, Schizophoria, Athyris,							
Brice and Mistiaen, 1992	Franco	Atrypa, Douvillina, Nervostrophia, Eoschuchertella		Forgue				9.10%	
1992	France	Cyrtospirifer, Schizophoria, Athyris,		Ferque				9.10%	
Brice and Mistiaen,		Atrypa, Douvillina, Nervostrophia,							
1992	France	Eoschuchertella		Ferque				18.90%	
1332	Trunce	Cyrtospirifer, Schizophoria, Athyris,		rerque				10.50%	
Brice and Mistiaen,		Atrypa, Douvillina, Nervostrophia,							
1992	France	Eoschuchertella		Ferque				15.40%	
		Cyrtospirifer, Schizophoria, Athyris,							
Brice and Mistiaen,		Atrypa, Douvillina, Nervostrophia,							
1992	France	Eoschuchertella						2%	
		Cyrtospirifer, Schizophoria, Athyris,							
		Atrypa, Douvillina, Nervostrophia,						same as	
Mistiaen et al, 2012	France	Eoschuchertella	auloporid specific					1992	
Brett and Bordeaux									
(unpublished)	CNY	Spinocyrtia	varied		moderate				34
Brett and Bordeaux	CNIV	Calacanatia	ded		d		1/		2
(unpublished)	CNY	Spinocyrtia	varied		deep	1	70		3
Pordonus and Prott			Hederellids, spirorbids, cornulitids, Ascodictyon,	single strat interval is					
Bordeaux and Brett, 1990	CNY	17 species	holdfasts, pleurodictyum	single strat interval in Kashong Shale	shallow	20-30%			25+
1770	Central Devonian Field,	17 species	noiarasts, pieuroaictyum	rasiiulig Silale	SIIdliUW	20-30%			25+
	Eastern European			transgressive pulse in clay					
Zaton and Borszcz, 201	•	Cyrtospirifer, Rhipidorhynchus		and marly limestone				56%	7 taxa

 $\textbf{TABLE 11}-Compilation\ of\ relevant\ sclerobiont\ assemblage\ data.$

TABLE 11 (cont'd)

			vermiformichnus;						
Thayer, 1974	CNY		hederellid scars, and trepostome scars noted	Catskill Delta	Delta Platform, proxima	al to distal			
	Michigan Basin	Paraspirifer		Silica Shale levels 7c-11 (upper clay mud flats)	,,,		3.1		42
Bose et al., 2011		Pseudoatrypa	trepostomes, hederellids, cornulitids, microconchids, Ascodictyon	lower Genshaw Fm., shale mbr				74%	
Bose et al., 2010	Dundee Fm., Iowa Basin	Pseudoatrypa	endoliths					35%	
Furlong and McRoberts, 2014	CNY	varied brachiopods	endoliths	Otisco Sh, transitional horizon between shales and silts				50%+	
Barringer, 2008	Michigan Basin	Strophodonta, Mucrospirifer	microconchs	Potter Farm, Alpena; Widder Fm., Arkona, ONT				18.10%	
Pitrat and Rogers, 1978	BMichigan Basin	Spinocyrtia	varied	Norway Point Fm.	precise interval, Ludlov	vville equiva	lent	71%	
Smrecak and Brandt, in prep	Michigan Basin	Mucrospirifer, Athyris, Pseudoatrypa, Strophodonta, Devonochonetes, Atrypa		Silica Shale, varied horizons	shallow	15%	4	75%	27
Smrecak and Brandt, in prep	Michigan Basin	Mucrospirifer, Athyris, Pseudoatrypa, Strophodonta, Devonochonetes, Atrypa		Ferron Point, Widder Shale	moderate, possibly higher sedimentation region	5.50%	1.4	41%	15
Alvarez and Taylor,	NW Spain	Anathyris	microconchs, hederellids, trepostomes, auloporids	Raneces Group (Emsian Stage)	shallow			71%	
Alvarez and Taylor, 1987	NW Spain	Anathyris	microconchs, hederellids, trepostomes, auloporids	Raneces Group (Emsian Stage)	shallow			75%	
Alvarez and Taylor, 1987	NW Spain	Anathyris	microconchs, hederellids, trepostomes, auloporids	Raneces Group (Emsian Stage)	shallow			63%	
Alvarez and Taylor, 1987	NW Spain	Anathyris	microconchs, hederellids, trepostomes, auloporids	Raneces Group (Emsian Stage)	shallow			60%	
Wallace, 1969	Northern France	Cyrtospirifer	microconchs, auloporids, hederellids, Paleschara	Ferques	shallow/moderate, pos	sibly sedime	nt rich	10%	
Smrecak and Brandt, in prep	Michigan Basin	Mucrospirifer, Athyris, Pseudoatrypa, Strophodonta, Devonochonetes, Atrypa		Bell Shale	deep	3.60%	1.3	49%	16
Ager, 1960	Iowa Basin (Upper Devonian)	Spinacyrtia	auloporids, paleschara, hederellids, spirorbids	Cedar Valley Limestone	shallow			89%	

TABLE 11 (cont'd)

012)										
rom Brett et al., 2	Smrecak and Brett, 2014	Cincinnati Arch, Ordovician	Rafinesquina	trepostomes, inarticulates, microconchs, cornulitids, holdfasts	Mt. Auburn	shallow	20%	2.7	80%	24
	S 1 10 11 2044	6	D. C.	trepostomes, inarticulates, microconchs, cornulitids,			120/		5504	10
n Patterns (Smrecak and Brett, 2014	Cincinnati Arch, Ordovician	Katinesquina	holdfasts trepostomes, inarticulates, microconchs, cornulitids,	Fairview	moderate	12%	1.4	66%	19
station	Smrecak and Brett, 2014	Cincinnati Arch, Ordovician	Rafinesquina	holdfasts	Коре	deep	0.70%>>1		6%	9
ısta	Lescinsky, 1997	varied	varied brachiopods	varied		shallow				20+
Encri	Lescinsky, 1997	varied	varied brachiopods	varied		moderate	17%		47%	16
ed Er	Lescinsky, 1997	varied	varied brachiopods	varied		deep				50
Observ	SSETI and Rodland et al., 2004	Bahamas, Brazilian Bight; Modern	brachiopods and deployed hosts	varied		shallow	18%	75	100%	70
	SSETI and Rodland et al., 2004	Bahamas, Brazilian Bight; Modern	brachiopods and deployed hosts	varied		moderate	14%)-44%	25
0	SSETI and Rodland et al., 2004	Bahamas, Brazilian Bight; Modern	brachiopods and deployed hosts	varied		deep	0.19%)-44%	

REFERENCES

REFERENCES

- AGER, DEREK, 1960, The epifauna of a Devonian spiriferid: Quarterly Journal of the Geological Society of London, v. 117(1).
- ALEXANDER, R.R. AND SCHARPF, C.D., 1990, Epizoans on Late Ordovician brachiopods from southeastern Indiana: Historical Biology, v. 4, p. 179-202.
- ALVAREZ AND TAYLOR, P.D., 1987, Epizoan ecology and interactions in the Devonian of Spain, Palaeogeography, Palaeoclimatology, Palaeoecology, v. 61, p. 17-31.
- BAIRD, GORDON C., AND BRETT, CARLTON E., 2008, Late Givetian Taghanic bioevents in New York State: new discoveries and questions: Bulletin of Geosciences, v. 83(1), p. 1-14.
- BARCLAY, KRISTINA M., SCHNEIDER, CHRIS L., AND LEIGHTON, LINDSEY R., 2013, Paleoecology of Devonian sclerobionts and their hosts from the Western Canadian Sedimentary Basin, Palaeogeography, Palaeoclimatology, Palaeoecology, v. 383, p. 79-91.
- BARRINGER, J.E., 2008, Analysis of the occurrence of microconchids on Middle Devonian brachiopods from the Michigan Basin: implications for microconchid and brachiopod autecology: unpublished M.S. thesis, Michigan State University, 117 p.
- BARTHOLOMEW, A.J., BRETT, C.E., DESANTIS, M, BAIRD, G.C., AND TSUJITA, C., 2006, Sequence stratigraphy of the Middle Devonian at the Border of the Michigan Basin: correlations with New York and implications for sea-level change and paleogeography, Northeastern geology and environmental sciences, v. 28(1), p. 2-33.
- BARTHOLOMEW, A.J., AND BRETT, C.E., 2007, Correlation of Middle Devonian Hamilton Group-equivalent strata in east-central North America: implications for eustacy, tectonics, and faunal provinciality, Geological Society of London Special Publications, v. 278, p. 105-131.
- BORDEAUX, Y.L., and BRETT, C.E., 1990, Medium specific associations of epibionts on Middle Devonian brachiopods: implications for paleoecology: Historical Biology, v. 4, p. 203-220.
- BOSE, R., SCHNEIDER, C., POLLY, P.D., and YACOBUCCI, M.M., 2010, Ecological interactions between *Rhipidomella* (Orthides, Brachiopoda) and its endoskeletobionts and predators from the Middle Devonian Dundee Formation of Ohio, United States: Palaios, v. 25(3), p. 196-208.
- BOSE, R., SCHNEIDER, C.L., LEIGHTON, L.R., AND POLLY, P.D., 2011, Influence of atrypid morphological shape on Devonian episkeletobiont assemblages from the lower Genshaw

- formation of the Traverse Group of Michigan: A geometric morphometric approach: Palaeogeography, Palaeoclimatology, Palaeoecology, v. 310, p. 427-441.
- BRANDT, DANITA S., 1996, Epizoans on *Flexicalymene (Trilobita)* and implications for trilobite paleoecology: Journal of Paleontology, v. 70, p. 442-449.
- BRICE, D. AND MISTIAEN, B., 1992, Epizoaires des Brachiopodes frasniens de Ferques (Boulonnais, Nord de la France), Geobios (Mem Spec), v. 14, p. 45-58.
- BRETT, CARLTON E., AND BAIRD, GORDON C., 1986, Comparative Taphonomy: a key to paleoenvironmental interpretation based on fossil preservation, *in* Thomas, R.D.K., Taphonomy: Ecology's loss is sedimentology's gain: Palaios 3(1), p. 205-344.
- BRETT, CARLTON E., AND BAIRD, GORDON C., 1996, Middle Devonian sedimentary cycles and sequences in the northern Appalachian Basin, *in* Witzke, B.J., Ludvigson, G.A., and Day, J., Paleozoic Sequence Stratigraphy: views from the North American Craton: Boulder, Colorado, Geological Society of America Special Paper 306, p. 213-241.
- BRETT, CARLTON E., 1998, Sequence stratigraphy, paleoecology, and evolution: biotic clues and responses to sea-level fluctuations, Palaios, v. 13, p. 241-262.
- Brett, C.E., Parsons-Hubbard, K., Walker, S.E., Ferguson, C., Powell, E.N., Staff, G., Ashton-Alcox, K.A., and Raymond, A., 2011a, Gradients and patterns of sclerobionts on experimentally deployed bivalve shells: Synopsis of bathymetric and temporal trends on a decadal time scale: Palaeogeography, Palaeoclimatology, Palaeoecology, v. 312, p. 278-304.
- Brett, C.E, Baird, Gordon C., Bartholomew, A.J. DeSantis, Michael K., and Verstraeten, Charles A., 2011b, Sequence stratigraphy and a revised sea-level curve for the Middle Devonian of eastern North America, Palaeogeography, Palaeoclimatology, Palaeoecology, v. 304, p. 21-53.
- BRETT, C.E., SMRECAK, T., PARSONS-HUBBARD, K.M., AND WALKER, S.E., 2012, Marine sclerobiofacies: Encrusting communities on shells through time and space, *in* Talent, J., ed., Global Biodiversity, Extinction Intervals and Biogeographic Perturbations through Time, UNESCO/International Year of Planet Earth Special Volume, p. 129-155.
- CLARKE, K.R., 1993, Non-parametric multivariate analyses of changes in community structure: Australian Journal of Ecology v. 18, p. 117-143.
- DAVIES, D.J., POWELL, ERIC N., STANTON, R.J. Jr., 1989, Taphonomic signature as a function of environmental process: shells and shell beds in a hurricane influenced inlet on the Texas coast: Palaeogeography, Palaeoclimatology, Palaeoecology, v. 72, p. 317-356.
- ETTENSOHN, F.R., 2004, Modeling the nature and development of major Paleozoic clastic wedges in the Appalachian Basin, USA: Journal of Geodynamics, v. 37, p. 657-681.

- ETTENSOHN, F.R., 2008, Chapter 4: The Appalachian Foreland Basin in Eastern United States, *in* Miall, A.D., ed., Sedimentary Basins of the World, Vol. 5, The Sedimentary Basins of the United States and Canada, p. 105-179.
- FURLONG, C. AND MCROBERTS, C.A., 2014, Commensal borings from the Middle Devonian of central New York: ecologic and taxonomic review of *Clionoides*, *Clinolithes*, and *Canaliparva* n. ichnogen., Journal of Paleontology, v. 88, p. 131-145.
- GLAUB, I., AND BUNDSCHUH, M., 1997, Comparative study on Silurian and Jurassic/lower Cretaceous microborings, Courier Forschungsinstitut Senckenberg, v. 201, p. 123-135.
- GLAUB, I., GOLUBIC, M., GEKTIDIS, M., RADTKE, G., AND VOGEL, K., 2007, Microborings and microbial endoliths: geological implications: Trace Fossils: concepts, problems, prospects, p. 368-381.
- HOWELL, P.D., AND VAN DER PLUIJM, B.A., 1999, Structural sequences and styles of subsidence in the Michigan Basin, GSA Bulletin, v. 111(7), 974-991.
- KAESLER, R.L., 1997, Part H: Brachiopoda, Treatise on Invertebrate Paleontology, 560 pp.
- KESLING, R.V., HOARE, R.D., SPARKS, D.K., 1980, Epizoans of the Middle Devonian brachiopod *Paraspirifer bownockeri*: their relationships to one another and to their host: Journal of Paleontology, v. 54(6), p. 1141-1154.
- KEY, MARCUS M., JR., WINSTON, JUDITH E., VOLPE, JARED W., JEFFRIES, WILLIAM B., VORIS, HAROLD K., 1999, Bryozoan fouling of the blue crab *Callinectes sapidus* at Beaufort, North Carolina: Bulletin of Marine Science, v. 64(3), p. 513-533.
- KEY, MARCUS M., JR., JEFFRIES, WILLIAM B., VORIS, HAROLD K., AND YANG, CHANG M., 2000, Bryozoan fouling pattern on the horseshoe crab *Tachypleus gigas* (Muller) from Singapore: Proceedings of the 11th International Bryozoology Association Conference, p. 265-271.
- KRAUSE, R.A., Jr., BARBOUR WOOD, S.L., KOWALEWSKI, M., KAUAN, D., ROMANEK, C.S. SIMOES, M.G., and WEHMILLER, J.F., 2010, Quantitative comparisons and models of time averaging in bivalve and brachiopod shell accumulations: Paleobiology, v. 36, p. 304-320.
- KOLBE, SARAH E., ZAMBITO, JAMES J. IV, BRETT, CARLTON E., WISE, JULIA L., AND WILSON, RYAN D., 2011, Brachiopod shell discoloration as an indicator of taphonomic alteration in the deep-time fossil record, Palaios 26(11), p. 682-692.
- LEBOLD, JOSEPH G., 2000, Quantitative analysis of epizoans on Silurian stromatoporoids within the Brassfield Formation, Journal of Paleontology, v.74(3), p. 394-403.

- LESCINSKY, H.L., 1993, Taphonomy and paleoecology of epibionts on the scallops *Chlamys hastate* (Sowerby 1843) and *Chlamys rubida* (Hinds 1845): Palaios, v.8, p. 267-277.
- LESCINSKY, H.L., 1997, Epibiont communities: recruitment and competition on North American carboniferous brachiopods: Journal of Paleontology, v. 71, p. 34-53.
- LESCINSKY, H.L., EDINGER, E., and RISK, M.J., 2002, Mollusc shell encrustation and bioerosion rates in a modern epeiric sea: taphonomy experiments in the Java Sea, Indonesia: Palaios, v. 17, p. 171-191.
- MISTIAEN, B., BRICE, D., ZAPALSKI, M.K., and LOONES, C., 2012, Brachiopods and their auloporid epibionts in the Devonian of Boulonnais (France): Comparison with other associations globally, *in* Talent, J., ed., Global Biodiversity, Extinction Intervals and Biogeographic Perturbations through Time, UNESCO/International Year of Planet Earth Special Volume, p. 159-189.
- PARSONS-HUBBARD, KARLA M., CALLENDER, W. RUSSELL, POWELL, ERIC N., BRETT, CARLTON E., WALKER, SALLY E., RAYMOND, ANNE L., STAFF, GEORGE M., 1999, Rates of burial and disturbance of experimentally-deployed molluscs; implications for preservation potential, Palaios v. 14(4), p. 337-351.
- PITRAT, C.W. AND ROGERS, F.S., 1978, *Spinocyrtia* and its epibionts in the Traverse Group (Devonian) of Michigan: Journal of Paleontology, 52(6), p. 1315-1324.
- POWELL, E.N., STAFF, G.M., CALLENDER, W.R., ASHTON-ALCOX, K.A., BRETT, C.E., PARSONS-HUBBARD, K.M., WALKER, S.E., and RAYMOND, A., 2011, The influence of molluscan taxon on taphofacies development over a broad range of environments of preservation, the SSETI experience: Palaeogeography, Palaeoclimatology, Palaeoecology, v. 312, p. 233-264.
- RICHARDS, R.P., 1972, Autecology of Richmondian brachiopods (Late Ordovician of Indiana and Ohio): Journal of Paleontology, v. 46, p. 386-405.
- RICKARD, L.V., 1984, Correlation of the subsurface Lower and Middle Devonian of the Lake Erie region, Geological Society of America Bulletin, v. 13, p.149-186.
- RODLAND, D.L., KOWALEWSKI, M., CARROLL, M., and SIMOES, M.G., 2004, Colonization of a 'Lost World': Encrustation Patterns in Modern Subtropical Brachiopod Assemblages: Palaios, v. 19, p. 381-395.
- RODRIGUES, S.C., SIMOES, M.G., KOWALEWSKI, M., PETTI, M.A.V., NONATO, E.F., 2008, Biotic interaction between spionid polychaetes and boucardiid brachiopods: paleoecological, taphonomic, and evolutionary implications, Acta Palaeontologica Polonica, v. 53(4), p. 657-668.
- SCOTESE, C., 2003, PALEOMAP Project, <u>www.scotese.com</u>. Last accessed 7/17/2015.

- SMRECAK, T.A., 2013, Comparing sclerobiont coverage of *Rafinesquina alternata* in hardground and soft-bottom substrate settings in the Cincinnati Arch region (Cincinnatian, Upper Ordovician), Geological Society of America North-Central Section, 47th Annual Meeting, Abstracts with Programs.
- SMRECAK, T.A., AND BRETT, C.E., 2014, Establishing patterns in sclerobiont distribution in a Late Ordovician (Cincinnatian) depth gradient: toward a sclerobiofacies model; Palaios, v. 19, p. 381-395.
- SMRECAK, T.A, AND BRANDT, D., *Chapter 1*, Sclerobiont encrustation patterns in the Middle Devonian Michigan Basin: characterizations with depth.
- SMRECAK, T.A, AND BRANDT, D., *Chapter 2*, Assessment of techniques used to describe sclerobiont abundance and distribution.
- SPARKS, D.K., HOARE, R.D., KESLING, R.V., 1980, Epizoans on the brachiopod *Paraspirifer bownockeri* (Stewart) from the Middle Devonian of Ohio: Museum of Paleontology, The University of Michigan, Ann Arbor, MI, 105 p.
- TAYLOR, P.D, M.A., 2002, A new terminology for marine organisms inhabiting hard media: Palaios, v. 17(5), p. 522-525.
- TAYLOR, P.D., AND WILSON, M.A., 2003, Palaeoecology and evolution of marine hard substrate communities: Earth-Science Reviews, v. 62(1-2), p. 1-103.
- THAYER, C.W., 1974, Substrate specificity of Devonian epizoa: Journal of Paleontology, v. 48(5), p. 881-894.
- TOMASOVYCH, A., FURSICH, F.T., OLSZEWSKI, T.D., 2006, Modeling shelliness and alteration in shell beds: variation in hardpart input and burial rates leads to opposing predictions: Paleobiology, v. 32(2), p. 278-298.
- TOMASOVYCH, A., and ZUSCHIN, M., 2009, Variation in brachiopod preservation along a carbonate shelf-basin transect (Red Sea and Gulf of Aden): environmental sensitivity of taphofacies: Palaios, v. 24, p. 697-716.
- VERSTRAETEN, C.A., 2007, Basinwide stratigraphic synthesis and sequence stratigraphy, upper Pragian, Emsian, and Eifelian stages (Lower to Middle Devonian), Appalachian Basin, Geological Society, London, Special Publications, v. 278, p. 39-81.
- VINN, OLEV and WILSON, MARK A., 2012, Encrustation and bioerosion on late Sheinwoodian (Wenlock, Silurian) stromatoporoids from Saaremaa, Estonia, Carnets de Geologie, 2012/07, p. 183-191.
- VOGEL, KLAUS, AND BRETT, CARLTON E., 2009, Record of microendoliths in different face of the Upper Ordovician in the Cincinnati Arch region USA: the early history of light-

- related microendoliths zonation, Palaeogeography, Palaeoclimatology, Palaeoecology, 281, p. 1-24.
- VOGEL, KLAUS, GOLUBIC STJEPKO, AND BRETT, CARLTON E., 1987, Endolith associations in the Middle Devonian of New York State, U.S.A., Lethaia, v. 20, p. 263-290.
- WALKER, S.E., PARSONS-HUBBARD, K., POWELL, E.N., and BRETT, C.E., 1998, Bioerosion or bioaccumulation? Shelf-slope trends for epi- and endobionts on experimentally deployed gastropod shells: Historical Biology, v. 13, p. 61-72.
- WALKER, S.E., PARSONS-HUBBARD, K., RICHARDSON-WHITE, S., BRETT, C.E., and POWELL, E.N., 2011, Alpha and beta diversity of encrusting foraminifera that recruit to long-term experiments along a carbonate platform-to-slope gradient: paleoecological and paleoenvironmental implications: Palaeogeography, Palaeoclimatology, Palaeoecology, v. 312, p. 325-349.
- WALLACE, PEIGI, 1969, Specific frequency and environmental indicators in two horizons of the Calcaire de Ferques (Upper Devonian), Northern France, Palaeontology, v. 12 (3), p. 366-381.
- ZAMBITO, JAMES, 2013, A revised stratigraphic framework for the Middle and Upper Devonian of the Northern Michigan Basin, AAPG Annual Convention and Exhibition, Pittsburgh, Pennsylvania, May 19-22, 2013.
- ZATON, M., and BORSZCZ, T., 2012, Encrustation patterns on post-extinction early Famennian (Late Devonian) brachiopods from Russia: Historical Biology, p.1-12.